Doklady Physics, Vol. 48, No. 12, 2003, pp. 657–659. Translated from Doklady Akademii Nauk, Vol. 393, No. 4, 2003, pp. 465–467.

PHYSICS

Beam Curvature in the Magnetic Field of a Neutron Star for an Arbitrary Angle between the Magnetic Dipole Moment and Incident Beam

V. I. Denisov, I. P. Denisova, I. V. Krivchenkov, and P. A. Vshivtseva

Presented by Academician V.V. Kozlov June 24, 2003

Received June 24, 2003

One of most impressive effects of nonlinear vacuum electrodynamics, which must manifest themselves in the strong magnetic fields of pulsars and magnetars, is the effect of curvature of beams of electromagnetic waves. However, in the scientific literature, due to the nonlinearity of the corresponding equations, this effect is analyzed only in two particular cases [1–3]. These are the cases when the beam lies in the planes of the magnetic-equator or magnetic meridian of the dipole magnetic field of a neutron star.

In this paper, we analyze the general case when the beam of an electromagnetic wave enters the star's magnetic field at an arbitrary angle with respect to the vector **m** of its magnetic dipole moment. In this case, as a result of nonlinear electrodynamic curvature, the beam is not represented by a planar line. Thus, the complexity of solving the problem critically depends on the successful choice of the coordinate-system orientation and on the parametrization used for parametric description of a spatial (twisted) curve. Since the expected values of the nonlinear electrodynamic and gravitational curvature of beams in the problem under consideration do not exceed $\frac{\pi}{2}$, it is convenient to choose the relevant coordinate system in the following manner.

Let vector **m** of the magnetic dipole moment of a neutron star and its rotation axis have an arbitrary direction in a certain coordinate system. At the same time, we always consider the origin of beams of electrodynamic waves to be at the point $r = \infty$, $\varphi = \pi$, $\theta = \frac{\pi}{2}$ of a spherical coordinate system and to have the impact parameter b. In this case, enumerating various orientations of vector **m** and of the rotation axis of a rotating neutron star is equivalent to enumerating beams incident onto the neutron star from different directions and at different initial angles but with the impact parameter b. In the chosen coordinate system, it is convenient to take as a parameter the polar angle φ. Thus, our first task is reduced to finding the beam parametric equations $r = r(\varphi)$ and $\theta = \theta(\varphi)$.

In the presence of external electromagnetic F_{ik} and gravitational $g^{ik}_{(0)}$ fields, by virtue of the equations of nonlinear vacuum electrodynamics [2], a weak electromagnetic wave propagates in a certain pseudo-Riemannian spacetime whose metric tensor for two normal modes has the form

$$g^{ik}_{1,2} = g^{ik}_0 + 4\xi\eta_{1,2}F^{il}F^{.k}_{l.}. \quad (1)$$

Here, subscripts of the electromagnetic-field tensor F_{ik} ascend with the help of the metric $g^{ik}_{(0)}$.

In the problem under consideration, it is reasonable to choose the metric Schwarzschild tensor as the metric tensor $g^{ik}_{(0)}$. Denoting the star's gravitational radius by r_g, we arrive at

$$g^{(0)}_{00} = 1 - \frac{r_g}{r}, \quad g^{(0)}_{rr} = -\frac{1}{g^{(0)}_{00}},$$
$$g^{(0)}_{\theta\theta} = -r^2, \quad g^{(0)}_{\varphi\varphi} = -r^2\sin^2\theta.$$

We now construct expressions for the components of the electromagnetic-field tensor F_{ik} for a neutron star rotating at a frequency of Ω_1 about the axis passing through the center of mass but not coinciding with the vector **m** of its magnetic dipole moment. In addition, the rotation axis performs a regular precession at the frequency Ω_2.

Further, we assume that, in the mobile coordinate system, the magnetic dipole moment of the neutron star is tilted at the angle α_0 to the x_3 axis and that its projection onto the $X_1O'X_2$ plane forms the angle β_0 to the positive direction of the x_1 axis. In this case, the vector **m**

Moscow State University,
Vorob'evy gory, Moscow, 119992 Russia

1028-3358/03/4812-0657$24.00

has the following components in terms of the *x*, *y*, and *z* coordinates:

$$\begin{aligned} m_x(t) &= |\mathbf{m}|\{\sin\alpha_0[\cos\psi\cos(\Phi+\beta_0) \\ &- \cos\Theta\sin\psi\sin(\Phi+\beta_0)] + \sin\Theta\sin\psi\cos\alpha_0\}, \\ m_z(t) &= |\mathbf{m}|\{\cos\alpha_0\cos\Theta + \sin\Theta\sin\alpha_0\cos(\Phi+\beta_0)\}, \\ m_y(t) &= |\mathbf{m}|\{\sin\alpha_0[\cos\Theta\cos\psi\sin(\Phi+\beta_0) \\ &+ \sin\psi\cos(\Phi+\beta_0)] - \sin\Theta\cos\psi\cos\alpha_0\}. \end{aligned} \quad (2)$$

In addition to the spatial rotation, the neutron star, being part of a double system, participates in precessional motion. Therefore, in accordance with laws of theoretical mechanics, the angles Φ and ψ entering into these expressions are time-dependent: $\Phi = \Omega_1 t + \Phi_0$, $\psi = \Omega_2 t + \psi_0$ and Ω_1 exceeding Ω_2. However, for the majority of typical neutron stars possessing a strong magnetic field, the periods $T_1 = \frac{2\pi}{\Omega_1}$ and $T_2 = \frac{2\pi}{\Omega_2}$ of this motion turn out to be considerably longer than the propagation time $T \approx \frac{2R}{c}$ for an electromagnetic signal within the domain of the presence of strong magnetic field. Therefore, while solving our problem on the nonlinear electrodynamic and gravitational curvature of beams in the neutron-star field, we may consider the angles Φ and ψ to be independent of time. Hence, expressions (2) should be taken into account only in final expressions.

We now employ a new intermediate parametrization of expression (2). We make use of auxiliary angles α and β in accordance with the relationships

$$\begin{aligned} m_x &= m\sin\alpha\cos\beta, \quad m_y = m\sin\alpha\sin\beta, \\ m_z &= m\cos\alpha. \end{aligned} \quad (3)$$

After the problem has been solved in terms of variables α and β, using relationships (2) and (3), we come back to the original angles α_0, β_0, Θ, ψ, and Φ.

In the spherical coordinates, the nonzero components of the tensor F_{ik} describing the dipole magnetic field of the neutron star have the form

$$\begin{aligned} F_{12} &= F_{r\theta} = -\frac{|\mathbf{m}|}{r^2}\{\sin\alpha\sin(\varphi-\beta)\}, \\ F_{32} &= F_{\varphi\theta} \\ &= \frac{2|\mathbf{m}|\sin\theta}{r}\{\cos\theta\cos\alpha + \sin\theta\sin\alpha\cos(\varphi-\beta)\}, \\ F_{13} &= F_{r\varphi} \\ &= \frac{|\mathbf{m}|\sin\theta}{r^2}\{\sin\theta\cos\alpha - \cos\theta\sin\alpha\cos(\varphi-\beta)\}. \end{aligned} \quad (4)$$

We write out the equation of motion for photons in an arbitrary pseudo-Riemannian spacetime:

$$\frac{dk^n}{d\sigma} + \Gamma^n_{mp}k^m k^p = 0, \quad g_{mp}k^m k^p = 0,$$

where $k^n = \frac{dx^n}{d\sigma}$ and σ is an affine parameter.

After the transformations, we reduce these equations to the form

$$\begin{aligned} \frac{d^2\theta}{d\varphi^2} + \left[\Gamma^\theta_{\alpha\beta} - \Gamma^\varphi_{\alpha\beta}\frac{d\theta}{d\varphi}\right]\frac{dx^\alpha}{d\varphi}\frac{dx^\beta}{d\varphi} &= 0, \\ \frac{d^2r}{d\varphi^2} + \left[\Gamma^r_{\alpha\beta} - \Gamma^\varphi_{\alpha\beta}\frac{dr}{d\varphi} - \frac{r_g}{2r^2}g_{\alpha\beta}\right]\frac{dx^\alpha}{d\varphi}\frac{dx^\beta}{d\varphi} &= 0. \end{aligned} \quad (5)$$

Using expressions (1) and (4), we construct nonzero components of metric tensor (1), as well as the Christoffel symbols. We perform all the calculations to within an accuracy of $\frac{r_g^2}{r^2} \ll 1$ and $\frac{\xi|\mathbf{m}|^2}{r^6} \ll 1$. As a result, Eqs. (5) acquire the form

$$\begin{aligned} &\frac{d^2Q_1}{d\varphi^2} + Q_1 = 6\eta_{1,2}\xi|\mathbf{m}|^2u^4\sin2\alpha \\ &\times\left\{2u\frac{du}{d\varphi}\sin(\varphi-\beta) - 3\left(\frac{du}{d\varphi}\right)^2\cos(\varphi-\beta)\right\}, \\ &\frac{d^2u}{d\varphi^2} + u - \frac{3r_g}{2}u^2 + 6\eta_{1,2}\xi|\mathbf{m}|^2u^4 \\ &\times\left\{4u^2\frac{du}{d\varphi}\sin2(\varphi-\beta)\sin^2\alpha\right. \\ &-u\left(\frac{du}{d\varphi}\right)^2[2+5\sin^2\alpha+9\sin^2\alpha\cos2(\varphi-\beta)] \\ &-u^3[2+\sin^2\alpha+\sin^2\alpha\cos2(\varphi-\beta)] \\ &\left.-3\left(\frac{du}{d\varphi}\right)^3\sin^2\alpha\sin2(\varphi-\beta)\right\} = 0. \end{aligned}$$

(Here, new auxiliary variables $Q_1 = \theta - \frac{\pi}{2}$ and $u = \frac{1}{r}$ are introduced.)

Because $r_g u \ll 1$ and $\eta_{1,2}\xi\mathbf{m}^2 u^6 \ll 1$, we seek the solution to these equations by the successive approximation method. Integrating these equations with the initial conditions $u(\pi) = 0$, $\frac{du(\pi)}{d\varphi} = -\frac{1}{b}$, $\theta(\pi) = \frac{\pi}{2}$, $\frac{d\theta(\pi)}{d\varphi}$, we arrive at

$$
\begin{aligned}
u = \frac{1}{b}\Bigg\{ & \sin\varphi + \frac{r_g}{4b}[3 + \cos 2\varphi + 4\cos\varphi] + \frac{r_g^2}{64b^2} \\
& \times [60(\pi - \varphi)\cos\varphi - 32\sin 2\varphi - 3\sin 3\varphi + 5\sin\varphi] \\
& + \frac{\eta_{1,2}\xi\mathbf{m}^2}{1024b^6}\{\sin^2\alpha[24(\varphi - \pi)[39\cos(\varphi + 2\beta) \\
& - 120\cos\varphi + 91\cos(\varphi - 2\beta)] - 9\sin(9\varphi - 2\beta) \\
& - 8\sin 7\varphi + 43\sin(7\varphi - 2\beta) \\
& - 2\sin(5\varphi + 2\beta) + 32\sin 5\varphi \\
& - 30\sin(5\varphi - 2\beta) - 18\sin(3\varphi + 2\beta) + 192\sin 3\varphi \\
& - 414\sin(3\varphi - 2\beta) - 747\sin(\varphi - 2\beta) \\
& - 1137\sin(\varphi + 2\beta) + 2200\sin\varphi] \\
& - 32[120(\varphi - \pi)\cos\varphi + \sin 5\varphi \\
& - 15\sin 3\varphi - 80\sin\varphi]\}\Bigg\},
\end{aligned}
\tag{6}
$$

$$
\begin{aligned}
\theta = \frac{\pi}{2} + \frac{\eta_{1,2}\xi\mathbf{m}^2}{512b^6}\sin 2\alpha\{ & 24(\varphi - \pi)[13\sin(\varphi + \beta) \\
& - 12\sin(\varphi - \beta)] + 5\cos(7\varphi - \beta) \\
& + 2\cos(5\varphi + \beta) - 28\cos(5\varphi - \beta) \\
& + 12\cos(3\varphi + \beta) + 42\cos(3\varphi - \beta) \\
& + 271\cos(\varphi + \beta) - 304\cos(\varphi - \beta)\}.
\end{aligned}
$$

We now analyze the expressions obtained. First of all, we find angles $\delta\varphi$ and $\delta\theta$ that characterize the beam curvature as a result of nonlinear electromagnetic and gravitational effects. Since the angles $\delta\varphi$ and $\delta\theta$ must be small, substituting $\varphi = \delta\varphi$ and $\theta = \frac{\pi}{2} + \delta\theta$ into expressions (6) and solving the relationships obtained, we find within the limits of the required accuracy

$$
\begin{aligned}
\delta\theta &= \frac{75\pi\eta_{1,2}\xi\mathbf{m}^2}{64b^6}\sin\beta\sin 2\alpha, \\
\delta\varphi &= -\frac{2r_g}{b} - \frac{15\pi r_g^2}{16b^2} \\
&\quad - \frac{15\pi\eta_{1,2}\xi\mathbf{m}^2}{64b^6}\{[12 - 13\cos 2\beta]\sin^2\alpha + 16\}.
\end{aligned}
\tag{7}
$$

Analysis of expressions (7) shows that the nonlinear electrodynamic part of $\delta\varphi$ has a fixed sign and is negative for arbitrary values of the angles α and β. The angle $\delta\theta$ is not a fixed-sign function of the angles α and β of the orientation of the neutron star's magnetic dipole moment.

If the neutron star rotates at a frequency $\Omega_1 \ll \frac{c}{R}$ and performs precessional motion, then the time dependence of the curvature angles can be found from expressions (2), (3) and (7):

$$
\begin{aligned}
\delta\varphi(t) &= -\frac{2r_g}{b} - \frac{15\pi r_g^2}{16b^2} \\
&\quad - \frac{15\pi\eta_{1,2}\xi}{64b^6}\{15\mathbf{m}^2 + 26m_y^2(t) + m_z^2(t)\}, \\
\delta\theta &= -\frac{75\pi\eta_{1,2}\xi}{32b^6}m_y(t)m_z(t),
\end{aligned}
$$

where the time-dependent components of the vector $\mathbf{m}$ are given by expressions (2).

Thus, because of the time dependence of the angles $\delta\varphi$ and $\delta\theta$, the intensity of electromagnetic radiation propagating through the magnetic field of a rotating neutron star and being registered by an observer is also time-dependent, and this dependence is different for the two normal modes of the electromagnetic wave. This property can form the basis for experimental investigation of regularities of nonlinear vacuum electrodynamics in domains with moderately strong ($\mathbf{m}^2/b^6 < B_q^2$) magnetic fields of neutron stars.

REFERENCES

1. V. L. Ginzburg and V. N. Tsytovich, Usp. Fiz. Nauk **126**, 553 (1978).
2. V. I. Denisov, Teor. Mat. Fiz. **132**, 211 (2002).
3. V. I. Denisov, I. P. Denisova, and I. V. Krivchenkov, Dokl. Akad. Nauk **388** (1), 23 (2003) [Dokl. Phys. **48**, 325 (2003)].

Translated by G. Merzon

Doklady Physics, Vol. 48, No. 12, 2003, pp. 660–664. Translated from Doklady Akademii Nauk, Vol. 393, No. 4, 2003, pp. 468–472.

PHYSICS

On the Interaction of a Thermal Wave with a Thermal-Decomposition Front under Intensely Heating Nonvolatile Condensed Systems

O. F. Shlensky

Presented by Academician V.V. Osiko July 4, 2003

Received August 28, 2003

Interaction of a thermal wave with a combustion front in liquid nonvolatile condensed systems in the case of boiling on a surface was studied in [1]. There it was established that the heating wave propagates in the forward direction, whereas the domain of liquid, which is heated up to the boiling temperature, is expanded (see [1]).

In the present paper, we consider mutual effects associated with the motion of a thermal wave and of the thermal-decomposition front. We analyze the dependence of these effects on thermophysical properties of a substance involved in the decomposition reaction and on kinetics of this reaction in the case of intensely heating nonvolatile condensed systems (in particular, during heat-shielding coatings and combustion).

In volatile condensed systems, the elevation of the surface temperature associated with the heat supply is naturally limited by the boiling temperature T_b. When intensely heating nonvolatile substances, the temperature rise is limited by the ultimate temperature T_l (temperature of attainable superheating). At lower temperatures, stability of the substance metastable state preserves [2–4].

Processes of thermal decomposition in nonvolatile substances are associated with formation of heterogeneous and homogeneous nuclei (the latter dominate at elevated temperatures). This complicates the behavior of nonvolatile liquids compared to volatile ones. The velocity of a heating wave, or of the front thermal propagation (thermal wave, in the terminology of Frank-Kamenetskiĭ [5]) is determined by the heat conduction equation

$$c\rho\frac{\partial T}{\partial t} = \lambda\frac{\partial^2 T}{\partial x^2} + F(T), \qquad (1)$$

having a solution of running-wave type: $T = T(z)$, $z = x + u_T t$ [6]. Here, u_T is the thermal-wave propagation velocity, c is the specific heat, $F(T)$ is the heat-release function, and other notation is traditional.

As was noted in [1], the amount of heat $W = c(T_s - T_0)$ released in the k-phase, where T_s is the surface temperature, attains only a small portion of the total thermal effect of the completed reaction by virtue of the dispersion effect, $T_s < T_0 + \frac{Q}{c}$. Therefore, following to from [1], we furthermore ignore the variation in concentration of reacting molecules in the k-phase. It is well known that for volatile substances, the front motion velocity during heating of their surface is determined by the evaporation rate (described by the Knudsen–Langmuir equation) or by the rate of boiling off a liquid from the surface. In contrast, for nonvolatile substances, the propagation velocity of the thermal-decomposition front is determined by the mass transport equation

$$\frac{\partial\eta}{\partial t} - w(T) = 0. \qquad (2)$$

This equation also has a solution of the running-wave type $\eta = \eta(y)$, $y = x + ut$, where η is the transformation depth (degree of conversion) and u is the combustion wave velocity. Hence, as is seen, $u_T \neq u$. Following [1], we consider the relation between the indicated velocities and write out Eqs. (1) and (2) in coordinate systems moving at constant velocities:

$$\lambda\frac{d^2 T}{dx^2} - c\rho u_T\frac{dT}{dt} + F(T) = 0, \qquad (3)$$

$$-u\frac{d\eta}{dx} + w(T) = 0. \qquad (4)$$

Thus, $u = u_T$ only in a particular case and in the steady-state regime. It was found in [1] by means of

Mendeleev University of Chemical Technology, Miusskaya pl. 9, Moscow, 125820 Russia

1028-3358/03/4812-0660$24.00

excluding the second term in Eq. (3) that

$$u_T = \frac{\left[2\lambda\frac{RT_s^2}{E}QB\exp\left(-\frac{E}{RT_b}\right)\right]^{1/2}}{\rho C(T_s - T_0)}, \quad (5)$$

where T_s is the surface temperature equal to T_b for volatile condensed systems. According to Zel'dovich [1], the thermal-wave velocity (6) differs from the front propagation velocity being measured in experiments and can be determined by integrating Eq. (5) within the limits $x = 0$ and $x = \infty$ (in the latter case, $\eta = 0$):

$$u\eta_d = \int_0^\infty w(T)dx. \quad (6)$$

Here, η_d is the degree of dispersing the substance (i.e., of carrying away particles of the unreacted substance). For substances (e.g., ammonium perchlorate (APC), hydroxyl ammonium perchlorate (HAP), trimethyl ammonium perchlorate, etc. [8]) in which processes associated with the heat absorption proceed simultaneously with the exothermic reaction, the following expression for velocity is derived in the Zel'dovich approximation:

$$u_T^2 = \frac{2\lambda\frac{RT_s^2}{E}k_0\exp\left(-\frac{E}{RT_b}\right)}{\rho E(1-\eta_s)(Q_d - (Q_d + Q_s)\eta_s)}. \quad (7)$$

Here, Q_s is the sublimation heat, Q_d is the decomposition heat, η_s is the sublimation fraction. In contrast to [1], many publications including [7, 8] do not distinguish the velocities u and u_T. We find the interrelation between the velocities u_T and u on the basis of Eq. (3). As a result of integrating Eq. (3) within the limits from $x = 0$ (where $q = -\lambda\frac{dT}{dx}$ is the heat flux through the surface) to $x = \infty$ (where $T = T_0$), we arrive at

$$-\lambda\frac{dT}{dx}\bigg|_{x=0} - c\rho u_T(T_w - T_0) + \int_0^\infty F(T)dx = 0. \quad (8)$$

We determine the velocity u_T from Eq. (8):

$$u_T = \frac{q + \int_0^\infty F(T)dx}{c\rho(T_s - T_0)}. \quad (9)$$

In the case of the thermal decomposition of condensed systems, $F(T) = f_0 Qw(T)$, where Q is the thermal effect of the reaction. The coefficient f_0 is introduced in order to allow for the incompleteness of the heat release in the decomposition reaction, since $W < Q$. The incompleteness of the heat release arises by virtue of a number of reasons. Among them, we can indicate the inconsistency of the reagent content with the stoichiometric relation of the components presented and the removal of particles of the unreacted substance from the reaction zone as a result of gas filtration. All these reasons decrease the coefficient f_0. After substituting the obtained value of the velocity into Eq. (9), we establish the relation between the two velocities in the form

$$u_T = \frac{q + f_0 Q\rho\eta_d u}{c\rho(T_s - T_0)}. \quad (10)$$

It follows from Eq. (10) that the velocities u and u_T are the same only under the following conditions: $q = 0$ and $Q\rho f = c\rho(T_s - T_0)\, f = f_0\eta_d$. Equating these velocities results in the loss of important information on the process. The velocity u_T exceeds the velocity u if $Q\rho f > c\rho(T_s - T_0)$ and $q > 0$. The relation between these velocities determines the stability or instability of combusting condensed systems. For example, a decrease in the thermal flux q down to zero at $Q\rho f < c\rho(T_s - T_0)$ implies that the thermal wave is delayed with respect to the thermal-decomposition wave and does not provide sufficient heat supply to the front, which results in the attenuation of the process. The thermal effect can enter into Eq. (10) with a plus or minus sign. Therefore, Eq. (10) is applicable in the case of heating of both power-consuming and heat-shielding condensed systems. An effect of the heat flux being supplied on the combustion stability of condensed systems was determined experimentally in [7, 8]. At lowering pressure, the convective heat supply to the surface decreases, and the combustion of various condensed systems either becomes unstable or entirely ceases.

We now present a numerical example for comparison of velocities of heating waves and combustion waves in the well-studied substance, namely, APC. The characteristic parameters of APC, which are necessary in the calculation, are borrowed from [8]: the density is $\rho = 1.94$ g cm^{-3}, the total thermal effect of the reaction in the combustion front with allowance for sublimation is $Q_d - (Q_d + Q_s)\eta_s = 120$ cal g^{-1}, the specific heat is $c = 0.3$ cal g^{-1}, the thermal conductivity is $\lambda = 10^{-4}$ cal cm^{-1} K^{-1} s^{-1}, and the coefficient f_0 is $f_0 = 0.64$. For a pressure of 0.1 MPa and in the absence of a thermal flux on the surface, we obtain, as a result of substituting these values into Eq. (10),

$$u_T = 0 + \frac{0.64 \times 120 \times 1.94u}{1.94 \times 0.3(750 - 300)} = 0.569u.$$

Thus, $u_T < u$, and in accordance with the calculation results, there occurs the retardation of the thermal wave from the combustion front, and this wave ceases to maintain combustion. The results of the experiment described in [8] testify to the fact that APC taken at a pressure of 0.1 MPa and at the initial temperature $T =$ 300 K is not capable of independently combusting.

Thereby, the assumption that $q = 0$ and the conclusion obtained in the calculation are confirmed. It is worth noting that Eq. (7) in itself does not allow us to make the conclusion on the absence of combustion. Indeed, according to this equation, we can calculate the combustion rate for an arbitrary value of the thermal effect (even as small as is wished), and the combustion is stable.

As is indicated in [8], APC is capable of independently combusting after it has obtained the additional heat $\Delta Q = 100$ cal g^{-1} in the form of radiative energy with the help of a small addition of combustible or by preliminarily heating. Furthermore, we analyze an effect of such an addition on the calculation results in the case of $q = 0$. In order to do this, we increase the thermal effect by $\Delta Q = 100$ cal g^{-1}:

$$u_T = 0 + \frac{0.64(120 + 100)1.94u}{1.94 \times 0.3 \times (750 - 300)} = 1.04u.$$

We have $u_T > u$. This indicates that the thermal wave advances the decomposition front and provides its heat supply. In this case, the process is stable, which is observed in the experiments described in [8].

Allowance for the heat flux q enhances the above statement. At pressures of 0.1 MPa, the temperature gradients at the APC surface are on the order of 7×10^5 K cm^{-1} [8]. In this case, $q = 7 \times 10^5 \times 10^{-4} = 7$ cal cm^{-2} s^{-1}. Then,

$$u_T = 7 + \frac{0.64(120 + 100)1.94u}{1.94 \times 0.3 \times (750 - 300)}$$
$$= 0.0267 + 1.04u > 1.04u,$$

which ensures additional stabilization of the process.

The calculation on the basis of Eq. (7) at higher pressures (40 and 100 MPa) was performed in [8]. The calculated value of the thermal-wave velocity [this is the thermal-wave velocity that is determined by Eq. (8)] was shown to exceed by a factor of 5 the experimental velocity of the front motion. This fact cannot be explained by simple spreading characteristics of the substance. Thus, the inequality $u_T > u$ testifies to stability of the process, which is confirmed by experimental data: the process turns out to proceed stably at high pressures.

In accordance with Eq.(10), lowering the initial temperature T_0 results in a decrease in the velocity u_T. Hence, the combustion stability also decreases, which is confirmed by the experimental data of [8].

The limitation of the surface temperature of the APC combustion by temperature T_l corresponds to the experimental data of [7, 9]. Introducing various polymeric admixtures into APC resulted in the variation of the combustion rate by a factor of 7. However, in this case, the surface temperature did not vary and remained close to $T_l = 495$°C at 0.1 MPa [3]. At the same time, according to Eq. (6), the variation in the velocity by a factor of 7 corresponds to a change in the thermal effect by a factor of 49, which was not observed in experiments. Introducing additions to compositions based on nitrocellulose [7] leads to a similar conclusion: the surface temperature varies negligibly and does not exceed the ultimate temperature of the nitrocellulose decomposition, which is $T_l = 320$°C at 0.1 MPa. Thus, the Zel'dovich formula and Eq. (7) can also be used for determination of the thermal-wave velocity of nonvolatile condensed systems, provided that the boiling temperature T_b for them is changed by the temperature T_l of the attainable superheating. An example of the calculation is given in [6]. However, the Zel'dovich formula and other solutions to Eq. (9) cannot determine the value of the velocity u if it is not equal to u_T. We now make use of the heat flux method proposed by Frank-Kamenetskiĭ [5]. This method is based on both deriving heat flux equations in the reaction surface zone

$$q + f_0 Q\rho w\delta_T = -\lambda\left.\frac{dT}{dx}\right|_{x=0} = c\rho(T_s - T_0)$$

(here, δ_T is the thickness of the near-surface layer in which the heat release takes place) and the equation for the amount of heat going out of this layer and arriving at the heating zone:

$$(q + f_0 Q\rho w\delta_T)t = c\rho(T_s - T_0)\frac{a}{u}.$$

We now multiply the heat flux equation by the propagation time $t = \frac{f_0}{w}$ of the heating wave and equate the right-hand sides of this and subsequent equations. As a result, we obtain the approximate expression for the velocity

$$u_T = \sqrt{\frac{aw}{f_0}}, \quad (11)$$

where a is the thermal diffusivity. Taking into account the fact that the reaction accompanied by the mass loss proceeds in the narrow layer with a thickness δ, we can rewrite Eq. (6) in the form

$$u\eta_d = w\delta. \quad (12)$$

The interrelation between the quantities δ and δ_T, which was called by Frank-Kamenetskiĭ "chemical" interrelation or the "front thermal thickness" (see [5, p. 366]) was established by him as $\delta = F\delta_T$. Substituting this value into Eq. (12), we arrive at $u = \frac{Ff_0}{\eta_d}u_T$, whence it follows

$$u_T = \frac{\eta_d}{Ff_0}u. \quad (13)$$

As was shown in [10], the calculated velocities determined by the heat flux method satisfactorily corre-

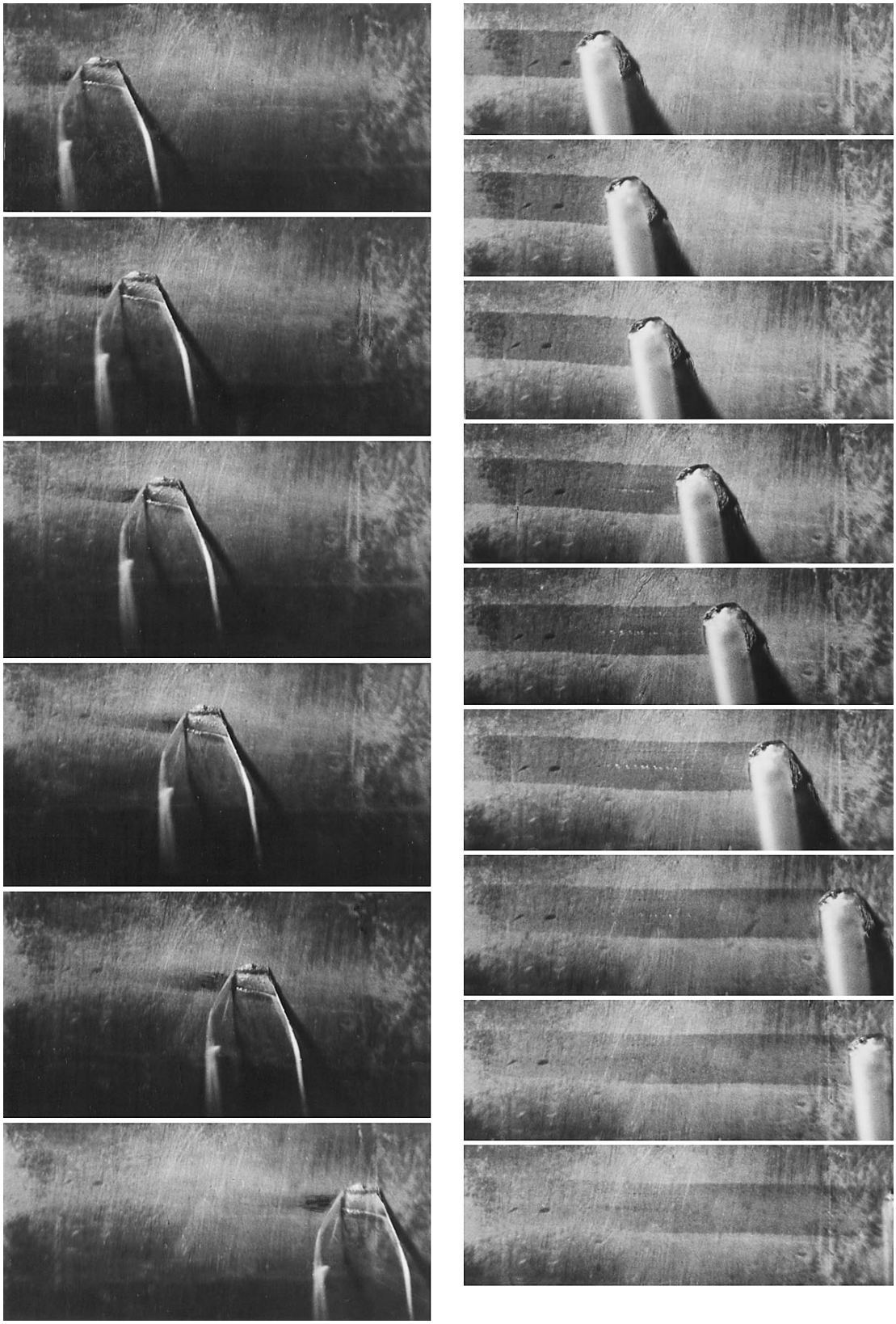

Filming frames of the process of depositing thin layers of (on the left) polymethyl methacrylate (on the left) and (on the right) polyethylene (on the right) melts on a heated metallic substrate. The velocity of motion for the original sample is 150 m s^{-1}, the residence times for the sample on the substrate are 0.03 and 0.18 s, respectively.

spond to experimental data for a number of condensed systems. Equating the right-hand sides of Eqs. (13) and (10), we find the coefficient F:

$$F^2 = \frac{\eta_d^2 Q}{c(T_s - T_0)}.$$

Hence, it follows that while decreasing the dispersion intensity, for example, as a result of elevating pressure, the thermal front thickness increases, which causes the same phenomenon that was analyzed by Zel'dovich for volatile condensed systems.

By contrast, lowering pressure causes a decrease in the convective heat supply of the surface and enhances the dispersion. In the framework of the model under consideration, this occurs by virtue of a rise in the velocity of motion of gaseous decomposition products. This is a result of reducing the gas density in the case of a pressure drop so that the coefficient f decreases. Strong dispersion at lowered pressures facilitates the decrease in heat release (the fQ product is reduced). This leads to deceleration of decomposition front motion, which was observed in the experiments of [7] not only for APC but also for other condensed systems.

The thickness of the thermal-wave zone was measured while intensely heating the lateral surfaces of condensed systems being decomposed. To this aim, substance layers were deposited onto a metallic substrate preliminary heated to a high temperature. Figure 1 illustrates the results obtained by the frame filming in the visible spectra of polymethyl methacrylate and polyethylene melt layers at temperatures slightly different from T_l, namely, 490 and 512°C, respectively. Testing samples of different thicknesses has demonstrated that for thicknesses up to 9–10 μm, the heating process was not accompanied by dispersing the substance. The decomposition proceeded as a result of homogeneous nucleation and evaporation of products from the surface. Thus, under the indicated test conditions, we dealt with δ_T = 9–10 μm. With increasing the layer thickness, the decomposition is accompanied by a strong frothing and dispersing of a sample. The similar results of filming samples in the infrared spectral range were reported in [10].

Thus, the conclusion made by Zel'dovich on the difference in the velocities of the thermal and combustion waves in the case of boiling liquid volatile condensed systems can be propagated on nonvolatile condensed systems under the condition of intensely heating their surfaces.

We can conclude that on the basis of the heat-conduction and mass-transport equations, the quantitative connection is established for the velocities of the thermal wave and decomposition front motion. We also have presented examples of calculation results obtained according to the formulas given above and experimental data related to the determination of the thermal-layer thickness in the case of intensely heating surfaces of volatile-substance samples.

REFERENCES

1. Ya. B. Zeldovich, *Selected Papers*, Vol. 1: *Chemical Physics and Hydrodynamics* (Nauka, Moscow, 1984; Princeton Univ. Press, Princeton, 1992).
2. P. A. Pavlov, *Dynamics of Boiling of Strongly Superheated Liquids* (Ural. Otd. Akad. Nauk SSSR, Sverdlovsk, 1988).
3. O. F. Shlenskiĭ, N. V. Afanas'ev, and A. G. Shashkov, *Thermal Decomposition of Materials* (Énergoatomizdat, Moscow, 1996).
4. V. P. Skripov, E. N. Sinitsyn, P. A. Pavlov, and G. V. Ermakov, *Thermodynamic Properties of Liquids in Metastable State* (Atomizdat, Moscow, 1980).
5. V. F. Zaĭtsev and A. D. Polyanin, *Handbook of Exact Solutions for Partial Differential Equations* (CRC Press, Moscow, 1996).
6. K. K. Andreev, *Thermal Decomposition and Combustion of Explosive Substances* (Nauka, Moscow, 1966).
7. G. B. Manelis, G. M. Nazin, Yu. I. Rubtsov, and V. A. Strunin, *Thermal Decomposition and Combustion of Explosive Substances and Powders* (Nauka, Moscow, 1996).
8. J. Powling and W. A. Smith, Combust. Flame **7**, 269 (1963).
9. O. F. Shlensky and Yu. V. Zelenev, Dokl. Akad. Nauk **385**, 482 (2002) [Dokl. Phys. **47**, 571 (2002)].
10. O. F. Shlensky and N. N. Lyasnikova, Dokl. Akad. Nauk **391**, 179 (2003) [Dokl. Phys. **48**, 347 (2003)].

Translated by G. Merzon

Doklady Physics, Vol. 48, No. 12, 2003, pp. 665–668. Translated from Doklady Akademii Nauk, Vol. 393, No. 6, 2003, pp. 762–765.

PHYSICS

Two-Threshold Cavitation Regime

G. N. Sankin and V. S. Teslenko

Presented by Academician V.M. Titov May 13, 2003

Received May 27, 2003

The effect of the heterogeneous structure of the medium on the formation processes and dynamics of cavitation clusters must be taken into account when studying the propagation of acoustic pulses in a liquid under the cavitation conditions. The corresponding problems concern both the known problems of the propagation of acoustic waves in heterogeneous media [1–3] and active development of investigations of the luminescence of liquids under cavitation conditions [4, 5].

Cavitation processes are complex because liquids usually have the potential heterogeneous properties determined by various cavitation nuclei. Water can include inhomogeneities such as gas microbubbles with a radius of about 1.5 μm and a density of 10^3–10^4 cm^{-3} [6], solid particles with gas bubbles [6, 7], and nanobubbles (bubstones) with a radius of about 2 nm [8]. Nanobubbles can be jointed into clusters with a density of about 10^4 cm^{-3} [8].

The experiment described in [7] shows that cavitation nuclei are not removed by multiple water purifications. In a real liquid, nanonuclei coexist with micronuclei and can be detected by studying the dynamics of the formation of cavitation clusters.

In this work, we investigate the early stages of the formation of a two-fraction cavitation cluster in distilled water.

Cavitation was induced by a generator of a spherically focused acoustic pulse (F = 55 mm) with pressures 75 and –42 MPa in the positive and negative phases, respectively, and with a decrease rate of about –40 MPa/μs [9]. A rarefaction wave arising due to diffraction at the radiator edges induces cavitation in the liquid. Cavitation was studied by high-speed (including microscopic) filming (10^8 fps, resolution was equal to 5–50 μm/pixel). The pressure field was measured by a FOPH 300 fiber-optic hydrophone [10] (fiber diameter was equal to 140 μm). Time was measured from the arrival of the compression wave front at the observation point.

Lavrent'ev Institute of Hydrodynamics, Siberian Division, Russian Academy of Sciences,
pr. Akademika Lavrent'eva 15, Novosibirsk, 630090 Russia

Figure 1 shows the typical frames of shadow filming of the development of hydrodynamic processes when the acoustic wave is focused far from the liquid boundary, which corresponds to developed cavitation. The processes are (*1*) the focusing of the acoustic shock wave, (*2*) the formation of a cluster of bubbles at the rarefaction phase, and (*3*) the formation of the compression pulse with the front from expanded bubbles, which is called the secondary cavitation compression wave (SCCW) [9, 11]. The distance between the fronts of the primary and secondary waves was measured to be 3.8 mm, which corresponds to a time interval of 2.5 μs, and is seen on pressure oscillograms (Fig. 2) [9].

Points in Fig. 3 are the bubble sizes obtained from the set of enlarged frames. As is seen, for time t from 3 to 4 μs, bubbles are separated into two kinematic fractions of (I) expanded and (II) collapsing bubbles. Figure 3 indicates that the bubble dynamics depends critically on the time of their growth up to detectable sizes. Data demonstrate the existence of two groups of bubbles that reach detectable size with the time difference $|t_{crI} - {}_{crII}| = 0.5$ μs.

It was ascertained that bubbles of (*4*) the first group become detectable in $\Delta t_{crI} = 1.6$ μs after the arrival of the compression wave front. Bubbles of (*5*) the second group become detectable after $\Delta t_{crII} = 2.1$ μs, when the pressure in the compression phase is $|p_-| \geq 33$ MPa (Fig. 2). The first-pulsation period was more than 100 μs and less than 3 μs for bubbles of the first and second groups, respectively.

Films show that small bubbles are concentrated at the center of the cluster. The distribution of small bubbles in the cluster over the distance from the radiator axis is maximal in the axis and has a FWHM of 1.2 mm (Fig. 4). The width of the small-bubble cloud increases with the initial pressure on the membrane for the almost constant FWHM 5.0 ± 0.5 mm of the distribution of the negative pressure phase. The distribution of larger bubbles is approximately uniform over the radius in the observation region $|r| < 1.7$ mm. The z distribution of bubbles in both groups is virtually uniform in the observation region $|\Delta z| < 2$ mm in agreement with the distribution of pressure. The average density of bubbles in the first and second groups does not exceed $n_I = 1.6 \times 10^2$ cm^{-3} and $n_{II} = 5.3 \times 10^3$ cm^{-3}, respectively.

1028-3358/03/4812-0665$24.00

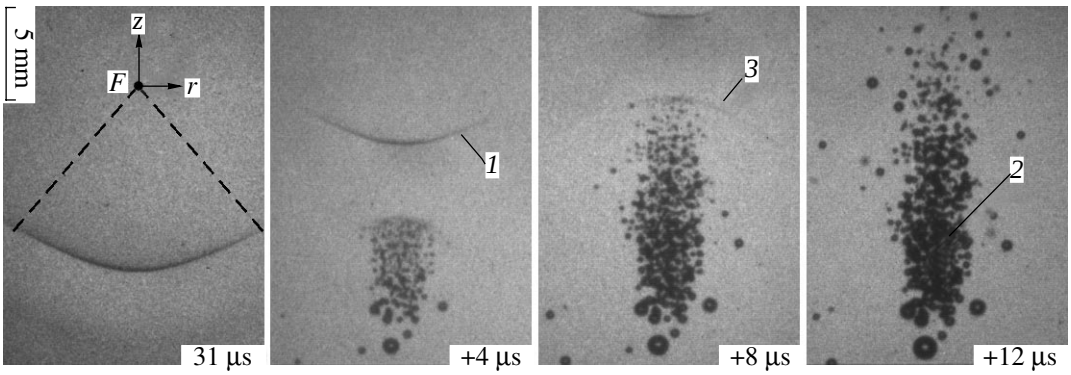

Fig. 1. Dynamics of the cavitation cloud induced when focusing an acoustic pulse in water for p_{max} = 9.7 MPa, F is the focus (z = r = 0).

The collapse of bubbles of the second group is induced by neighboring larger bubbles. Expanding by inertia (gained in the initial rarefaction wave), bubbles of the first group emit spherical compression waves. An SCCW is formed due to the interference of waves from individual bubbles. In the compression wave (*3* in Fig. 1) corresponding to the SCCW field, small bubbles collapse in the time interval 3.5–4.5 μs, emitting the third series of slightly phased shock waves. The amplitude of shock waves from the collapse of the second group of bubbles was below the sensitivity threshold of the FOPH hydrophone of about 1 MPa, which was much lower than the pressure in the SCCW. Therefore, the presence of small bubbles only slightly affects the dynamics of large bubbles.

As is known, the spherical shape of a bubble compressed by an external plane shock wave is distorted. In the case under consideration, the spherical shape of the bubble is conserved at early times (t < 4.5 μs) in the pulsation period following the first collapse [9].

The experimental data discussed above show that bubbles of the first and second groups behave differently when a bipolar acoustic wave passes through a liquid in the presence of cavitation. To reveal the origin of this difference, we numerically simulated the effect of a pulse action on a single bubble with variation in its initial diameter. The dynamics of a single bubble including nonstationary pressure in the SCCW was calculated in the Rayleigh–Plesset model with the numerical constants taken from [12]. The calculation was carried out for the measured time dependence of p_∞ (Fig. 2) and for the initial bubble radius R_0 from 0.01 to 1 μm. The initial time t_0 of the nucleation of the bubble varied from 0 to 2.5 μs.

According to the calculations shown in Fig. 3 (lines *a*, *b*, *c*), bubbles with the initial radius R_0 > 2.2 nm collapse later than the SCCW arrival time t_B (lines *a*, *b*). Bubbles with the initial radius in the interval 1.8–2.2 nm collapse in the positive phase of the SCCW (line *c*). Such bubbles grow to a detectable size of 10 μm in the time interval 2.0–2.2 μs, which agrees with the measured time τ_{crII} in which bubbles of the second group reach the same size (points in Fig. 3). Nuclei with the initial radius R_0 < 1.8 nm did not become detectable, because pressure in the rarefaction phase exceeded the critical pressure for these bubble radii. A similar collapse effect in the compression pulse of the SCCW was observed for a bubble that had the initial radius 0.01–1 μm and originated in the time interval 2.0–2.4 μs.

Thus, the use of a spherically focused pulse far from the liquid boundaries revealed a number of new cavitation properties. The analysis of the time dependence of the radius of bubbles shows that a two-fraction bubble cluster is formed. Measurements of the time in which bubbles became detectable indicate that the mechanisms of the formation of bubbles of different groups are different.

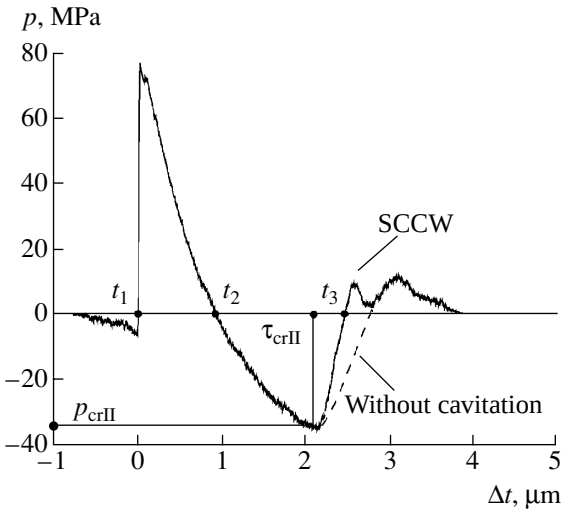

Fig. 2. Pressure measured by the FOPH 300 hydrophone at the focus of the radiator (z = r = 0) for the cavitation case (p_{max} = 7.7 MPa). Pressure is equal to zero at times t_1, t_2, and t_3.

These experimental data imply the two-fraction initial distribution of cavitation nuclei in the liquid. Simple estimates by formulas for the homogeneous nucleation rate [13] show that the probability of the formation of vapor nuclei far from the boiling point of the liquid is very low. For the appearance of a detectable nucleus in the rarefaction wave in water, pressure must be lower than –160 MPa, which is several times lower than pressure used in the experiment.

Stable micro- and nanonuclei whose size distribution has two maxima at about 1 μm and 2 nm can serve as cavitation nuclei. Nuclei whose initial radius exceeds 0.01 μm can be classified among the first group, because calculations show that such bubbles become detectable almost simultaneously.

The critical pressure p_{cr} at which the bubble is expanded is given by the formula [6]

$$p_{cr} = p_v - 2\left[\frac{\left(\frac{2\sigma}{R_0}\right)^3}{3\left(p_0 - p_v + \frac{2\sigma}{R_0}\right)}\right]^{1/2}, \qquad (1)$$

where R_0 is the initial radius of the nucleus. Formula (1) with values σ = 0.071 N/m, p_v = 0.002 MPa, p_0 = 0.1 MPa, and bubstone radius R_{0II} = 3.6 nm [14] yields p_{crII}^{theor} = –45 MPa close to the experimental value. This implies the presence of nanonuclei with R_{0II} = 2–4 nm in our experiments.

The two-fraction distribution of detected bubbles in the cluster can be attributed to the presence of stable nanobubbles (bubstones). The transition to the two-threshold cavitation regime occurs when the critical pressure is exceeded for both types of nuclei with micro- and nanosizes. This is due to the fact that bubbles of the first group are formed from micronuclei, while bubbles of the second group are formed from nanonuclei, which became detectable at the rarefaction-phase amplitude $|p_{crII}|$ = |–33 MPa| that is much larger than the amplitude at which microbubbles became detectable ($0.07 < |p_{crII}| < 33$ MPa).

Numerical simulation of pulse compression in the cluster well reproduces both the contraction of the oscillation period and the enhancement of the collapse of bubbles of the second group. Pulse compression of bubbles when the rarefaction wave transforms to the compression wave occurs at the internal cluster pressure up to 20 MPa. Owing to the internal pressure arising in the cluster due to the expanded nuclei of the first group, the collapse of bubbles of the second group becomes more spherical than the collapse of bubbles in a plane acoustic wave. Therefore, such polydisperse bubble systems are promising for practical usage in sonochemistry due to higher thermodynamic parameters when a bubble collapses in a cluster.

The observed kinetic bimodality of bubble pulsation in a water cavitation cluster can considerably simplify experiments related to sonoluminescence. In such experiments, the necessity to specially purify the liquid and initiate bubbles using inaccessible neutron sources can be excluded [15].

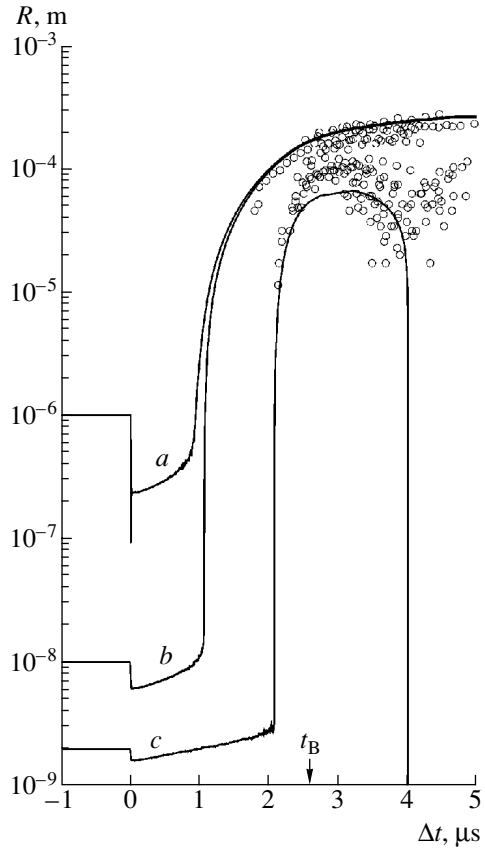

Fig. 3. Radius of bubbles at the center of the cluster vs. the time delay for the pressure p_{max} = 7.7 MPa above the critical pressure: (points) experiment and calculations of the dynamics of the nucleus with the initial radius (*a*) 1, (*b*) 0.01 μm, and (*c*) 1.99 nm.

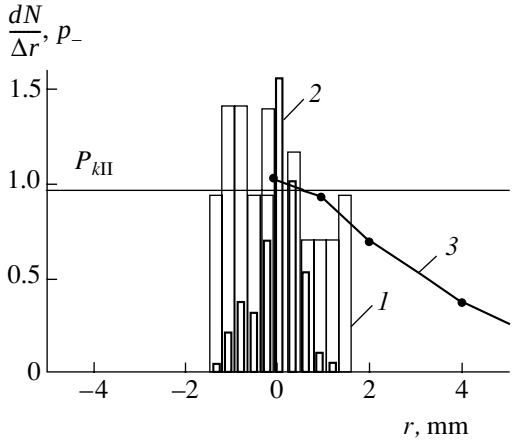

Fig. 4. Distribution of the number of bubbles of the (*1*) first and (*2*) second groups and (*3*) amplitude of the negative pressure phase over the distance from the axis (z = –4.5 mm, observation region $|r| < 1.7$ mm).

The proposed method can make it possible to approach higher threshold parameters in investigations of the strength properties of liquids without application of labor-intensive technologies of multistage purification.

This simple method can be applied in devices for monitoring the purity of liquids to detect technogenic nano- and microparticles in drinking and specially purified water.

ACKNOWLEDGMENTS

This work was supported by the German Academic Exchange Service (DAAD, grant no. A/00/01480), the Russian Foundation for Basic Research (project nos. 00-02-17992, 03-02-17682, 01-02-06444-mas, 02-02-06838-mas, and 03-02-06212-mas), and the US Civilian Research and Development Foundation for the Independent States of the Former Soviet Union (grant no. 1210/1). We are grateful to W. Lauterborn (Universität Göttingen, Göttingen, Germany) for the opportunities of high-speed filming and measurement of pressure and to V.M. Titov, M.E. Topchiyan, S.A. Zhdan, S.F. Urmancheev, and V.E. Dontsov for stimulating discussions.

REFERENCES

1. S. S. Kutateladze and V. E. Nakoryakov, *Heat and Mass Transfer in Liquid–Gas Systems* (Nauka, Novosibirsk, 1984).
2. R. I. Nigmatullin, *Dynamics of Heterogeneous Media* (Nauka, Moscow, 1987).
3. V. K. Kedrinskiĭ, *Hydrodynamics of Explosion: Experiment and Models* (Izd. Sib. Otd. Ross. Akad. Nauk, Novosibirsk, 2000).
4. M. A. Margulis, Usp. Fiz. Nauk **170**, 263 (2000) [Phys. Usp. **43**, 259 (2000)].
5. V. S. Teslenko, G. N. Sankin, and A. P. Drozhzhin, Fiz. Goreniya Vzryva **35**, 125 (1999).
6. A. D. Pernik, *Cavitation Problems* (Sudpromgiz, Leningrad, 1963).
7. A. V. Butenin and B. Ya. Kogan, Opt. Spektrosk. **37**, 1000 (1974).
8. N. F. Bunkin and F. V. Bunkin, Zh. Éksp. Teor. Fiz. **101**, 512 (1992) [Sov. Phys. JETP **74**, 271 (1992)].
9. D. V. Voronin, G. N. Sankin, V. S. Teslenko, *et al.*, Prikl. Mekh. Tekh. Fiz. **44** (1), 22 (2003).
10. J. Staudenraus and W. Eisenmenger, Ultrasonics **31**, 267 (1993).
11. V. S. Teslenko, Pis'ma Zh. Tekh. Fiz. **20** (5), 51 (1994) [Tech. Phys. Lett. **20**, 199 (1994)].
12. I. Sh. Akhatov, O. Lindau, A. Topolnikov, *et al.*, Phys. Fluids **13**, 2805 (2001).
13. V. P. Skripov, *Metastable Liquids* (Nauka, Moscow, 1972).
14. N. F. Bunkin, O. I. Vinogradova, A. I. Kuklin, *et al.*, Pis'ma Zh. Éksp. Teor. Fiz. **62**, 659 (1995) [JETP Lett. **62**, 685 (1995)].
15. R. P. Taleyarkhan, C. D. West, J. S. Cho, *et al.*, Science **295**, 1868 (2002).

Translated by R. Tyapaev

Doklady Physics, Vol. 48, No. 12, 2003, pp. 669–673. Translated from Doklady Akademii Nauk, Vol. 393, No. 4, 2003, pp. 473–477.

MECHANICS

Factorization Method in the Theory of Vibration-Strength Viruses

Academician V. A. Babeshko and O. M. Babeshko

Received August 6, 2003

We develop the theory of vibration-strength viruses (viruses, in what follows) introduced both for ordering sets of various inhomogeneities—inclusions, cracks, defects, strip transmission lines, etc.—in continua independently of their physical properties and for revealing their behavior [1]. Media, not necessarily deformable, can be hydroacoustic, electromagnetic, and thermal, described by systems of linear partial differential equations. Viruses localize physical processes and are responsible for resonances [1, 2].

In this work, we solve the problem for such simple viruses, which can be particularly realized as the set of plane-parallel inclusions, cavity cracks, and their combinations located on parallel planes in a deformable medium [3–6]. Such objects often appear in problems of mechanics, electronics, scattering theory, and ecology. In addition, they were observed in lithospheric plates when American scientists used a Y-3000 heavy mobile vibration seismic source to study the Earth's depths by vibration seismic methods. The first such observation was likely made by Prof. R. Williams, University of Tennessee.

Seismological interest in such objects is motivated by two reasons. First, viruses are strong concentrators of stresses under certain conditions. Their destruction can give rise to the destruction of a large section of a lithospheric plate. This circumstance is possibly responsible for the internal location of earthquake centers. Second, although proper experimental possibilities are absent, we assume that gradual destruction and propagation of cracks such as class-2 viruses (cracks) leads to so-called quiet earthquakes, where high energy is not released and which are associated with the loss of the strength of cracked structures even under low stresses. Thus, invisibly developing under certain stresses and approaching the ground, these sets of cracks can accumulate high elastic energy under other forms of stress and can be manifested as a distinct fracture on the ground. At present, these objects can be observed only by vibration seismic exploration that can determine changes in the dimensions of fractures. To calculate stress concentration in a fracture, it is necessary to develop a theory taking into account both a complex structure of domains occupied by cracks and their location on parallel planes. Analyzing these problems, one can develop a system for prediction of their behavior and control over them. Problems concerning a single inhomogeneity—crack or inclusion—have been studied in detail. At the same time, problems concerning sets of such inhomogeneities are poorly studied due primarily to mathematical difficulties. Viruses can be studied by the factorization method that was considerably modified to this end [7–9].

1. Systems of integral equations for simple viruses of types 1 (set of rigid inclusions) and 2 (set of cracks, terminology introduced in [1]) in bounded, semibounded, and unbounded domains of an isotropic elastic medium, where inhomogeneities are located on parallel planes, were derived in [3–6]. Reducing the boundary conditions if necessary, the systems of integral equations can be represented in the form

$$\sum_{r=1}^{L}\sum_{n=1}^{N_r}\sum_{m=1}^{3}\int\int_{\Omega_{nr}} k^0_{spmr}(x_1-\xi_1, x_2-\xi_2)q^0_{mnr} \times (\xi_1, \xi_2)d\xi_1 d\xi_2 = f^0_{spl}(x_1, x_2),$$
$$x_1, x_2 \in \Omega_{pl}, \quad s = 1, 2, 3, \quad p = 1, 2, \ldots, N_r, \quad l = 1, 2, \ldots, L. \tag{1}$$

Here, for a type-1 virus, q^0_{mnr} is the mth component of an unknown jump of stresses acting on the area Ω_{nr}, which is located on the rth level (plane) and has the number n, and f^0_{spl} is the displacement component specified in accordance with the stress component. For a type-2 virus, the displacement jumps and stress components are replaced with each other.

Kuban State University,
ul. Karla Libknekhta 149, Krasnodar, 350640 Russia
e-mail: babeshko@kubsu.ru

1028-3358/03/4812-0669$24.00

We introduce the Fourier transform

$$\mathbf{V}(\alpha_1, \alpha_2)k(x_1, x_2)$$

$$= \int\int_{R^2} k(x_1, x_2)e^{i\langle \alpha, x\rangle}dx_1dx_2 \equiv K(\alpha_1, \alpha_2),$$

$$\mathbf{V}^{-1}(x_1, x_2)K(\alpha_1, \alpha_2)$$

$$= \frac{1}{4\pi^2}\int\int_{R^2} K(\alpha, \alpha_2)e^{-i\langle \alpha, x\rangle}d\alpha_1 d\alpha_2 \equiv k(x_1, x_2),$$

$$\langle \alpha, x\rangle = \alpha_1 x_1 + \alpha_2 x_2$$

and the matrix function

$$K^0(\alpha_1, \alpha_2) = \{\mathbf{V}(\alpha_1, \alpha_2)k^0_{spmr}(x_1, x_2)\}, \qquad (2)$$

which consists of third-order matrix blocks. The effect of levels on the coefficients is described by exponentials with real and imaginary arguments (for details, see [3–6]).

Integral equations (1) are convenient for transparent description of a virus. For investigation, it is necessary to represent them in another form. We introduce the notation leading to the standard representation of matrices and vectors. United numbering is used for functions on the left- and right-hand sided. For a type-1 virus, we arrange all stress components in a certain sequence as the components of one unknown vector by numbering all levels in succession, regions at levels, and vector components in them if they exist. Similarly, we introduce united numbering for the vector on the right-hand side of the system.

As a result, system (1) can be represented in the form

$$\sum_{r=1}^{R}\int\int_{\Omega_r} k_{mr}(x_1 - \xi_1, x_2 - \xi_2)q_r(\xi_1, \xi_2)d\xi_1 d\xi_2$$
$$= f_m(x_1, x_2), \quad x_1, x_2 \in \Omega_m, \ m = 1, 2, \ldots, R \qquad (3)$$

or in the operator form

$$\mathbf{K}q \equiv \int\int_{\sigma_1\sigma_2} K(\alpha)\mathbf{V}(\alpha_1, \alpha_2)q\exp(-i\langle \alpha, x\rangle)d\alpha = f, \qquad (4)$$
$$q = \{q_r\}, \quad K = \{K_{mr}\}, \quad f = \{f_m\},$$
$$F(\alpha) \equiv F(\alpha_1, \alpha_2), \quad F(x) \equiv F(x_1, x_2).$$

We note that some functions k_{mr} in this notation can be identical for different r values.

A similar method is applied for a type-2 virus.

2. System (3) is considered for an arbitrary anisotropic stratified elastic medium in the presence of possible thermoelectroelastic, magnetostatic, aggressive chemical actions, and other characteristics, which is a more general case than that considered for systems constructed in [3–6].

The elements of the matrix function $K(\alpha_1, \alpha_2)$ are generally analytic functions. They are described by the ratio of analytic functions of two complex variables. For layer blocks, they are ratios of integer functions, and the elements are meromorphic functions.

We assume that the asymptotic behavior of the matrix function $K(\alpha_1, \alpha_2)$ for real γ_k values has the form

$$M(\gamma_1, \gamma_2) = M(\gamma_1)\gamma_2^{-1}[1 + O(\gamma_2^{-1})],$$
$$0 \le \gamma_1 \le 2\pi, \quad \gamma_2 \to \infty, \quad \alpha_1 = \gamma_2\cos\gamma_1, \qquad (5)$$
$$\alpha_2 = \gamma_2\sin\gamma_1,$$
$$M(\gamma_1, \gamma_2) = K(\gamma_2\cos\gamma_1, \gamma_2\sin\gamma_1),$$

which is the case for a type 1 virus.

The elements of the matrix function $M(\gamma_1, \gamma_2)$ can have a finite number of poles $\gamma_2 = \xi_m(\gamma_1)$ for real γ_k values. The determinant of this function can have a finite number of zeros $\gamma_2 = z_n(\gamma_1)$ on the real axis. Integration contours pass around poles according to certain rules described in [10, 11]. Functions q and f belong to a certain space $\mathbf{H}_s$.

In what follows, the approximation of functions with poles on the real axis is treated as the approximation of functions in C that are multiplied by a polynomial having these poles.

Lemma 1 [10, 11]. *The elements of the matrix function $M(\gamma_1, \gamma_2)$ on the real axis can be approximated by meromorphic functions with conservation of real poles and asymptotic behavior* (5). *If system* (3) *is correctly solvable in a certain space $\mathbf{H}_s$, the system with the approximate matrix is also solvable, and the approximation error depends linearly on the errors of approximations on the integration constants δ_1 and δ_2.*

Lemma 2 [12]. *The matrix function $M(\gamma_1, \gamma_2)$ on the real axis can be approximated as*

$$M(\gamma_1, \gamma_2) = M_0(\gamma_1, \gamma_2)\Pi(\gamma_1, \gamma_2),$$

where the elements of the matrix function $M_0(\gamma_1\ \gamma_2)$ are meromorphic functions of the parameter γ_2. The poles of these elements and zeros of the determinant of this function lie beyond a certain band η including the real axis. The elements of the matrix function $\Pi(\gamma_1, \gamma_2)$ are rational functions, whose poles coincide with the poles of the respective elements of the matrix function $M(\gamma_1, \gamma_2)$ in the band η. The zeros of the determinant of the matrix function $\Pi(\gamma_1, \gamma_2)$ coincide with the zeros of the determinant of the matrix function $M_0(\gamma_1\ \gamma_2)$ in the band η.

Let the polynomials $p_1(\gamma_1, \gamma_2)$ and $p_2(\gamma_1, \gamma_2)$ have zeros $\gamma_2 = z_n(\gamma_1)$ and $\gamma_2 = \xi_m(\gamma_1)$, respectively, that can be expanded into Fourier series in the coordinate γ_1. For simplicity, we consider the common case where the

polynomials have even orders and zeros are conjugate; i.e.,

$$z_n^{\pm}(\gamma_1) = \sum_{s=-S}^{S} z_{n,2s+1} e^{i(2s+1)\gamma_1} \pm \sum_{s=-S}^{S} z_{n,2s} e^{i\cdot 2s\gamma_1},$$
$$\xi_n^{\pm}(\gamma_1) = \sum_{s=-S}^{S} \xi_{n,2s+1} e^{i(2s+1)\gamma_1} \pm \sum_{s=-S}^{S} \xi_{n,2s} e^{i\cdot 2s\gamma_1}, \quad (6)$$
$$S \to \infty, \quad 0 \le \gamma_1 \le 2\pi.$$

Lemma 3 [2, 13]. *The rational function* $\dfrac{p_1(\gamma_1, \gamma_2)}{p_2(\gamma_1, \gamma_2)}$ *on the real axis can be approximated by the rational function*

$$\frac{p_1(\alpha_1, \alpha_2, S)}{p_2(\alpha_1, \alpha_2, S)},$$

which is the ratio of polynomials of two complex variables. The approximating polynomials have at least the same number of zeros as the polynomials of the original functions, which merge for $S \to \infty$.

According to the above lemmas, the matrix function $K(\alpha_1, \alpha_2)$ can be represented in the form

$$K = K_0 P, \quad K_0 = \{K_{0pr}(\alpha_1, \alpha_2)\},$$
$$P = \left\{\frac{p_{1rn}(\alpha_1, \alpha_2, S)}{p_{2rn}(\alpha_1, \alpha_2, S)}\right\}. \quad (7)$$

We consider the differential equation generating the characteristic polynomial $p_{1mm}(\alpha_1, \alpha_2, S)$ of the order $2M$:

$$-p_{1mm}(i\partial x_1, i\partial x_2, S)\varphi_m(x_1, x_2) = 0,$$
$$m = 1, 2, \ldots, R, \quad x_1, x_2 \in \Omega_m. \quad (8)$$

The boundary value problem for this equation in the $\mathbf{H}_s(\Omega_m)$ space is obtained with the boundary conditions for derivatives along to the outer normal to the domain boundary, i.e.,

$$\partial^{k-1} n\varphi_m(x) = g_{mk}(x), \quad x \in \partial\Omega_m,$$
$$k = 1, 2, \ldots, M. \quad (9)$$

Solving the boundary value problem by the factorization method [7–9], we obtain the representation

$$p_{1mm}(\alpha_1, \alpha_2, S)\Phi_m(\alpha_1, \alpha_2) = \int_{\partial\Omega_m} \theta_m \equiv \Theta_m. \quad (10)$$

Here, θ_m is the exterior form generated by differential expression (8) and

$$\Phi_m(\alpha_1, \alpha_2) = \int\int_{\Omega_m} \varphi_m(x)\exp(i\langle\alpha, x\rangle)dx.$$

We emphasize that g_{mk}, $k = 1, 2, \ldots, 2M$, on the right-hand side of Eq. (10) are derivatives along to the outer normal to the boundary $\partial\Omega_m$ of orders from zeroth to $2M - 1$ [7]. Therefore, the solution of the boundary value problem for given g_{mk}, $k = 1, 2, \ldots, M$, reduces to the determination of M functions g_{mk}, $k = M + 1, 2, \ldots, 2M$ in terms of the first group of functions [7–9].

Let the inverse operator $\mathbf{K}_0^{-1}$ be constructed for the operator $\mathbf{K}_0$ defined as

$$\mathbf{K}_0\varphi \equiv \int\int_{\sigma_1\sigma_2} K_0(\alpha)\mathbf{V}(\alpha)\varphi\exp(-i\langle\alpha, x\rangle)d\alpha. \quad (11)$$

Various methods of construction of these operators were described, e.g., in [10, 11, 13].

According to the introduced topology, the boundary value problem specified by Eqs. (8) and (9) are considered on two-dimensional orientable manifolds Ω_m with the oriented boundaries $\partial\Omega_m$ [7–9]. Domains Ω_m are located to the left of the boundary $\partial\Omega_m$. When factorizing, they are denoted by the plus sign, while those located to the right from $\partial\Omega_m$, by the minus sign. Domains Ω_m can be bounded, unbounded, and multiply connected with smooth boundaries including those extended to infinity. We apply the concept of the factorization of functions with respect to domains, which was introduced in [7–9], to boundary value problems. We do not discuss the choice and application of a particular form of factorization, classical or generalized, which were discussed in [7–9]. Thus, factorization accompanied by the construction of classes of functions with a support either in or beyond Ω_m will be denoted by

$$\{f(\mathbf{x})\}^{\pm}_{\Omega_m}, \quad \{F(\alpha)\}^{\pm}_{\Omega_m},$$

respectively. The vector component with the number m is denoted as $(\cdot)_m$.

Theorem 1. *The exact or approximate solutions of the system of integral equations* (3) *for a type* 1 *virus have the form*

$$q_m(x) = p_m(x) + \varphi_m(x), \quad m = 1, 2, \ldots, R,$$
$$p_m(x) = \mathbf{V}^{-1}\Pi^{-1}\left\{\left\{\sum_{r=1}^{R}\frac{p_{1mr}\Theta_r}{p_{2mr}p_{1rr}}\right\}^{+}_{\Omega_m} + (\mathbf{K}_0^{-1}f)_m\right\},$$
$$\varphi_m(x) = \left\{\mathbf{V}^{-1}p_{1mm}^{-1}(\alpha_1, \alpha_2, S)\int_{\partial\Omega_m}\theta_m\right\}^{+}_{\Omega_m}; \quad (12)$$
$$\left\{\mathbf{V}^{-1}p_{1mm}^{-1}(\alpha_1, \alpha_2, S)\int_{\partial\Omega_m}\theta_m\right\}^{-}_{\Omega_m} = 0,$$
$$\left\{\mathbf{V}^{-1}\Pi^{-1}\left\{\left\{\sum_{r=1}^{R}\frac{p_{1mr}\Theta_r}{p_{2mr}p_{1rr}}\right\}^{+}_{\Omega_m} + (\mathbf{K}_0^{-1}f)_m\right\}\right\}^{-}_{\Omega_m} = 0.$$

The last two relations are normally solvable systems of integral equations. They serve for the determination of unknown boundary functions $g_{km}(x)$, $k = 1, 2, \ldots, 2M$ and $m = 1, 2, \ldots, R$. Their number coincides with the number of unknowns. They are regularized, i.e., represented in the form of second-kind integral equations, such as it was done in [7–9].

Let us consider the case of a type-2 virus, which is somewhat more difficult than the case of a type-1 virus, because it has additional conditions. Inhomogeneities are sets of cracks that have arbitrary shapes in plan view and are located on parallel planes, i.e., levels. The system of integral equations has form (3), where the asymptotic behavior of coefficients at infinity has the form

$$M(\gamma_1, \gamma_2) = M(\gamma_1)\gamma_2[1 + O(\gamma_2^{-1})], \quad \gamma_2 \to \infty,$$

and the unknown vector components must vanish at the boundaries of their domains; i.e.,

$$q_m(x) = 0, \quad x \in \partial\Omega_m, \quad m = 1, 2, \ldots, R.$$

A certain transformation reduces the solution of the system for a type-2 virus to the case considered above. To this end, we represent system (4) in the form

$$\mathbf{K}_1 q \equiv \int\limits_{\sigma_1\sigma_2}\int (\alpha_1^2 + \alpha_2^2 + B^2)^{-1} K(\alpha)\mathbf{V}(\alpha_1, \alpha_2)q \times \exp(-i\langle\alpha, x\rangle)d\alpha = f_1 + g, \quad B > 0,$$

where the asymptotic behavior of the elements of the new matrix function has form (5). The components of the vector on the right-hand side are solutions of the boundary value problems

$$(-\partial^2 x_1 - \partial^2 x_2 + B^2)g_m = 0,$$
$$g_m(x) = g_m^0, \quad x \in \partial\Omega_m, \quad g = \{g_m\} \in \mathbf{H}_s$$

in the domains Ω_m. These solutions can be constructed by the factorization method [7–9]. The function f_1 is any partial solution of this differential equation with the right-hand side f. The functions g_m^0 must be determined.

Theorem 2. *The solution of the system of integral equations for a type-2 virus has the form*

$$q_m(x) = p_m(x) + \varphi_m(x), \quad m = 1, 2, \ldots, R,$$
$$p_m(x) = \mathbf{V}^{-1}\Pi^{-1}\left\{\left\{\sum_{r=1}^{R}\frac{p_{1mr}\Theta_r}{p_{2mr}p_{1rr}}\right\}_{\Omega_m}^{+} + (\mathbf{K}_{10}^{-1}(f_1 + g))_m\right\}, \quad (13)$$

$$\varphi_m(x) = \left\{\mathbf{V}^{-1}p_{1mm}^{-1}(\alpha_1, \alpha_2, S)\int\limits_{\partial\Omega_m}\theta_m\right\}_{\Omega_m}^{+},$$

$$\left\{\mathbf{V}^{-1}p_{1mm}^{-1}(\alpha_1, \alpha_2, S)\int\limits_{\partial\Omega_m}\theta_m\right\}_{\Omega_m}^{-} = 0;$$

$$\left\{\mathbf{V}^{-1}\Pi^{-1}\left\{\left\{\sum_{r=1}^{R}\frac{p_{1mr}\Theta_r}{p_{2mr}p_{1rr}}\right\}_{\Omega_m}^{+} + (\mathbf{K}_{10}^{-1}(f_1 + g))_m\right\}\right\}_{\Omega_m}^{-} = 0,$$

$$p_m(x) + \varphi_m(x) = 0, \quad x \in \partial\Omega_m.$$

The representation $K = K_{10}P$ is an analogue of representation (7) for this problem.

The last system of equations serves for the determination of the functions g_m^0 at the boundaries of the domains Ω_m.

The solution for the mixed virus combining inclusions and cracks is constructed similarly.

Systems of one-dimensional integral equations in theorems 1 and 2 reduce by the tangent fiber bundle at $\partial\Omega_m$ to second-kind integral equations with a smooth kernel and admit various discretizations.

Note. We do not discuss numerous methods facilitating the study of problems by these methods. We only note that the factorization method is more general than the method of fictitious absorption, because it allows, in contrast to the latter, the investigation of mixed problems not only for convex domains. In particular, a problem for a plane with a removed convex domain cannot be solved by the method of fictitious absorption but can be solved by the factorization method.

ACKNOWLEDGMENTS

This work was supported by the Ministry of Education of the Russian Federation (project nos. E02-4.0-190, Z/N-241, 379, 380, GN-374); the Russian Foundation for Basic Research (project no. 03-01-00694); the R2003YuG Program, the Russian Foundation for Basic Research (project nos. 03-01-96537, 03-01-96527, 03-01-96519, 03-01-96584); the "Integratsiya" Program (project no. B0121); and the US Civilian Research and Development Foundation for the Independent States of the Former Soviet Union (grant no. REC-004).

REFERENCES

1. V. A. Babeshko, Izv. Ross. Akad. Nauk, Mekh. Tverd. Tela, No. 3, 5 (2000).

2. V. A. Babeshko and P. V. Syromyatnikov, Dokl. Akad. Nauk **367**, 186 (1999) [Dokl. Phys. **44**, 460 (1999)].
3. V. A. Babeshko, R. Williams, A. V. Pavlova, and S. V. Ratner, Dokl. Akad. Nauk **382**, 625 (2002) [Dokl. Phys. **47**, 141 (2002)].
4. V. A. Babeshko, A. V. Pavlova, S. V. Ratner, and R. Williams, Dokl. Akad. Nauk **386**, 43 (2002) [Dokl. Phys. **47**, 677 (2002)].
5. V. A. Babeshko, V. V. Buzhan, and R. Williams, Dokl. Akad. Nauk **382**, 765 (2002) [Dokl. Phys. **47**, 156 (2002)].
6. V. A. Babeshko, V. V. Buzhan, and R. Williams, Dokl. Akad. Nauk **385**, 332 (2002) [Dokl. Phys. **47**, 538 (2002)].
7. V. A. Babeshko and O. M. Babeshko, Dokl. Akad. Nauk **389**, 184 (2003) [Dokl. Phys. **48**, 134 (2003)].
8. V. A. Babeshko and O. M. Babeshko, Dokl. Akad. Nauk **392**, 185 (2003) [Dokl. Phys. **48**, 512 (2003)].
9. V. A. Babeshko and O. M. Babeshko, Dokl. Akad. Nauk **392**, 767 (2003) [Dokl. Phys. **48**, 594 (2003)].
10. I. I. Vorovich and V. A. Babeshko, *Mixed Dynamic Problems of Elasticity Theory in Unbounded Domains* (Nauka, Moscow, 1979).
11. V. A. Babeshko, *Generalized Factorization Method in Spatial Mixed Dynamic Problems of Elasticity Theory* (Nauka, Moscow, 1984).
12. V. A. Babeshko, Dokl. Akad. Nauk **335**, 55 (1994) [Phys. Dokl. **39**, 186 (1994)].
13. V. A. Babeshko, E. V. Glushkov, and Zh. F. Zinchenko, *Dynamics of Inhomogeneous Linearly Elastic Media* (Nauka, Moscow, 1984).

Translated by R. Tyapaev

Doklady Physics, Vol. 48, No. 12, 2003, pp. 674–678. Translated from Doklady Akademii Nauk, Vol. 393, No. 4, 2003, pp. 478–482.

MECHANICS

On the Condition of Rigidity in the Joukowski Sense for Trajectories of Dynamical Systems

O. V. Druzhinina and A. A. Shestakov

Presented by Academician V.V. Rumyantsev July 1, 2003

Received July 4, 2003

Fundamental results on the stability of motion and rigidity of trajectories have been established, respectively, by A.M. Lyapunov [1] and N.E. Joukowski [2]. Russian and foreign scientists contributed greatly to the development of theories of both stability and rigidity [3–10]. The problem on bundles of rigid and nonrigid trajectories of a mechanical system with two degrees of freedom was first analyzed in [11]. In this paper, we consider rigidity of trajectories of a dynamical system described by a moving Frenet n-hedron in n-dimensional Euclidean space. We also find conditions for the existence of bundles of asymptotically rigid and nonrigid trajectories of the dynamical system described by the time-independent differential equation

$$\frac{dx}{dt} = g(x), \quad x \in R^n, \quad t \in I ::= [t_0, +\infty). \qquad (1)$$

In particular, we construct sets M^+ and M^- of the phase space such that only asymptotically rigid and nonrigid semitrajectories pass through all points of M^+ and of M^-, respectively.

We consider the positive semitrajectory $C^+(p_0)$ of motion $x = \varphi(t)$, $\varphi(t_0) = p_0$ of dynamical system (1), where g is a continuously differentiable function of $x = (x_1, x_2, \ldots, x_n) \in R^n$. In what follows, the semitrajectory $C^+(p_0)$ and the positive semitrajectory $C^+(q_0)$ passing through a point $q_0 \neq p_0$ close to the point p_0 are referred to as a base (unperturbed) and roundabout (perturbed) semitrajectory of Eq. (1), respectively. Motions along the base and roundabout trajectories are described by the functions $p(t)$ and $q(t)$, with $p(t_0) = p_0$ and $q(t_0) = q_0$.

Russian Open State Technical University of Railway Transport, ul. Chasovaya 22/2, Moscow, 125808 Russia

Let $\bar{p}(t)$ be the point at which the base trajectory intersects the hyperplane perpendicular to it and passing through a point $q(t)$ of the roundabout trajectory.

The mappings $p(t) \to q(t)$ and $\bar{p}(t) \to q(t)$, which are called isochronous and normal (orthogonal) mappings, are bases for the definition of stability in the Lyapunov and Joukowski sense, respectively.

We now introduce notions of rigidity and nonrigidity in the Joukowski sense for the base semitrajectory $C^+(p_0)$ of system (1). Let e_0 be the vector tangent to the semitrajectory at the point $\bar{p}(t)$. The distance along the curve from the point p_0 to the point $\bar{p}(t)$ is denoted by $s(t)$, i.e., $s(t) = p_0\bar{p}$. The use of the distance $s(t)$ leads to a reparametrization of the semitrajectory $C^+(p_0)$. Let $(e_1, e_2, \ldots, e_{n-1})$ be a set of $n-1$ linearly independent normals to the semitrajectory $C^+(p_0)$ at the point $\bar{p}(t)$. If the curvatures of this semitrajectory are nonzero along the normals, the set $(e_1, e_2, \ldots, e_{n-1})$ is unambiguously defined [7], which is furthermore taken into account. The set $(e_0, e_1, \ldots, e_n)$ and the corresponding coordinates $(s, u_1, u_2, \ldots, u_{n-1})$ are referred to as a moving Frenet n-hedron and moving Frenet coordinates along the base semitrajectory $C^+(p_0)$, respectively.

It is easy to verify that differential equation (1) can be written out in the moving Frenet coordinates $(s, u_1, u_2, \ldots, u_{n-1})$ as

$$\frac{ds}{dt} = \sum_{j=0}^{n-1} b_j u_j + U_0(s, u), \qquad (2)$$

$$\frac{du}{dt} = Bu + U(s, u), \quad B = \|b_{ij}\|, \quad i, j = 1, 2, \ldots, n-1, \qquad (3)$$

where $u = (u_1, u_2, \ldots, u_{n-1})$. The quantities b_{0j} and b_{ij} are functions of the coordinates of the representation point

1028-3358/03/4812-0674$24.00

$p(t)$ for the base semitrajectory $C^+(p_0)$. They are determined by the formulas

$$b_{00} = \frac{d|g(\varphi(t, p_0))|}{ds} = \frac{1}{|g(\varphi(t, p_0))|^2} p_{ij} g_i g_{ji},$$

$$b_{01} = \frac{|g(\varphi(t, p_0))|}{\rho_1} + \frac{\partial |g(\varphi(t, p_0))|}{\partial x_j} \gamma_{j1},$$

$$b_{0s} = \frac{\partial |g(\varphi(t, p_0))|}{\partial x_j} \gamma_{js}, \quad s = 2, 3, \ldots, n-1,$$

$$b_{ms} = p_{kj} \gamma_{km} \gamma_{js}, \quad m = 1, 2, \ldots, n-1,$$
$$s = 1, 2, \ldots, n-1, \quad s \neq m-1, \quad s \neq m+1, \tag{4}$$

$$b_{m, m-1} = -\frac{|g(\varphi(t, p_0))|}{\rho_m} + p_{ij} \gamma_{im} \gamma_{j, m-1},$$

$$m = 2, 3, \ldots, n-1,$$

$$b_{m, m+1} = -\frac{|g(\varphi(t, p_0))|}{\rho_m} + p_{ij} \gamma_{i, m-1} \gamma_{im},$$

$$m = 1, 2, \ldots, n-2.$$

Here, γ_{ij} denote the direction cosines between the $x_1, x_2, \ldots, x_n$ axes and the $z_0, z_1, \ldots, z_n$ axes in the directions of the unit tangent vector and of the unit vectors $e_1, e_2, \ldots, e_{n-1}$ perpendicular to the semitrajectory $C^+(p_0)$ of the motion $\varphi(t, p_0)$. The quantity ρ_i corresponds to the radius of curvature along the normal e_i ($i = 1, 2, \ldots, n-1$). As $u_1 \to 0, u_2 \to 0, \ldots, u_{n-1} \to 0$, the order of smallness of the functions $U_j(s, u_1, u_2, \ldots, u_{n-1})$ is higher than the first one. In this case,

$$U_i(s, 0, \ldots, 0) = 0, \quad i = 1, 2, \ldots, n-1. \tag{5}$$

In what follows, we assume that the quantities b_{ij} and the terms $U_j(s, u_1, u_2, \ldots, u_{n-1}), j = 0, 1, 2, \ldots, n-1$, of higher order of smallness are continuous functions of time t and bounded in modulus within the range of variables under consideration. Moreover, we assume that the functions $U_i(s, u)$ tends to zero uniformly with respect to $s \geq 0$:

$$U_i(s, u) = o(|u|), \quad i = 1, 2, \ldots, n-1, \quad u \to 0. \tag{6}$$

As follows from (6), there exists a continuous scalar function $\mu(s, u)$ such that

$$U_i(s, u) = |u| \mu(s, u), \quad i = 1, 2, \ldots, n-1, \tag{7}$$

as both u and $\mu(s, u)$ tend to zero uniformly with respect to $s \geq 0$.

Definition 1. A base semitrajectory $C^+(p_0)$ of system (1) is referred to as (asymptotically) rigid in the Joukowski sense if the trivial solution $u_1 = u_2 = \ldots = u_{n-1} = 0$ of differential equation (3) is (asymptotically) stable in the Lyapunov sense with respect to the function $u_1^2 + u_2^2 + \ldots + u_{n-1}^2$.

Definition 2. A base semitrajectory $C^+(p_0)$ of system (1) is referred to as nonrigid in the Joukowski sense if it is not rigid in the Joukowski sense.

Definition 3. A base semitrajectory $C^+(p_0)$ of system (1) is referred to as exponentially rigid in the Joukowski sense if the solution $u = 0$ of Eq. (3) is exponentially stable with respect to $u_1^2 + u_2^2 + \ldots + u_{n-1}^2$, i.e., if there exists a number $\omega > 0$ such that, for each $\varepsilon > 0$, a number $\delta(\varepsilon) > 0$ can be found such that the solution $u(t) = (u_1(t), u_2(t), \ldots, u_{n-1}(t))$ of Eq. (3) under the initial condition $u(t_0)| < \delta(\varepsilon)$ satisfies the inequality

$$|u(t)| < \varepsilon \exp\{-\omega(t - t_0)\}, \text{ for } t > t_0.$$

Definitions 1–3 are specific cases of those given in [12–14], applicable to Eq. (3).

According to Definitions 1 and 2, the rigidity in the Joukowski sense for the semitrajectory $C^+(p_0)$ of the solution $\varphi(t, p_0)$ follows from the stability in the Lyapunov sense for this solution, and the instability in the Lyapunov sense for the solution $\varphi(t, p_0)$ follows from the nonrigidity in the Joukowski sense for the semitrajectory $C^+(p_0)$. The rigidity in the Joukowski sense for the semitrajectory $C^+(p_0)$ does not guarantee stability in the Lyapunov sense for the solution $\varphi(t, p_0)$.

Definition 4. A base semitrajectory $C^+(p_0)$ of system (1) is referred to as steady-state if all quantities b_{ij} entering into relations (4) are constant along this trajectory.

If none of the radii of curvature is equal to zero along the normals, then the definition of steady-state motion is independent of the choice of these normals.

It is worth noting that an arbitrary semitrajectory steady-state in the Whitteker sense [7] is steady-state in the sense of Definition 4.

The following theorems are valid.

Theorem 1. *Let $C^+(p_0)$ be a steady-state base semitrajectory of dynamical system* (1). *If the real part of at least one of roots of the characteristic equation*

$$\det(B - \lambda E) = 0, \quad B = \|b_{ij}\|, \quad i, j = 1, 2, \ldots, n-1 \tag{8}$$

[*where E is the unit matrix and the quantities a and b_{ij} are defined in Eq.* (4)] *is positive, then the semitrajectory $C^+(p_0)$ of dynamical system* (1) *is not rigid in the Joukowski sense.*

Let the real part of at least one of the roots of Eq. (8) be positive. In this case, the solution $u_1 = u_2 = \ldots = u_{n-1} = 0$ of Eq. (3) is unstable in the Lyapunov sense and, therefore, the semitrajectory $C^+(p_0)$ is not rigid in the Joukowski sense.

Theorem 2. *Let $C^+(p_0)$ be a steady-state base semitrajectory of dynamical system* (1). *In this case, the semitrajectory $C^+(p_0)$ is exponentially rigid in the*

Joukowski sense if and only if the real parts of all roots of characteristic equation (8) *are negative.*

Proof. Let the real parts of all roots of Eq. (8) be negative. In this case, the solution $u = 0$ of Eq. (3) is exponentially stable in the Lyapunov sense, i.e., there exist numbers $c > 0$, $\delta > 0$, and $\omega > 0$ such that any solution $u(t)$ of Eq. (3) satisfies the inequality

$$|u(t_0)| \le c|u(0)|\exp\{-\omega(t, t_0)\} \quad \forall t > t_0.$$

According to Definition 3, the semitrajectory $C^+(p_0)$ is exponentially rigid in the Joukowski sense.

Let the solution $u = 0$ of Eq. (3) be exponentially stable in the Lyapunov sense. In this case, the semitrajectory $C^+(p_0)$ of a motion $\varphi(t, p_0)$ is exponentially rigid in the Joukowski sense. Indeed, substituting $v = u\exp(\omega t)$ into Eq. (3), with ω given in Definition 3, we arrive at

$$\frac{dv}{dt} = Av + V(s, v), \quad A ::= B - \omega E, \tag{9}$$

where $V(s, v) ::= |v|\mu(s, e^{-\omega t}v)$ and $\mu(s, u)$ is a scalar function satisfying Eq. (7). It is evident that the function $V(s, v)$ meets the condition

$$V(s, v) = o(|v|) \text{ as } v \text{ tends to zero uniformly with respect to } t \ge 0. \tag{10}$$

Let $\varepsilon > 0$ be a given number. Then, for an arbitrary $t_0 \ge 0$, there exists the number $\delta = \delta(\varepsilon, t_0) > 0$ such that the solution $u(t)$ of Eq. (3) under $|u(t_0)| < \delta(\varepsilon, t_0)$ satisfies the inequality

$$|u(t_0)| < \varepsilon\exp(-\omega t_0)\exp-\omega(t - t_0), \quad \forall t \ge t_0,$$

and, consequently,

$$|u(t_0)| < \varepsilon\exp(-\omega t), \quad \forall t \ge t_0.$$

We assume that $v(t)$ is the solution of Eq. (9), such that $|v(t_0)| < \delta$. It is evident that

$$|u(t_0)|\exp(\omega t_0) < \delta.$$

In this case,

$$|u(t)| < \varepsilon\exp(-\omega t), \quad \forall t \ge t_0,$$

i.e.,

$$|v(t)|\exp(-\omega t) < \varepsilon\exp(-\omega t_0), \quad \forall t \ge t_0.$$

Therefore, the solution $v = 0$ of Eq. (9) is stable in the Lyapunov sense. We then use the following statement, which can easily be proved. Let the function V in Eq. (9) satisfy condition (10), let A be a constant matrix, and let the solution $v = 0$ of Eq. (9) be stable in the Lyapunov sense. In this case, the real parts of all eigenvalues of the matrix A are nonnegative. Indeed, we assume that the real part of one of the eigenvalues of matrix A is positive. The perturbation $V(s, v)$ satisfies condition (10). Therefore, according to the Lyapunov theorem on the instability in the first approximation, the solution $v = 0$ of Eq. (9) is unstable as $t \to +\infty$, which is contradictory to the hypothesis of this theorem. In this case, the matrix A is semistable, i.e., the real parts of all its eigenvalues are nonpositive. Therefore, all eigenvalues of the matrix B are smaller than the negative number $-\omega$. Thus, Theorem 2 is proved.

We now pass to consideration of conditions under which the unsteady semitrajectory $C^+(p_0)$ is not rigid or is asymptotically rigid in the Joukowski sense.

The following theorems are valid.

Theorem 3. *Let there exist the constants* $c_i \ne 0$, $i = 1, 2, \ldots, n-1$, *such that*

$$\Delta_1 > c_1^2, \quad \frac{\Delta_2}{\Delta_1} > c_2^2, \ldots, \frac{\Delta_{n-1}}{\Delta_{n-2}} > c_{n-1}^2 \quad \forall t \ge t_0, \tag{11}$$

where the quantities Δ_i, $i = 1, 2, \ldots, n-1$, *considered as functions of time, are determined by the formulas*

$$\Delta_1 = b_{11}, \quad \Delta_{k-1} \begin{vmatrix} b_{11} & b_{12} & \ldots & b_{1,k-1} \\ \ldots & \ldots & \ldots & \ldots \\ b_{1,k-1} & b_{k-1,2} & \ldots & b_{k-1,k-1} \end{vmatrix},$$

$$k = 3, \ldots, n.$$

In this case, the base semitrajectory $C^+(p_0)$ *of dynamical system* (1) *is not rigid in the Joukowski sense.*

Theorem 4. *Let there exist the constants* $c_i \ne 0$, $i = 1, 2, \ldots, n-1$ *such that*

$$\Delta_1 < -c_1^2, \quad \frac{\Delta_2}{\Delta_1} < -c_2^2, \ldots, \frac{\Delta_{n-1}}{\Delta_{n-2}} < -c_{n-1}^2 \quad \forall t \ge t_0. \tag{12}$$

In this case, the base semitrajectory $C^+(p_0)$ *of dynamical system* (1) *is asymptotically rigid in the Joukowski sense.*

Proof. Theorem 3 and 4 are proved by the method of Lyapunov functions, with $V = u_1^2 + u_2^2 + \ldots + u_{n-1}^2$ taken as a Lyapunov function.

The asymptotic rigidity in the Joukowski sense for the semitrajectory $C^+(p_0)$ of a motion $\varphi(t, p_0)$ of dynamical system (1) does not result in the asymptotic stability in the Lyapunov sense for the motion $\varphi(t, p_0)$. However, the following theorem holds.

Theorem 5. *Let* (1) *the semitrajectory* $C^+(p_0)$ *of a motion* $\varphi(t, p_0)$ *of dynamical system* (1) *be asymptotically rigid in the Joukowski sense and* (2) *let the zero solution of Eq.* (2) *be asymptotically stable in the Lyapunov sense with respect to the function* s^2, *provided that* $u_1 = u_2 = \ldots = u_{n-1} = 0$. *In this case the motion* $\varphi(t, p_0)$ *of system* (1) *is asymptotically stable in the Lyapunov sense.*

As follows from Theorem 5, it is advisable to introduce the notion of the longitudinal rigidity for a semitrajectory $C^+(p_0)$ of system (1).

Definition 5. A semitrajectory $C^+(p_0)$ of system (1) is referred to as (asymptotically) longitudinally rigid if the solution $s = 0$ of Eq. (2) is (asymptotically) stable in

the Lyapunov sense with respect to the function s^2, provided that $u_1 = u_2 = \ldots = u_{n-1} = 0$.

By virtue of Definition 5, the study of the longitudinal rigidity reduces to the analysis of the stability in the Lyapunov sense for the solution $s = 0$ of the scalar differential equation

$$\frac{ds}{dt} = b_{00}s + U_0(s, 0, 0, \ldots, 0).$$

Because of this, the asymptotic rigidity in the Joukowski sense for a semitrajectory is below referred to as transverse asymptotic rigidity. Therefore, we reformulate Theorem 5 as follows: *if a semitrajectory of dynamical system* (1) *is both longitudinally and transversely asymptotically rigid, then it is asymptotically stable in the Lyapunov sense.*

If the set of the initial conditions under which a semitrajectory is longitudinally (transversely) rigid is empty, this semitrajectory can be referred to as completely nonrigid. It is evident that if a semitrajectory $C^+(p_0)$ of the dynamical system is completely nonrigid, it is unstable in the Lyapunov sense.

We define sets $A_1, A_2, \ldots, A_{n-1}$ in the x-space, with $\Delta_1 > 0, \Delta_2 > 0, \ldots, \Delta_{n-1} > 0$, and sets $B_1, B_2, \ldots, B_{n-1}$, with $\Delta_1 < 0, \Delta_2 < 0, \ldots, \Delta_{n-1} < 0$. We also define the sets

$$\begin{aligned} M^+ &::= A_1 \cap A_2 \cap \ldots \cap A_{n-1}, \\ M^- &::= B_1 \cap B_2 \cap \ldots \cap B_{n-1}. \end{aligned} \tag{13}$$

The following theorems are valid.

Theorem 6. *Let a base semitrajectory $C^+(p_0)$ of dynamical system* (1) *belong to M^+, i.e., $C^+(p_0) \subset M^+$, and let*

$$\inf_{C^+(p_0)}\left(\Delta_1, \frac{\Delta_2}{\Delta_1}, \ldots, \frac{\Delta_{n-1}}{\Delta_n}\right) = m > 0. \tag{14}$$

In this case, the base semitrajectory $C^+(p_0)$ is not rigid in the Joukowski sense.

Theorem 7. *Let a base semitrajectory $C^+(p_0)$ of dynamical system* (1) *belong to M^-, i.e., $C^+(p_0) \subset M^+$, and let*

$$\sup_{C^+(p_0)}\left(\Delta_1, \frac{\Delta_2}{\Delta_1}, \ldots, \frac{\Delta_{n-1}}{\Delta_n}\right) = l < 0. \tag{15}$$

In this case, the base semitrajectory $C^+(p_0)$ is asymptotically rigid in the Joukowski sense.

Theorems 6 and 7 are corollaries of Theorems 3 and 4, respectively.

Thus, for all points of M^- (M^+), the phase bundles of the trajectories contract (expand) monotonically when their parameter increases.

Example. We now consider a dynamical system described by the linear differential equation in the R^2 plane:

$$\frac{dx}{dt} = Ax, \quad x = (x_1, x_2), \quad A = \begin{Vmatrix} a & b \\ c & d \end{Vmatrix}. \tag{16}$$

The corresponding determinant has the form

$$\begin{aligned} \Delta_1 &= \begin{vmatrix} 0 & ax_1 + bx_2 & cx_1 + dx_2 \\ ax_1 + bx_2 & a & b + c \\ cx_1 + dx_2 & b + c & d \end{vmatrix} \\ &= \alpha x_1^2 + 2\beta x_1 x_2 + \gamma x_2^2, \end{aligned} \tag{17}$$

where

$$\alpha = a(c^2 + 2bc - ad), \quad \beta = \frac{1}{2}d(b^2 + 2bc - ad),$$
$$\text{and } \gamma = 2bc(b + c).$$

The set M^- of all the points $(x_1, x_2) \in R^2$, for which

$$\Delta_1 = \alpha x_1^2 + 2\beta x_1 x_2 + \gamma x_2^2 < 0,$$

defines the bundle of asymptotically rigid semitrajectories of Eq. (16).

The inequalities

$$\alpha > 0, \quad \begin{vmatrix} \alpha & \gamma \\ \gamma & \beta \end{vmatrix} < 0 \tag{18}$$

are the necessary and sufficient conditions of negative definiteness of the quadratic form $\alpha x_1^2 + 2\beta x_1 x_2 + \gamma x_2^2$.

Substituting the expressions for α, β, and γ into (18), we obtain the conditions determining the bundle of asymptotically rigid semitrajectories of Eq. (16). It is easy to verify that these conditions have the form

$$a(c^2 + 2abc - ad) > 0,$$
$$\frac{1}{2}ad(c^2 + 2bc - ad)(b^2 + 2bc - ad)$$
$$- 4b^2c^2(b + c)^2 < 0.$$

ACKNOWLEDGMENTS

We are sincerely grateful to Academician V.V. Rumyantsev for his attention to this work.

REFERENCES

1. A. M. Lyapunov, *The General Problem of the Stability of Motion* (Kharkovsk. Mat. Obshchestvo, Kharkov, 1892; Taylor & Francis, London, 1992).
2. N. E. Joukowski, Uchen. Zap. Mosk. Univ., Otd. Fiz.-Mat., No. 4, 1 (1882).
3. N. G. Chetaev, *Papers on Analytical Mechanics: Stability of Motion* (Akad. Nauk SSSR, Moscow, 1962).
4. V. V. Rumyantsev and A. S. Oziraner, *Stability and Stabilization of Motion with Respect to a Part of Variables* (Nauka, Moscow, 1987).
5. V. I. Vorotnikov and V. V. Rumyantsev, *Stability and Control of Coordinates Concerning a Part of the Phase Vector in Dynamical Systems: Theory, Methods and Applications* (Nauchn. Mir, Moscow, 2001).
6. V. V. Rumyantsev, Diff. Uravneniya **19**, 739 (1983).
7. J. L. Synge and A. Schild, *Tensor Calculus* (Univ. Toronto Press, Toronto, 1949; Inostrannaya Literatura, Moscow, 1947).
8. M. Sh. Aminov, Tr. Kazan. Aviats. Inst. **24**, 3 (1949).
9. V. I. Zubov, *Dynamics of Controlled Systems* (Vysshaya Shkola, Moscow, 1982).
10. G. A. Leonov and D. V. Ponomarenko, Izv. Vyssh. Uchebn. Zaved. Mat., No. 4, 88 (1993).
11. V. V. Stepanov, Astron. Zh. **13**, 435 (1936).
12. O. V. Druzhinina, Dokl. Akad. Nauk **355**, 51 (1997) [Phys. Dokl. **42**, 374 (1997)].
13. O. V. Druzhinina and V. V. Rumyantsev, Dokl. Akad. Nauk **355**, 476 (1997) [Phys. Dokl. **42**, 433 (1997)].
14. O. V. Druzhinina and A. A. Shestakov, Dokl. Akad. Nauk **384**, 52 (2002) [Dokl. Phys. **47**, 382 (2002)].

Translated by V. Chechin

Doklady Physics, Vol. 48, No. 12, 2003, pp. 679–684. Translated from Doklady Akademii Nauk, Vol. 393, No. 4, 2003, pp. 483–488.

MECHANICS

Effect of Small Dissipative and Gyroscopic Forces on the Stability of Nonconservative Systems

A. P. Seĭranyan* and O. N. Kirillov**

Presented by Academician S.S. Grigoryan July 28, 2003

Received July 30, 2003

We analyze the effect of small forces proportional to the generalized velocity vector on the stability of a linear autonomous mechanical system with nonconservative positional forces. It is known that arbitrarily small dissipation generally destabilizes a nonconservative system [1–5]. Necessary and sufficient conditions on the matrix of dissipative and gyroscopic forces under which the system is asymptotically stable are obtained. The two-dimensional system is studied in detail. The problem of the stability of the Ziegler–Herrmann–Jong pendulum is considered as a mechanical example.

1. We consider a linear mechanical system with nonconservative positional forces and small forces proportional to the velocity vector:

$$\mathbf{M}\ddot{\mathbf{q}} + \varepsilon\mathbf{D}\dot{\mathbf{q}} + \mathbf{A}\mathbf{q} = 0, \tag{1}$$

where $\mathbf{M}$, $\mathbf{D}$, and $\mathbf{A}$ are constant real $m \times m$ matrices determining inertial, dissipative, and gyroscopic along with nonconservative positional forces, respectively; $\varepsilon \geq 0$ is the small parameter, $\mathbf{q}$ is the generalized coordinate vector, and the dot denotes the time differentiation. The matrix $\mathbf{M}$ is assumed nonsingular.

Substituting $\mathbf{q} = \mathbf{u}e^{\lambda t}$, we arrive at the eigenvalue problem

$$(\mathbf{M}\lambda^2 + \varepsilon\mathbf{D}\lambda + \mathbf{A})\mathbf{u} = 0. \tag{2}$$

Eigenvalues $\lambda_1, \lambda_2, \ldots, \lambda_{2m}$ are determined from the characteristic equation

$$\det(\mathbf{M}\lambda^2 + \varepsilon\mathbf{D}\lambda + \mathbf{A}) = 0. \tag{3}$$

We now consider system (1) in the absence of forces proportional to the velocity vector ($\varepsilon = 0$). This system is called the circulatory system [1, 2]. In this case, as follows from Eq. (3), if λ is an eigenvalue, $-\lambda$, $\bar{\lambda}$, and $-\bar{\lambda}$ are also eigenvalues. Therefore, the circulatory system is stable (not asymptotically) if and only if all eigenvalues $\pm i\omega_j$, $\omega_j \geq 0_j$ are imaginary and semisimple. This means that the number r of independent eigenvectors corresponding to an eigenvalue is equal to its algebraic multiplicity k. When $r < k$, the general solution of system (1) contains secular terms proportional to $t^\alpha e^{\lambda t}$, $\alpha \leq k - 1$ (instability). Thus, the system having a pair of algebraically double eigenvalues $\pm i\omega_0$, $\omega_0 > 0$ with one eigenvector, where other eigenvalues are imaginary and simple, corresponds to the boundary between the regions of stability and instability (flutter) [6]. Let us analyze this case in more detail.

The right ($\mathbf{u}_0$, $\mathbf{u}_1$) and left ($\mathbf{v}_0$, $\mathbf{v}_1$) eigenvectors and adjoint vectors corresponding to the double eigenvalue $\lambda_0 = i\omega_0$ are determined from the equations [7, 8]

$$\begin{aligned}(\mathbf{A} - \omega_0^2\mathbf{M})\mathbf{u}_0 &= 0,\\ (\mathbf{A} - \omega_0^2\mathbf{M})\mathbf{u}_1 &= -2i\omega_0\mathbf{M}\mathbf{u}_0,\end{aligned} \tag{4}$$

$$\begin{aligned}\mathbf{v}_0^{\mathrm{T}}(\mathbf{A} - \omega_0^2\mathbf{M}) &= 0,\\ \mathbf{v}_1^{\mathrm{T}}(\mathbf{A} - \omega_0^2\mathbf{M}) &= -2i\omega_0\mathbf{v}_0^{\mathrm{T}}\mathbf{M}.\end{aligned} \tag{5}$$

In addition, they are related as

$$\mathbf{v}_0^{\mathrm{T}}\mathbf{M}\mathbf{u}_0 = 0, \quad \mathbf{v}_0^{\mathrm{T}}\mathbf{M}\mathbf{u}_1 = \mathbf{v}_1^{\mathrm{T}}\mathbf{M}\mathbf{u}_0 \neq 0. \tag{6}$$

The vectors $\mathbf{u}_0$, $\mathbf{u}_1$, $\mathbf{v}_0$, and $\mathbf{v}_1$ are defined up to arbitrary constants. Since the matrix $\mathbf{A} - \omega_0^2\mathbf{M}$ is real, the eigenvectors $\mathbf{u}_0$ and $\mathbf{v}_0$ in Eqs. (4) and (5) can be taken real. In this case, the adjoint vectors $\mathbf{u}_1$ and $\mathbf{v}_1$ are imaginary.

In the presence of small dissipative and gyroscopic forces ($\varepsilon > 0$), the double eigenvalue $\lambda_0 = i\omega_0$ with one eigenvector generally splits into two simple eigenvalues. This splitting is determined by the expansion

$$\lambda = i\omega_0 + \varepsilon^{1/2}\lambda_1 + \varepsilon\lambda_2 + \ldots, \tag{7}$$

where the coefficient λ_1 is determined from the qua-

Institute of Mechanics, Moscow State University, Michurinskiĭ pr. 1, Moscow, 119192 Russia

** e-mail: seyran@imec.msu.ru*

*** e-mail: kirillov@imec.msu.ru*

1028-3358/03/4812-0679$24.00

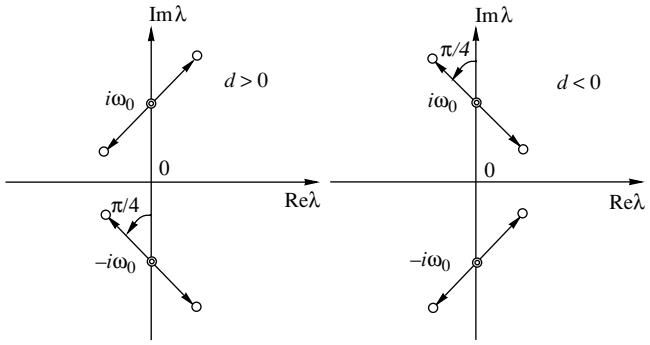

Fig. 1. Destabilization of the circulatory system by the small perturbation $\varepsilon\mathbf{D}$.

dratic equation [7, 8]

$$\lambda_1^2 = id, \quad d = -\frac{\mathbf{v}_0^{\mathrm{T}}\mathbf{D}\mathbf{u}_0}{2i\mathbf{v}_0^{\mathrm{T}}\mathbf{M}\mathbf{u}_1}. \tag{8}$$

We note that the quantity d is real, because the vectors $\mathbf{u}_0$ and $\mathbf{v}_0$ are real, while the vector $\mathbf{u}_1$ is imaginary. Therefore, in the presence of perturbation $\varepsilon\mathbf{D}$ ($\varepsilon > 0$), the double eigenvalue $\lambda_0 = i\omega_0$ splits into two simple eigenvalues

$$\lambda = i\omega_0 \pm \sqrt{id\varepsilon} + O(\varepsilon).$$

For $d \neq 0$, these eigenvalues lie on the opposite sides of the imaginary axis (Fig. 1). This means destabilization of the circulatory system ($\varepsilon = 0$) by arbitrarily small forces proportional to the velocity vector.

Therefore, $d = 0$, i.e.,

$$\frac{\mathbf{v}_0^{\mathrm{T}}\mathbf{D}\mathbf{u}_0}{2i\mathbf{v}_0^{\mathrm{T}}\mathbf{M}\mathbf{u}_1} = 0 \tag{9}$$

is a necessary condition of stabilization of the system. Under this condition, splitting of the double eigenvalue is determined by the expansion $\lambda = i\omega_0 + \lambda_2\varepsilon + o(\varepsilon)$, where the coefficient λ_2 is determined from the quadratic equation [7]

$$\lambda_2^2 + \lambda_2\frac{\mathbf{v}_1^{\mathrm{T}}\mathbf{D}\mathbf{u}_0 + \mathbf{v}_0^{\mathrm{T}}\mathbf{D}\mathbf{u}_1}{2\mathbf{v}_0^{\mathrm{T}}\mathbf{M}\mathbf{u}_1} - i\omega_0\frac{\mathbf{v}_0^{\mathrm{T}}\mathbf{D}\mathbf{G}(\mathbf{D}\mathbf{u}_0)}{2\mathbf{v}_0^{\mathrm{T}}\mathbf{M}\mathbf{u}_1} = 0. \tag{10}$$

Here, $\mathbf{G}$ is the operator inverse to the operator $\mathbf{A} - \omega_0^2\mathbf{M}$. In particular, this operator can be represented in the form

$$\mathbf{G} = (\mathbf{A} - \omega_0^2\mathbf{M} + 2i\omega_0\mathbf{v}_0\mathbf{v}_1^{\mathrm{T}}\mathbf{M})^{-1}, \quad \det\mathbf{G} \neq 0.$$

The coefficients of Eq. (10) are real. If the circulatory system is stabilized by small forces proportional to the velocity vector, both roots λ_2 must satisfy the condition $\mathrm{Re}\,\lambda_2 \leq 0$. This condition is equivalent to the weakened Routh–Hurwitz conditions for polynomial (10):

$$\frac{\mathbf{v}_1^{\mathrm{T}}\mathbf{D}\mathbf{u}_0 + \mathbf{v}_0^{\mathrm{T}}\mathbf{D}\mathbf{u}_1}{2\mathbf{v}_0^{\mathrm{T}}\mathbf{M}\mathbf{u}_1} \geq 0, \tag{11}$$

$$-i\omega_0\frac{\mathbf{v}_0^{\mathrm{T}}\mathbf{D}\mathbf{G}(\mathbf{D}\mathbf{u}_0)}{2\mathbf{v}_0^{\mathrm{T}}\mathbf{M}\mathbf{u}_1} \geq 0. \tag{12}$$

Strict inequalities (11) and (12) for sufficiently small values $\varepsilon > 0$ ensure splitting of the double eigenvalue $\lambda_0 = i\omega_0$ into two eigenvalues lying in the left half-plane.

In addition to a double pair $\pm i\omega_0$, the behavior of simple eigenvalues $\pm i\omega_j$, $j = 3, 4, \ldots, m$ with the right $\mathbf{u}_j$ and left $\mathbf{v}_j$ eigenvectors must be studied. When introducing small dissipative and gyroscopic forces ($\varepsilon > 0$), increments of these eigenvalues are determined by the formula

$$\lambda_j = i\omega_j + \mu_j\varepsilon + O(\varepsilon^2),$$

where

$$\mu_j = -\frac{\mathbf{v}_j^{\mathrm{T}}\mathbf{D}\mathbf{u}_j}{2\mathbf{v}_j^{\mathrm{T}}\mathbf{M}\mathbf{u}_j}$$

are real. Thus, the conditions

$$\frac{\mathbf{v}_j^{\mathrm{T}}\mathbf{D}\mathbf{u}_j}{\mathbf{v}_j^{\mathrm{T}}\mathbf{M}\mathbf{u}_j} \geq 0, \quad j = 3, 4, \ldots, m \tag{13}$$

in the first approximation in ε mean that any simple eigenvalue λ_j does not transit to the right half-plane in the presence of the perturbation $\varepsilon\mathbf{D}$ ($\varepsilon > 0$). Strict inequalities (13) imply that perturbed eigenvalues λ_j belong to the left half-plane for sufficiently small $\varepsilon > 0$.

Conditions (9) and (11)–(13) are the constructive necessary conditions of stabilization of the circulatory system by small dissipative and gyroscopic forces. Correspondingly, sufficient conditions of stabilization of system (1) are derived from conditions (9) and (11)–(13) by replacing nonstrict inequalities with strict ones. These conditions impose constraints on the elements of the matrix $\mathbf{D}$. Conditions (9), (11), and (13) are linear, and condition (12) is quadratic in the elements of the matrix $\mathbf{D}$. To calculate the coefficients of linear and quadratic forms, it is necessary to know the spectrum of the circulatory system and corresponding right and left eigenvectors and adjoint vectors. We emphasize that one constraint specified by equality (9) and m con-

straints specified by inequalities (11)–(13) are imposed on the m^2 elements of the matrix $\mathbf{D}$.

2. We consider system (1) under the assumption that $m = 2$ and $\mathbf{M} = \mathbf{I}$, where $\mathbf{I}$ is the identity matrix. This assumption does not limit generality, and the results of this section can be extended to the case of the arbitrary mass matrix with $\det\mathbf{M} \neq 0$. The spectrum of the two-dimensional system at the boundary between regions of stability and flutter consists of only a pair of imaginary double eigenvalues $\pm i\omega_0$. Since simple eigenvalues are absent, the stability of the system is determined by the behavior of this pair.

The necessary and sufficient condition of the existence of the double eigenvalue $\lambda_0 = i\omega_0$ of the circulatory system can be represented as the equation

$$4a_{12}a_{21} + (a_{22} - a_{11})^2 = 0, \tag{14}$$

equivalent to the equality $\det\mathbf{A} = \left(\frac{\mathrm{tr}\mathbf{A}}{2}\right)^2$. In this case,

$$-\lambda_0^2 = \omega_0^2 = \frac{a_{11} + a_{22}}{2} > 0, \quad a_{12}a_{21} \le 0. \tag{15}$$

In view of conditions (14) and (15), the eigenvectors and adjoint vectors $\mathbf{u}_0$, $\mathbf{v}_0$, $\mathbf{u}_1$, and $\mathbf{v}_1$ corresponding to the double eigenvalue $\lambda_0 = i\omega_0$ are found from Eqs. (4) and (5) in the form

$$\mathbf{u}_0 = \begin{bmatrix} 2a_{12} \\ a_{22} - a_{11} \end{bmatrix}, \quad \mathbf{v}_0 = \begin{bmatrix} 2a_{21} \\ a_{22} - a_{11} \end{bmatrix}, \tag{16}$$

$$\mathbf{u}_1 = \begin{bmatrix} 0 \\ -4i\omega_0 \end{bmatrix}, \quad \mathbf{v}_1 = \begin{bmatrix} 0 \\ -4i\omega_0 \end{bmatrix}. \tag{17}$$

Therefore, the denominator of expressions (8) and (10) is equal to

$$2\mathbf{v}_0^{\mathrm{T}}\mathbf{M}\mathbf{u}_1 = -8i\omega_0(a_{22} - a_{11}). \tag{18}$$

In view of Eqs. (18) and (14), necessary condition (9) takes the form

$$\frac{\mathbf{v}_0^{\mathrm{T}}\mathbf{D}\mathbf{u}_0}{2i(\mathbf{v}_0^{\mathrm{T}}\mathbf{M}\mathbf{u}_1)} = \frac{(d_{22} - d_{11})(a_{22} - a_{11}) + 2(d_{12}a_{21} + d_{21}a_{12})}{8\omega_0} = 0. \tag{19}$$

This condition can be written in the compact form

$$2\mathrm{tr}(\mathbf{A}\mathbf{D}) = \mathrm{tr}\mathbf{A}\,\mathrm{tr}\mathbf{D}.$$

We now determine the coefficients of quadratic equation (10). The coefficient of the linear term is equal to

$$\begin{aligned}\mathbf{v}_1^{\mathrm{T}}\mathbf{D}\mathbf{u}_0 + \mathbf{v}_0^{\mathrm{T}}\mathbf{D}\mathbf{u}_1 &= -8i\omega_0(d_{22}(a_{22} - a_{11}) + d_{12}a_{21} + d_{21}a_{12}) \\ &= -4i\omega_0\mathrm{tr}\mathbf{D}(a_{22} - a_{11}).\end{aligned} \tag{20}$$

To determine the free term of Eq. (10), the vector $\mathbf{w}$ must be determined from the inhomogeneous equation

$$(\mathbf{A} - \omega_0^2\mathbf{I})\mathbf{w} = \mathbf{D}\mathbf{u}_0, \tag{21}$$

where the eigenvector $\mathbf{u}_0$ is given in Eqs. (16). Solving Eq. (21), we obtain

$$\mathbf{G}(\mathbf{D}\mathbf{u}_0) \equiv \mathbf{w} = \begin{bmatrix} -2d_{12} \\ 2d_{11} \end{bmatrix}. \tag{22}$$

Then,

$$\mathbf{v}_0^{\mathrm{T}}\mathbf{D}\mathbf{G}(\mathbf{D}\mathbf{u}_0) = 2(a_{22} - a_{11})\det\mathbf{D}. \tag{23}$$

Substituting Eqs. (18), (20), and (23) into quadratic equation (10), we arrive at the relation

$$\lambda_2^2 + \lambda_2\frac{1}{2}\mathrm{tr}\mathbf{D} + \frac{1}{4}\det\mathbf{D} = 0. \tag{24}$$

Thus, necessary conditions (9), (11), and (12) for the two-dimensional system ($m = 2$) take the compact form

$$2\mathrm{tr}(\mathbf{A}\mathbf{D}) = \mathrm{tr}\mathbf{A}\,\mathrm{tr}\mathbf{D}, \tag{25}$$

$$\mathrm{tr}\mathbf{D} \ge 0, \quad \det\mathbf{D} \ge 0. \tag{26}$$

We note that similar conditions and Eq. (24) were obtained in [5] by analyzing the characteristic polynomial of system (1).

Let us determine the stabilization region that is specified by strict conditions (25) and (26) in the space of the elements of the matrix $\mathbf{D}$. Two cases are naturally distinguished.

In the first case, where $a_{12} \neq 0$, d_{21} is expressed from equality (25), and the matrix of dissipative and gyroscopic forces is found in the form

$$\mathbf{D} = \begin{bmatrix} d_{11} & d_{12} \\ \dfrac{(d_{22} - d_{11})(a_{11} - a_{22}) - 2a_{21}d_{12}}{2a_{12}} & d_{22} \end{bmatrix}. \tag{27}$$

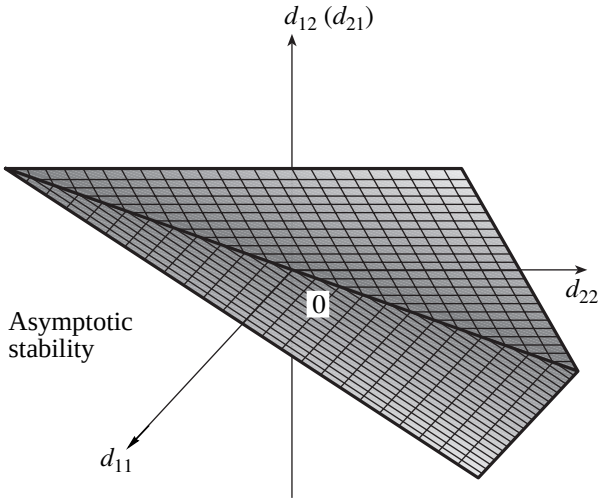

Fig. 2. Stabilization region for the asymmetric matrix **D** for $\frac{a_{11}-a_{22}}{2a_{12}}>0$ $\left(\text{or } \frac{a_{11}-a_{22}}{2a_{21}}>0\right)$.

Using condition (14) that the eigenvalue λ_0 is double, we transform inequalities (26) for matrix (27) to the form

$$d_{11}+d_{22}\geq 0, \tag{28}$$

$$\left(d_{11}-d_{12}\frac{a_{11}-a_{22}}{2a_{12}}\right)\left(d_{22}-d_{12}\frac{a_{22}-a_{11}}{2a_{12}}\right)\geq 0. \tag{29}$$

These inequalities are equivalent to the conditions

$$d_{11}\geq d_{12}\frac{a_{11}-a_{22}}{2a_{12}},\quad d_{22}\geq d_{12}\frac{a_{22}-a_{11}}{2a_{12}}. \tag{30}$$

Thus, in the three-dimensional space of the parameters d_{11}, d_{22}, and d_{12}, inequalities (30) define the dihedral angle that determine the region of stabilization of the circulatory system by small dissipative and gyroscopic forces specified by matrix **D** (27) (Fig. 2).

In the second case, where $a_{21}\neq 0$, the necessary conditions of stability have the form

$$d_{11}\geq d_{21}\frac{a_{11}-a_{22}}{2a_{21}},\quad d_{22}\geq d_{21}\frac{a_{22}-a_{11}}{2a_{21}}, \tag{31}$$

which corresponds to the dihedral angle in the three-dimensional space of the parameters d_{11}, d_{22}, and d_{21}. In this case, the matrix **D** has the form

$$\mathbf{D}=\begin{bmatrix} d_{11} & \dfrac{(d_{22}-d_{11})(a_{11}-a_{22})-2a_{12}d_{21}}{2a_{21}} \\ d_{21} & d_{22}\end{bmatrix}. \tag{32}$$

When $a_{12}\neq 0$ and $a_{21}\neq 0$, conditions (30) and (31) corresponding to matrices (27) and (30), respectively, are equivalent to each other.

Let us consider the case where $a_{11}=a_{22}$. In this case, $a_{12}=0$ or $a_{21}=0$. These equalities cannot be satisfied simultaneously. Otherwise, two linearly independent eigenvectors would correspond to the double eigenvalue λ_0 that contradicts the initial assumption. It follows from condition (25) that $d_{12}=0$ or $d_{21}=0$, respectively. According to strict conditions (30) and (31), the stabilization region in the three-dimensional space of the parameters d_{11}, d_{22}, and d_{12} (or d_{21}) is the right dihedral angle specified by the inequalities $d_{11}>0$ and $d_{22}>0$.

We now determine the form of the symmetric matrices **D** stabilizing the circulatory system. In this case, gyroscopic forces are absent, and inequalities (26) mean that the matrix **D** is nonnegative. We emphasize that strict inequalities (26) imply total dissipation. Expressing the coefficient $d_{12}=d_{21}$ from Eq. (25), we obtain

$$\mathbf{D}=\begin{bmatrix} d_{11} & \dfrac{(a_{22}-a_{11})(d_{11}-d_{22})}{2(a_{12}+a_{21})} \\ \dfrac{(a_{22}-a_{11})(d_{11}-d_{22})}{2(a_{12}+a_{21})} & d_{22}\end{bmatrix}. \tag{33}$$

We note that $a_{12}+a_{21}\neq 0$, because otherwise two linearly independent eigenvectors would correspond to the double eigenvalue λ_0 that contradicts the initial assumption. Calculating the determinant and trace of matrix (33) and writing the conditions that they are nonnegative, we arrive at the following necessary conditions in the space of the two parameters d_{11} and d_{22}:

$$\begin{gathered} d_{11},d_{22}\geq 0,\quad \frac{\sqrt{x}-1}{\sqrt{x}+1}d_{22}\leq d_{11}\leq d_{22}\frac{\sqrt{x}+1}{\sqrt{x}-1}, \\ x=1+\left(\frac{a_{22}-a_{11}}{a_{12}+a_{21}}\right)^2. \end{gathered} \tag{34}$$

Strict inequalities (34) specify the region of stabilization of system (1) by small forces proportional to the velocity vector. Thus, the region of stabilization of the circulatory system by symmetric matrices $\varepsilon\mathbf{D}$ of the form specified by Eqs. (33) and (34) is an angle on the plane of parameters d_{11} and d_{22} (Fig. 3). According to formula (34), this angle is generally acute and is right only for $a_{11}=a_{22}$.

3. Let us consider the Ziegler–Herrmann–Jong pendulum [1, 9] consisting of two rigid massless bars, which have the same length l and are connected by a hinge, and point-like masses $m_1=2m$ and $m_2=m$ located at the bar connection point and free end, respectively (Fig. 4). The pendulum is subject to the follower

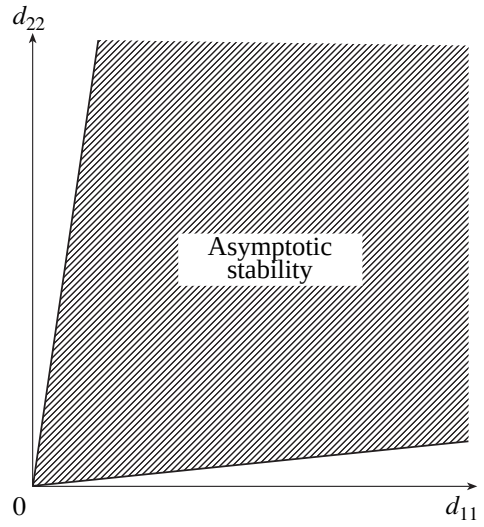

Fig. 3. Stabilization region for the symmetric matrix **D**.

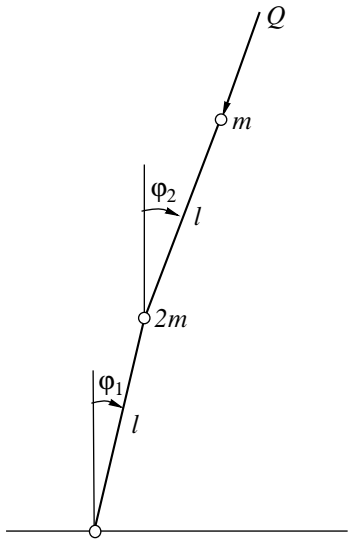

Fig. 4. Ziegler–Herrmann–Jong pendulum.

force Q applied to the free end. The viscoelastic hinges of the pendulum have the same rigidity c and different damping coefficients εb_1 and εb_2. In terms of the dimensionless quantities

$$q = \frac{Ql}{c}, \quad k_1 = \frac{b_1}{\sqrt{cml^2}}, \quad k_2 = \frac{b_2}{\sqrt{cml^2}},$$
$$\tau = t\sqrt{\frac{c}{ml^2}},$$

where τ is the time, the equations of small oscillations of the pendulum have the form

$$\frac{d^2\mathbf{y}}{d\tau^2} + \varepsilon\mathbf{D}\frac{d\mathbf{y}}{d\tau} + \mathbf{A}\mathbf{y} = 0, \quad \mathbf{y} = \begin{bmatrix}\varphi_1\\ \varphi_2\end{bmatrix}, \tag{35}$$

where

$$\mathbf{D} = \frac{1}{2}\begin{bmatrix} k_1 + 2k_2 & -2k_2 \\ -k_1 - 4k_2 & 4k_2\end{bmatrix}, \quad \mathbf{A} = \frac{1}{2}\begin{bmatrix}3-q & q-2\\ q-5 & 4-q\end{bmatrix}. \tag{36}$$

It is known that, in the absence of viscous friction, when $\varepsilon = 0$, the equilibrium position of the pendulum is stable for $q < q_0 = \frac{7}{2} - \sqrt{2}$ [9]. The critical load q_0 corresponds to the boundary between the regions of stability and flutter of the circulatory system. At this point, the spectrum of the system includes a pair of double imaginary eigenvalues $\pm i\omega_0$ and $\omega_0 = 2^{-1/4}$ with one eigenvector.

To determine the damping parameters k_1 and k_2 for which the perturbed system is asymptotically stable, we use stabilization conditions (25) and (26). Calculating the invariants of the matrices **A** and **D** for $q = q_0$

$$\mathrm{tr}\mathbf{A} = \sqrt{2}, \quad \mathrm{tr}\mathbf{D} = \frac{1}{2}k_1 + 3k_2, \quad \det\mathbf{D} = \frac{1}{2}k_1k_2,$$
$$\mathrm{tr}(\mathbf{AD}) = \left(-\frac{1}{2} + \frac{\sqrt{2}}{2}\right)k_1 + \left(-\frac{1}{2} + 3\sqrt{2}\right)k_2 \tag{37}$$

and substituting them into relations (25) and (26), we arrive at the necessary conditions of stabilization

$$k_1 = (5\sqrt{2} + 4)k_2, \quad k_2 \geq 0. \tag{38}$$

Thus, if the damping coefficients in the hinges satisfy strict conditions (38), the Ziegler–Herrmann–Jong pendulum is asymptotically stable.

We now determine the general form of the matrix **D** stabilizing circulatory system (1) without constrains (36). Substituting the coefficients of the matrix **A** calculated at the critical point $q = q_0$ into formulas (31) and (32), we obtain

$$\mathbf{D} = \begin{bmatrix} d_{11} & (17 - 12\sqrt{2})d_{21} + (3 - 2\sqrt{2})(d_{22} - d_{11}) \\ d_{21} & d_{22}\end{bmatrix} \tag{39}$$

with the constrains

$$-d_{22} \leq d_{21}(3 - 2\sqrt{2}) \leq d_{11}. \tag{40}$$

for the coefficients. It is easy to check that if the matrix **D** has form (36), conditions (39) and (40) lead to relations (38).

ACKNOWLEDGMENTS

This work was supported by the Russian Foundation for Basic Research and National Natural Science Foundation of China (project no. 02-01-39004), the Russian Foundation for Basic Research (project no. 03-01-00161), and the Basic Research and Higher Education Program, the US Civilian Research and Development Foundation for the Independent States of the Former Soviet Union and the Ministry of Education of the Russian Federation (grant no. Y1-MP-06-19).

REFERENCES

1. H. Ziegler, Ing. Arch. **20**, 49 (1952).
2. V. V. Bolotin, *Non Conservative Problems in the Theory of Elastic Stability* (Fizmatgiz, Moscow, 1961; Pergamon, London, 1963).
3. G. Herrmann, Appl. Mech. Rev. **20** (2), 103 (1967).
4. A. P. Seyranian, Usp. Mekh. **13** (2), 89 (1990).
5. O. N. Kirillov, in *Reports of Danish Center for Applied Mechanics and Mathematics (DCAMM), Copenhagen, 2003*, Rep. No. 681.
6. A. P. Seyranian and O. N. Kirillov, Theor. Appl. Mech. **26**, 135 (2001).
7. A. P. Seyranian, Preprint No. 446, IPM AN SSSR (Institute for Problems in Mechanics, Academy of Sciences of USSR, Moscow, 1990).
8. A. P. Seyranian, Stroinicki Cas. **42** (3), 193 (1991).
9. G. Herrmann and I. C. Jong, Trans. ASME, Ser. E, J. Appl. Mech. **33** (1), 125 (1966).

Translated by R. Tyapaev

Doklady Physics, Vol. 48, No. 12, 2003, pp. 685–687. Translated from Doklady Akademii Nauk, Vol. 393, No. 4, 2003, pp. 489–492.

MECHANICS

Exact Representation of Certain Axisymmetric Vortex Elements in a Viscous Incompressible Fluid

Yu. D. Shmyglevskiĭ* and A. V. Shcheprov**

Presented by Academician A.A. Petrov July 2, 2003

Received July 3, 2003

In cylindrical coordinates, steady axisymmetric flows of a viscous incompressible fluid rotating about the symmetry axis are described by the equations

$$u_x + v_r + \frac{1}{r}v = 0,$$

$$uu_x + vu_r + p_x = \frac{1}{\mathrm{R}}\left(u_{xx} + u_{rr} + \frac{1}{r}u_r\right),$$

$$uv_x + vv_r - \frac{1}{r}w^2 + p_r = \frac{1}{\mathrm{R}}\left(v_{xx} + v_{rr} + \frac{1}{r}v_r - \frac{1}{r^2}v\right), \quad (1)$$

$$uw_x + vw_r + \frac{1}{r}vw = \frac{1}{\mathrm{R}}\left(w_{xx} + w_{rr} + \frac{1}{r}w_r - \frac{1}{r^2}w\right).$$

Here, u, v, and w are axial, radial, and azimuthal velocity components, which correspond to axial (x), radial (r), and azimuthal (ϑ) cylindrical coordinates, respectively; p is the pressure divided by the constant density; and R is the Reynolds number.

Here, we consider flows with potential rotation about the x axis; i.e., $w = \frac{W}{r}$ and $p = P(x, r) - \frac{W^2}{2r^2}$, where W is an arbitrary constant and P is the new unknown function. In this case, the last of Eqs. (1) is satisfied, and the quantity W does not enter into the transformed equations.

Introducing the stream function

$$d\psi = ru\,dr - rv\,dx$$

and the function σ, where

$$\sigma = L\psi, \quad L = \frac{\partial^2}{\partial x^2} + \frac{\partial^2}{\partial r^2} - \frac{1}{r}\frac{\partial}{\partial r}$$

and eliminating P, we transform Eqs. (1) into the following system of equations for ψ and σ:

$$L\psi = \sigma, \quad L\sigma = Rr\frac{D\left(\frac{\sigma}{r^2}, \psi\right)}{D(x, r)}. \quad (2)$$

We consider the special class of solutions to system (2) for

$$\sigma = cr^2, \quad (3)$$

where c is an arbitrary constant. In this case, the second of Eqs. (2) is satisfied. To find the functions ψ analytic near the x axis, a solution to the first equation is sought in the form

$$\psi = \sum_{n=0}^{\infty} f_{2n}(x)r^{2n+2}, \quad (4)$$

where f_{2n} are the desired functions.

Substituting this expression for ψ into the first of Eqs. (2) and taking Eq. (3) into account, we arrive at the relation

$$\sum_{n=0}^{\infty}[f_{2n}^{(2)}(x)r^{2n+2} + 4n(n+1)f_{2n}(x)r^{2n}] = cr^2,$$

where the superscript in parentheses shows the order of derivative. This equality can be transformed to the form

$$\sum_{n=0}^{\infty}[f_{2n}^{(2)} + 4(n+1)(n+2)f_{2n+2}]r^{2n+2} = cr^2.$$

Therefore,

$$f_0^{(2)} + 8f_2 = c \quad \text{or} \quad f_2 = \frac{1}{8}(c - f_0^{(2)}). \quad (5)$$

In addition,

$$f_{2n}^{(2)} + 4(n+1)(n+2)f_{2n+2} = 0, \quad n = 1, 2, \ldots.$$

Computer Center, Russian Academy of Sciences, ul. Vavilova 40, Moscow, 117333 Russia

* *e-mail: yds@ccas.ru*

** *e-mail: and_ch@yahoo.com*

1028-3358/03/4812-0685$24.00

As a result,

$$f_{2n+2} = -\frac{1}{4(n+1)(n+2)} f^{(2)}_{2n}.$$

Induction on n yields

$$f_{2n} = k_{2n} f^{(2n)}, \quad k_{2n} = \frac{1}{(-4)^n (n!)^2 (n+1)}, \qquad (6)$$
$$n = 2, 3, \ldots.$$

Relations (4)–(6) lead to the equality

$$\psi = \frac{1}{8} c r^4 + \sum_{n=0}^{\infty} \frac{1}{(-4)^n (n!)^2 (n+1)} f^{(2n)} r^{2n+2}. \qquad (7)$$

In what follows, arbitrary functions $f(x)$ are assumed to be infinitely differentiable.

Let us investigate convergence of series (7). If $f(x)$ is a polynomial, the problem of convergence does not exist and formula (7) gives an exact solution. For the series

$$K = \sum_{n=2}^{\infty} |k_{2n}| r^{2n+2}, \qquad (8)$$

where k_{2n} is defined in (6), the ratio of two successive terms has the limit

$$\lim_{n \to \infty} \frac{r^2}{4(n+1)(n+2)} = 0$$

at a finite r value. Thus, series (8) is absolutely convergent. At bounded $|f^{(2n)}(x)| < M$, series (8) multiplied by M majorizes the series

$$\sum_{n=2}^{\infty} \left| k_{2n} f^{(2n)}(x) r^{2n+2} \right|.$$

Therefore, series (7) is absolutely and uniformly convergent if x and r are bounded and the function $f(x)$ is infinitely differentiable.

It is noteworthy that both sides of the second of Eqs. (2) are equal to zero for $\sigma = cr^2$. Consequently, the solution given by Eqs. (3) and (7) is independent of the Reynolds number and describes flows of both viscous and perfect fluids. Certain classes of similar solutions, which overlap with the

class of solutions found here, were found in [1–4]. However, the possibility of rotating a flow about the x axis was not pointed out in [1–3]. For example, solution (7) contains the spherical Hill's vortex $\psi = r^2(x^2 + r^2 - 1)$, which was described in [5], while the function $f = \cos x$ leads to an infinite chain of the Hill-type vortex elements, which can be found in [4].

If $f(x)$ is infinitely differentiable, the series entering into relation (7) can be differentiated infinitely term by term not only with respect to x but also with respect to r. Indeed, the series

$$\sum_{n=0}^{\infty} k_{2n} 2(n+1) f^{(2n)} r^{2n+1}$$

is uniformly convergent because of the uniform convergence of the series with the terms

$$\left| k_{2n} 2(n+1) r^{2n+1} \right| = \frac{2}{4^n (n!)^2} r^{2n+1}.$$

The m-fold differentiation of the series entering into relation (7) with respect to r leads to the relation

$$\left| \sum_{n \geq m}^{\infty} k_{2n} \frac{(2n+2)!}{(2n+2-m)!} f^{(2n)} r^{2n+2-m} \right|$$
$$\leq M \sum_{n \geq m}^{\infty} \frac{2(2n+1)! r^{2n+2-m}}{4^n (n!)^2 (2n+2-m)!}.$$

The ratio between the terms of the last series with $n = h + 1$ and $n = h$ is equal to

$$\frac{(2h+3) r^2}{2(h+1)(2h+4-m)(2h+3-m)} \to 0$$

at $n \to \infty$. Consequently, the m-fold differentiation of the series in relation (7) with respect to r yields a uniformly convergent series according to the d'Alembert ratio test, while formulas (3) and (7) represent a solution to Eqs. (2) if the function $f(x)$ is infinitely differentiable.

Certain steady axisymmetric vortex elements that rotate about the symmetry axis and satisfy the Navier–Stokes equations were found in [4, 5]. They are vortex rings, pairs of such rings, monolithic vortices with the structure of the spherical Hill's vortex, etc. Almost all of them are observed experimentally, but their existence is always associated with the rotation of a flow about its symmetry axis. Among vortex elements obtained experimentally, pairs of the coaxial Hill's structures observed in [6, 7] are of particular interest. The solution specified by Eqs. (3) and (7) with a polynomial function $f(x)$ gives exact description of the corresponding flows.

Both polynomial and nonpolynomial functions are used in the examples discussed below. For brevity, expressions for $\psi(x, r)$ are not presented there. However, they can be easily derived by substituting the expressions presented below for $f(x)$ and constant c into formula (7).

1. The relations $f = (x+3)(x+2)(x-1)(x-4)$ and $c = 170$ determine a pair of disconnected vortex elements. The corresponding flow pattern in the (x, r) plane is shown in Fig. 1. Vortices are bounded by the $\psi = 0$ lines. Flow directions are shown by arrows, while num-

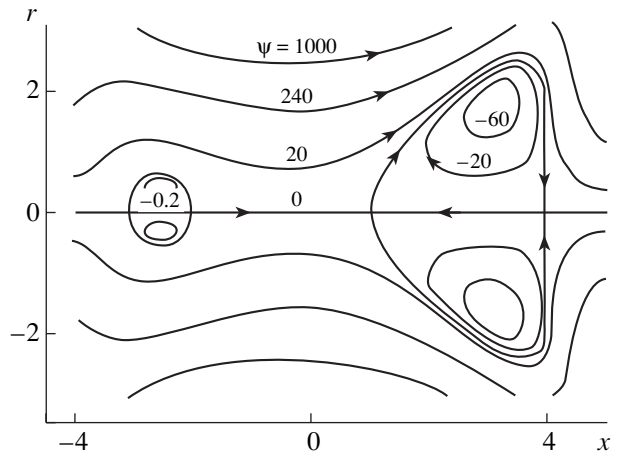

Fig. 1. Two disconnected vortex elements.

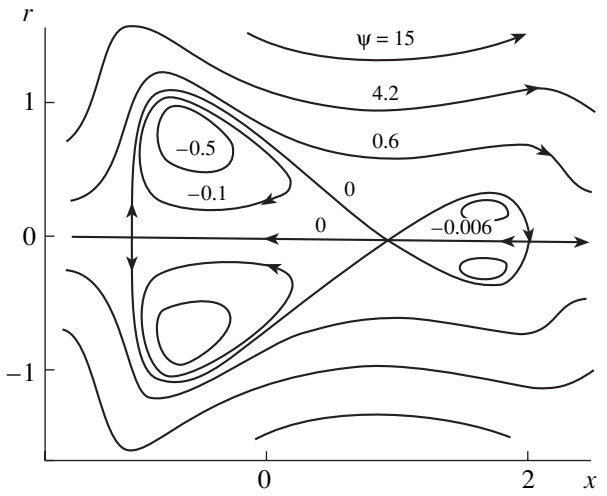

Fig. 2. Two touching vortex elements.

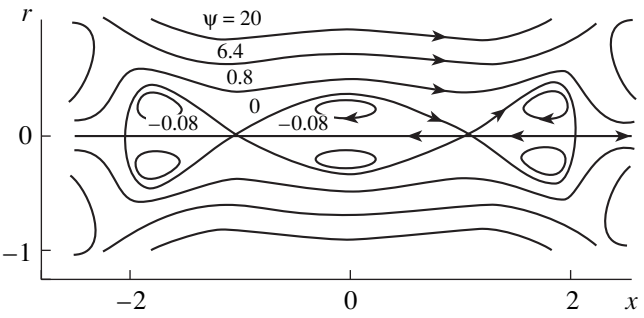

Fig. 3. Three vortex elements touching in pairs.

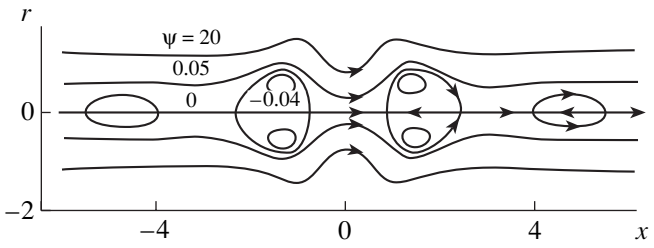

Fig. 4. Infinite vortex chain.

bers near the lines show ψ values. Vortices symmetric with respect to the *r* axis can be obtained by using symmetric zeros of the polynomial $f(x)$.

2 The relations $f = (x + 1)(x - 1)^2(x - 2)$ and $c = 35$ give a pair of touching vortex elements. Streamlines of the corresponding flow are shown in Fig. 2. Two vortices touch at the point $x = 1, r = 0$. In Figs. 1–4, the same notation is used.

3. Three Hill's vortices touching in pairs in the axis are obtained for $f = (x + 1)^2(x^2 - 4)(x - 1)^2$ and $c = 250$. The flow pattern is symmetric with respect to the *r* axis (Fig. 3). Neighboring pairs of three vortices touch by their points in the *x* axis at $x = -1$ and 1.

In the above examples, polynomial functions $f(x)$ are used. Therefore, both (3) and sums (7) represent exact solutions to Eqs. (2). Below, the function $f(x)$ is not a polynomial.

4. The function $f = \dfrac{\cos 2x}{1 + x^2}$ $(c = 4)$ describes a chain of the Hill-type vortices. In this case, ψ represents an infinite series. The flow part containing the largest vortices is shown in Fig. 4. The vortex width in the *r* direction decreases with an increase in the absolute value of *x*.

REFERENCES

1. U. Crudeli, Atti Accad. Naz. Lincei, Cl. Sci. Fis. Mat. Nat. Rend. **5**, 500 (1927).
2. U. Crudeli, Atti Accad. Naz. Lincei, Cl. Sci. Fis. Mat. Nat. Rend. **5**, 783 (1927).
3. U. Crudeli, Atti Accad. Naz. Lincei, Cl. Sci. Fis. Mat. Nat. Rend. **5**, 397 (1927).
4. Yu. D. Shmyglevskiĭ, *Analytic Investigations of Gas and Liquid Dynamics* (Editorial URSS, Moscow, 1999).
5. M. J. M. Hill, Rep. Br. Assoc. Adv. Sci., 696 (1893).
6. S. Leibovich, Annu. Rev. Fluid Mech. **10**, 221 (1978).
7. M. Escudier, Prog. Aerosp. Sci. **25**, 189 (1988).

Translated by Yu. Verevochkin

Doklady Physics, Vol. 48, No. 12, 2003, pp. 688–690. Translated from Doklady Akademii Nauk, Vol. 393, No. 5, 2003, pp. 615–617.

MECHANICS

Stability of a Longitudinally Inhomogeneous Elastic Rod

R. Yu. Amenzade, M. G. Gasymov, and S. S. Mirzoev

Presented by Academician G.G. Chernyĭ July 7, 2003

Received July 16, 2003

The problem of stability of non-prismatic rods in the Eulerian setting was intensely studied in the first half of 20th century [1, 2]. The solution to this problem is attained most easily in cases of piecewise variation of the rod stiffness or its variation according to a power law. The buckling of a rod with its stiffness varying according to a sinusoid law was analyzed by Dinnik [3]. Certain problems in the theory of rod stability for particular cases of stiffness variation have exact solutions in terms of Bessel functions [4].

In the present paper, we analyze stability of a hinged (at its ends) non-prismatic longitudinally inhomogeneous elastic rod for the case of weaker constraints imposed on the rod stiffness. The mathematically formulated problem is reduced to seeking the approximate minimal eigenvalue and the corresponding eigenfunction for the solution of the Sturm–Liouville equation with homogeneous boundary conditions. It is worth noting that in this setting of the problem, the well-known results are obtained as particular cases.

1. We now consider a hinged rod having the rectangular variable cross section $F = F(x) = 2ah(x)$, which is centrally compressed by force P. Furthermore, we suppose that $a = 1$. We also assume the Young modulus to be dependent on the longitudinal coordinate x: $E = E(x)$. Then, based on the hypothesis of plane cross sections and supposing the deformation of the rod to occur without its lengthening, we can reduce the problem on the rod buckling to integration of the differential equation with non-constant coefficients:

$$\{E(x)I(x)\}w'' + Pw = 0 \tag{1}$$

and with homogeneous boundary conditions

$$w(0) = w(l) = 0. \tag{2}$$

Here, w is the flexure, l is the rod length, and

$$I(x) = \int_{-h(x)}^{h(x)} z^2 dz = \frac{2}{3}h^3(x)$$

is the moment of inertia of the cross section with the longitudinal coordinate x.

Baku State University,
Baku, 370000 Azerbaijan

Henceforth, without lack of generality, we write out

$$E(x) = E_0\varphi_1(x), \quad I(x) = I_0\varphi_2(x), \tag{3}$$

where E_0 and I_0 are, respectively, the characteristic Young modulus and the moment of inertia, whereas $\varphi_1(x)$ and $\varphi_2(x)$ are the functions describing inhomogeneity and variability of the rod cross section.

We now impose on these functions conditions that do not contradict the physical sense: the functions $\varphi_1(x)$ and $\varphi_2(x)$ are measurable and limited from both above and below, their lower boundaries being positive. It follows from these conditions that the functions $\varphi_1(x)$ and $\varphi_2(x)$ are integrable in the Lebesgue sense:

$$\int_0^l \varphi_1(x)dx < +\infty, \quad \int_0^l \varphi_2(x) < +\infty. \tag{4}$$

The last expression also allows us to consider the case of piecewise inhomogeneity and the step-like variability of the cross section. Thus, introducing the notation

$$0 < \lambda = PE_0^{-1}I_0^{-1},$$

we can rewrite Eq. (1) in the form

$$w'' + \lambda q(x)w = 0 \tag{5}$$

for $q(x) = [\varphi_1(x)\varphi_2(x)]^{-1}$. It follows from (4)

$$\int_0^l q(x)dx < +\infty. \tag{6}$$

Finally, using dimensionless quantities

$$x = \bar{x}l, \quad \lambda l^2 = \bar{\lambda}, \quad w = \bar{w}l$$

and omitting, for simplicity, bars above the relevant quantities, the boundary value problem [formulas (5) and (2)] can be reduced to

$$\begin{aligned} w'' + \lambda q(x)w &= 0, \\ w(0) = w(1) &= 0. \end{aligned} \tag{7}$$

As is well known, the question related to conditions for the appearance of flexural forms of equilibrium corresponds to the problem on finding eigenvalues. The determination of the least nonzero critical force is associated with seeking the minimal value of λ for which

1028-3358/03/4812-0688$24.00

problem (7) has a nontrivial solution. In the general case, the determination of the exact minimal value of λ is impossible. Therefore, the object of our further study is constructing the approximate value of this quantity and the eigenfunction.

2. We consider problem (7) of eigenvalues in the space $L_2(0, 1)$. Since the Green's function of the problem

$$-y''(x) = f(x), \quad y(0) = y(1) = 0$$

has the form

$$G(x, \xi) = \begin{cases} x(1-\xi) & \text{for } x \le \xi \\ \xi(1-x) & \text{for } \xi \le x, \end{cases}$$

problem (7) is equivalent to the integral equation

$$w(x) = \lambda \int_0^1 G(x, \xi) q(\xi) w(\xi) d\xi. \tag{8}$$

It follows from the form of the kernel $G(x, \xi)$ and from properties of the function $q(\xi)$ that

(a) integral operator (8) is quite continuous and symmetrizable on the left in the case of its multiplying by the function $q(\xi)$;

(b) the eigenvalues of problem (7) are discrete and positive;

(c) the first eigenvalue λ_1 corresponds to the unique positive eigenfunction, all eigenfunctions forming a basis of the weight $q(\xi)$ [6].

Furthermore, denoting by S and D the operators

$$Sw = \int_0^1 G(x, \xi) w(\xi) d\xi,$$

$$Dw = q(x) w(x),$$

we obtain from the general theory of linear operators [7]:

$$\lambda_1^{-1} \le ||SD|| \le ||S|| \cdot ||D||.$$

Since S is the self-conjugated positive quite continuous operator having the eigenvalues $(\pi^2 n^2)^{-1}$, $n = 1, 2, \ldots$, then the norms of S and of D are $||S|| = \pi^{-2}$ and $||D|| = \sup_x q(x) = b$. It follows from the aforementioned that

$$0 < \frac{\pi^2}{b} \le \lambda_1 < \lambda_2 \le \lambda_3 \le \ldots \le \lambda_n \le \ldots.$$

We now calculate the approximate eigenvalue λ_1 using the method of successive approximations. To this aim, we consider the approximations

$$e_{1,0}(x) \equiv 1,$$

$$e_{1,k} = \int_0^1 G(x, \xi) q(x) e_{1,k-1}(\xi) d\xi, \quad k = 1, 2, \ldots. \tag{9}$$

We denote

$$\alpha = \int_0^1 q(\xi) d\xi > 0$$

and form the following sequence:

$$\lambda_{1,1} = \frac{\sqrt{\alpha}}{\left(\int_0^1 e_{1,1}(\xi) q(\xi) d\xi \right)^{\frac{1}{2}}}, \tag{10}$$

$$\lambda_{1,k} = \left\{ \frac{\int_0^1 e_{1,k-1}^2(\xi) q(\xi) d\xi}{\int_0^1 e_{1,k}^2(\xi) q(\xi) d\xi} \right\}^{\frac{1}{2}}, \quad k = 2, 3, 4, \ldots. \tag{11}$$

Here, we arrive at the estimate

$$0 < \lambda_{1,k} - \lambda_1 < \text{const} \left(\frac{\lambda_1}{\lambda_2} \right)^{2k-1},$$

from which by virtue of the rigorous inequality $\lambda_1 < \lambda_2$, it follows that $\lambda_{1,k} \to \lambda_1$ as $k \to \infty$. Thus, formulas (10) and (11), in combination with dependences (9), yield the constructive representation of the desired value. It should be noted that after a number of analogous reasonings, the final formula for the approximate calculation of the first eigenfunction is reduced to the expression

$$\chi_{1,k}(\xi) = \frac{e_{1,k}(\xi)}{\left(\int_0^1 e_{1,k}^2(\xi) q(\xi) d\xi \right)^{\frac{1}{2}}}.$$

3. For numerical realization, we consider a number of examples. Initially, we assume that $q(x) \equiv 1$. Then, the critical Eulerian force is determined as $\lambda_1 = \pi^2 \approx 9.8696$, whereas the three first approximations calculated on the basis of constructed formulas (10) and (11) are

$$\lambda_{1,1} \approx 10.9544, \quad \lambda_{1,2} \approx 9.8767, \quad \lambda_{1,3} \approx 9.8697.$$

Hence, it follows that even the second approximation yields a practical result, which is also the case in other examples given below. Furthermore, we analyze the stability of a combined rod with a constant cross section [$\varphi_2(x) \equiv 1$] for which

$$\varphi_1(x) = \begin{cases} 1, & 0 \le x \le 0.5 \\ 2, & 0.5 \le x \le 1. \end{cases}$$

For two approximations, we have obtained the val-

ues of the critical force

$$\lambda_{1,1} \approx 13.2116, \quad \lambda_{1,2} \approx 12.3264.$$

In the third example, we consider the case of a linear variation of the Young modulus, which can be represented in the form

$$\varphi_1(x) = 1 + \eta x, \quad \varphi_2(x) \equiv 1.$$

We now present the numerical values of the second approximation for $\lambda_{1,2}$ as functions of η:

η	−0.4	−0.2	0	1	2
$\lambda_{1,2}$	7.7957	8.8607	9.8767	14.4672	18.6900

In the examples listed above, the integrals were calculated using the Simpson method.

In conclusion, we would like to emphasize that by constructing an inhomogeneity, we can increase (decrease) the critical force and thereby, in a certain sense, optimize the construction.

REFERENCES

1. S. P. Timoshenko, *Stability of Elastic Systems* (Gostekhizdat, Moscow, 1955), p. 568.
2. A. S. Vol'mir, *Stability of Strained Systems* (Nauka, Moscow, 1967).
3. A. N. Dinnik, Vestn. Inzh. Tekh., No. 9 (1931).
4. B. G. Korenev, *Certain Problems of Elasticity and Thermal Conduction Theory: Solutions in Terms of Bessel Functions* (GIFML, Moscow, 1960).
5. M. A. Naimark, *Linear Differential Operators* (Nauka, Moscow, 1969; Ungar, New York, 1967).
6. V. S. Vladimirov, *Equations of Mathematical Physics* (Nauka, Moscow, 1971; Dekker, New York, 1971).
7. F. Riesz and B. Sz.-Nagy, *Functional Analysis* (Ungar, New York, 1955; Mir, Moscow, 1979).

Translated by G. Merzon

Doklady Physics, Vol. 48, No. 12, 2003, pp. 691–695. Translated from Doklady Akademii Nauk, Vol. 393, No. 5, 2003, pp. 618–623.

MECHANICS

Spectral Correlation Models of Fluctuations in the Earth's Rotation

Yu. G. Markov* and I. N. Sinitsyn**

Presented by Academician V.V. Kozlov June 2, 2003

Received June 5, 2003

Spectral and spectral correlation methods of processing measurements of the Earth's motion are commonly used to develop models of oscillations of the Earth's pole [1–3]. Linear and nonlinear analytical stochastic models of the motion of the deformable Earth were developed in [4–7] on the basis of celestial mechanics. In this paper, we construct spectral correlation models of fluctuations in the Earth's rotation and analyze the spectral correlation characteristics of fluctuations.

1. Under the assumptions considered in [8], the equations of the rotation of the deformable Earth can be written in the vector form

$$\dot{Y} = a(Y, t) + \mathbf{V}, \quad Y(t_0) = Y_0. \tag{1}$$

Here,

$$Y = [p_t q_t \delta r_t]^{\mathrm{T}}, \quad Y_0 = [p_0 q_0 \delta r_0]^{\mathrm{T}},$$
$$\mathbf{V} = [V_{1t} V_{2t} V_{3t}]^{\mathrm{T}},$$
$$a = a(Y, t) = [a_1 a_2 a_3]^{\mathrm{T}},$$

$$a_1 = -D_1 p_t - N_* q_t + \mathcal{P}_{10} + \mathcal{P}_{11}\cos\omega_* t + \mathcal{P}_{12}\cos 2\omega_* t - u_4[(r_* + \delta r_t)^2 - r_*^2], \tag{2}$$

$$a_2 = -D_2 q_t + N_* p_t + \mathcal{Q}_{10} + \mathcal{Q}_{11}\cos\omega_* t + \mathcal{Q}_{12}\cos 2\omega_* t - u_8[(r_* + \delta r_t)^2 - r_*^2],$$

$$a_3 = -D_3 \delta r_t + \mathcal{R}_{10} + \mathcal{R}_{11}\cos\omega_* t + \mathcal{R}_{12}\cos 2\omega_* t;$$

$$\mathcal{P}_{10} = -\frac{3}{2}u_4\omega_*^2\left(1 - \frac{3}{2}b_1^2\right) - \frac{3}{2}u_6\omega_*^2\left(1 - \frac{b_1^2}{2}\right) - \frac{3}{2}u_{11}\omega_*^2\left(1 - \frac{b_1^2}{2}\right) - u_4 r_*^2,$$

$$\mathcal{Q}_{10} = \frac{3}{2}u_7\omega_*^2\left(1 - \frac{b_1}{2}\right) + \frac{3}{2}u_8\omega_*^2\left(1 - \frac{3b_1^2}{2}\right) - \frac{3}{2}u_{10}\omega_*^2\left(1 - \frac{b_1^2}{2}\right) - u_8 r_*^2, \tag{3}$$

$$\mathcal{R}_{10} = \frac{3}{2}u_3\omega_*^2\left(1 - \frac{b_1^2}{2}\right) - 3u_{15}\omega_*^2\left(1 - \frac{b_1^2}{2}\right);$$

$$\mathcal{P}_{11} = 3u_1 b\omega_*^2 + \frac{3}{2}u_{13}b\omega_*^2,$$
$$\mathcal{Q}_{11} = -3u_2 b\omega_*^2 - 3u_{14}b\omega_*^2, \tag{4}$$
$$\mathcal{R}_{11} = -\frac{3}{2}u_5 b\omega_*^2 + 3u_9 b\omega_*^2,$$

$$\mathcal{P}_{12} = \frac{9}{4}u_4 b_1^2\omega_*^2 + \frac{3}{4}u_6 b_1^2\omega_*^2 + \frac{3}{4}u_{11}b_1^2\omega_*^2,$$
$$\mathcal{Q}_{12} = -\frac{3}{4}u_7 b_1^2\omega_*^2 - \frac{9}{4}u_8 b_1^2\omega_*^2 + \frac{3}{4}u_{10}b_1^2\omega_*^2, \tag{5}$$
$$\mathcal{R}_{12} = -\frac{3}{4}u_3 b_1^2\omega_*^2 - \frac{3}{2}u_{15}b_1^2\omega_*^2.$$

In Eqs. (1)–(5), p_t, q_t, and r_t are the projections of the instantaneous rotational velocity of the Earth on the body axes; $\delta r_t = r_t - r_*$, where r_* is the axial rotational velocity of the Earth; N_* is the Chandler frequency; the vector $\mathbf{u} = [u_1, \ldots, u_{15}]^{\mathrm{T}}$ describes variations in the axial and transverse moments of inertia of the Earth; V_{1t}, V_{2t}, and V_{3t} are the specific moments of external stochastic forces, which have the form of uncorrelated Gaussian

* *Moscow Aviation Institute (Technical University), Volokolamskoe sh. 4, Moscow, 125080 Russia*

** *Institute for Problems of Informatics, Russian Academy of Sciences, ul. Vavilova 30/6, Moscow, 117900 Russia*

1028-3358/03/4812-0691$24.00 © 2003 MAIK "Nauka/Interperiodica"

(normal) white noise and intensities $\nu_i = \nu(t)$ ($i = 1, 2, 3$); and $D_{1,2,3}$ are the specific coefficients of the moments of dissipative forces. The additive regular moments with the coefficients $\mathcal{P}_{10}$, …, $\mathcal{R}_{12}$, as well as the moments V_{1t}, V_{2t}, and V_{3t} of stochastic forces, are responsible for perturbations.

2. Equations (1) are linear in p_t and q_t and quadratic in δr_t. Taking

$$r_*^2 \approx (m_t^{\delta r})^2 + D_t^{\delta r} + 2r_* m_t^{\delta r} + 2(r_* + m_t^{\delta r})\delta r_t^0, \quad (6)$$

we linearize the nonlinear functions $u_{4,8}[(r_* + \delta r_t)^2 - r_*^2]$. In this case, Eqs. (1) lead to the following expressions for the mathematical expectations $m_t^{p,q,\delta r}$ and the centered components p_t^0, q_t^0, and δr_t^0:

$$\begin{aligned}
\dot m_t^p &= -D_1 m_t^p - N_* m_t^q - u_4\left[(m_t^{\delta r})^2 + D_t^{\delta r} + 2r_* m_t^{\delta r}\right] \\
&+ \mathcal{P}_{10} + \mathcal{P}_{11}\cos\omega_* t + \mathcal{P}_{12}\cos 2\omega_* t, \quad m_{t_0}^p = m_0^p, \\
\dot m_t^q &= -D_2 m_t^q + N_* m_t^p + u_8\left[(m_t^{\delta r})^2 + D_t^{\delta r} + 2r_* m_t^{\delta r}\right] \\
&+ \mathcal{Q}_{10} + \mathcal{Q}_{11}\cos\omega_* t + \mathcal{Q}_{12}\cos 2\omega_* t, \quad m_{t_0}^q = m_0^q, \\
\dot m_t^{\delta r} &= -D_3 m_t^{\delta r} \\
&+ \mathcal{R}_{10} + \mathcal{R}_{11}\cos\omega_* t + \mathcal{R}_{12}\cos 2\omega_* t, \quad m_{t_0}^{\delta r} = m_0^{\delta r}, \\
\dot p_t^0 &= -D_1 p_t^0 - N_* q_t^0 - 2u_4(r_* + m_t^{\delta r})\delta r_t^0 + V_{1t}, \\
p_{t_0}^0 &= p_0^0, \\
\dot q_t^0 &= -D_2 q_t^0 + N_* p_t^0 + 2u_8(r_* + m_t^{\delta r})\delta r_t^0 + V_{2t}, \\
q_{t_0}^0 &= q_0^0, \\
\delta\dot r_t^0 &= -D_3 \delta r_t^0 + V_{3t}, \quad \delta r_{t_0}^0 = \delta r_0^0.
\end{aligned} \quad (7), (8)$$

Equations (7) are nonlinear in $m_t^{p,q,\delta r}$, while Eqs. (8) are linear in p_t^0, q_t^0, and δr_t^0. Equations (7) and (8) represent a system of stochastic differential equations governing the mathematical expectations $m_t^{p,q,\delta r}$ and centered stochastic components p_t^0, q_t^0, and δr_t^0. Using numerical methods of statistical simulation [9, 10], we now estimate both the mathematical expectations and spectral correlation characteristics of the quantities p_t^0, q_t^0, and δr_t^0.

3. Since Eqs. (8) are linear, the covariance matrix K_t and the matrix $K_{t_1 t_2}$ of the covariance functions satisfy the equations [9, 10]

$$\dot K_t = a_1 K_t + K_t a_1^{\mathrm T} + \nu, \quad K_{t_0} = K_{0,} \quad (9)$$

$$\frac{dK_{t_1 t_2}}{dt_2} = K_{t_1 t_2} a_1(t_2)^{\mathrm T} \quad (10)$$

with $K_{t_1 t_2} = K_{t_1}$ for $t_1 < t_2$ and $K_{t_1 t_2} = K_{t_2 t_1}^{\mathrm T}$ for $t_2 < t_1$. Here, a_1 is the matrix of coefficients of Eqs. (8), i.e.,

$$a_1 = a_1(t, m_t^{\delta r}) = \begin{bmatrix} -D_1 & -N_* & -2u_4(r_* + m_t^{\delta r}) \\ N_* & -D_2 & 2u_8(r_* + m_t^{\delta r}) \\ 0 & 0 & -D_3 \end{bmatrix}, \quad (11)$$

$$\nu = \nu(t) = \begin{bmatrix} \nu_1(t) & 0 & 0 \\ 0 & \nu_2(t) & 0 \\ 0 & 0 & \nu_3(t) \end{bmatrix}.$$

Using Eqs. (9)–(11), we arrive at the following equations for the variances

$$\begin{aligned}
\dot D_t^p &= -2(D_1 D_t^p + N_* K_t^{pq}) \\
&+ 2u_4(r_* + m_t^{\delta r})K_t^{pr} + \nu_1, \\
\dot D_t^q &= 2(-D_2 D_t^q + N_* K_t^{pq}) \\
&+ 2u_8(r_* + m_t^{\delta r})K_t^{pr} + \nu_2, \\
\dot D_t^{\delta r} &= -2D_3 D_t^{\delta r} + \nu_3;
\end{aligned} \quad (12)$$

covariances

$$\begin{aligned}
\dot K_t^{pq} &= -(D_1 + D_2)K_t^{pq} - N_*(D_t^p - D_t^q) \\
&- 2u_4(r_* + m_t^{\delta r})K_t^{q\delta r} + 2u_8(r_* + m_t^{\delta r})K_t^{p\delta r}, \\
\dot K_t^{p\delta r} &= -(D_1 + D_3)K_t^{p\delta r} + N_* K_t^{q\delta r} \\
&- 2u_4(r_* + m_t^{\delta r})D_t^{\delta r}, \\
\dot K_t^{q\delta r} &= N_* K_t^{p\delta r} - (D_2 + D_3)K_t^{q\delta r} \\
&+ 2u_8(r_* + m_t^{\delta r})D_t^{\delta r},
\end{aligned} \quad (13)$$

and (for $t_1 < t_2$) covariance functions

$$\frac{\partial K^{pp}_{t_1t_2}}{\partial t_2} = -D_1K^{pp}_{t_1t_2} - N_*K^{pq}_{t_1t_2} - 2u_4(r_* + m^{\delta r}_{t_2})K^{p\delta r}_{t_1t_2},$$

$$\frac{\partial K^{pq}_{t_1t_2}}{\partial t_2} = -D_2K^{pq}_{t_1t_2} + N_*K^{pp}_{t_1t_2} + 2u_8(r_* + m^{\delta r}_{t_2})K^{p\delta r}_{t_1t_2},$$

$$\frac{\partial K^{p\delta r}_{t_1t_2}}{\partial t_2} = -D_3K^{p\delta r}_{t_1t_2}, \quad \frac{\partial K^{q\delta r}_{t_1t_2}}{\partial t_2} = -D_3K^{q\delta r}_{t_1t_2},$$

$$\frac{\partial K^{\delta r\delta r}_{t_1t_2}}{\partial t_2} = -D_3K^{\delta r\delta r}_{t_1t_2},$$

$$\frac{\partial K^{qp}_{t_1t_2}}{\partial t_2} = -D_1K^{qp}_{t_1t_2} - N_*K^{qq}_{t_1t_2} - 2u_4(r_* + m^{\delta r}_{t_2})K^{q\delta r}_{t_1t_2}, \quad (14)$$

$$\frac{\partial K^{qq}_{t_1t_2}}{\partial t_2} = -D_2K^{qq}_{t_1t_2} + N_*K^{qp}_{t_1t_2} + 2u_8(r_* + m^{\delta r}_{t_2})K^{q\delta r}_{t_1t_2},$$

$$\frac{\partial K^{\delta rp}_{t_1t_2}}{\partial t_2} = -D_1K^{\delta rp}_{t_1t_2} - N_*K^{\delta rq}_{t_1t_2} - 2u_4(r_* + m^{\delta r}_{t_2})K^{\delta r\delta r}_{t_1t_2},$$

$$\frac{\partial K^{\delta rq}_{t_1t_2}}{\partial t_2} = -D_2K^{\delta rq}_{t_1t_2} + N_*K^{\delta rp}_{t_1t_2} + 2u_8(r_* + m^{\delta r}_{t_2})K^{\delta r\delta r}_{t_1t_2}.$$

The initial conditions are

$$K^{ii}_{t_1t_2} = D^i_{t_1}, \quad K^{ij}_{t_1t_2} = K^{ij}_{t_1} \ (i, j = p, q, \delta r).$$

If the covariance functions for p^0_t, q^0_t, and δr^0_t depend only on the time difference $t_2 - t_1 = \tau$, the covariance functions and (mutual) spectral densities are given by the expressions

$$k^{p,q,\delta r}(\tau) = K^{p,q,\delta r}_{t,t+\tau} = \int_{-\infty}^{\infty} s^{p,q,\delta r}(\omega)e^{i\omega\tau}d\omega; \quad (15)$$

$$s^{p,q,\delta r}(\omega) = \frac{1}{2\pi}\int_{-\infty}^{\infty} k^{p,q,\delta r}(\omega)e^{-i\omega\tau}d\tau. \quad (16)$$

4. In the linear theory of fluctuations [6, 7], the terms

$$u_{4,8}[(r_* + \delta r_t)^2 - r_*^2]$$

are ignored in Eqs. (1). In this case, system (1) splits into two independent systems of stochastic equations in $\bar{Y} = [p_tq_t]^{\mathrm{T}}$ and δr_t, which describe the motion of the Earth's pole. If the terms containing the factors u_4 and u_8 are omitted, Eqs. (12)–(14) for the mathematical expectations and covariance characteristics are simplified.

According to [9, 10], the linear correlation models of fluctuations in the Earth's motion are based on the analysis of the weighting functions of white noise and its intensity. In particular, the mathematical expectations, covariance functions, and spectral densities are determined by the formulas

$$\bar{m}_t = \tilde{w}(t - t_0)\bar{m}_0 + \int_{t_0}^{t}\tilde{w}(t - \tau)\alpha_0(\tau)d\tau; \quad (17)$$

$$\bar{K}_{t_1t_2} = \tilde{\omega}(t_1 - t_0)\bar{K}_0\tilde{\omega}(t_2 - t_0)^* + \int_{t_0}^{\min(t_1, t_2)}\tilde{\omega}(t_1 - \tau)\bar{\nu}(\tau)\tilde{w}(t_2 - \tau)^*d\tau; \quad (18)$$

$$m^{\delta r} = \tilde{w}^{\delta r}(t - t_0)m^{\delta r}_0 + \int_{t_0}^{t}\tilde{w}^{\delta r}(t - \tau)\alpha'_0(\tau)dt; \quad (19)$$

$$K^{\delta r}_{t_1t_2} = \tilde{w}^{\delta r}(t_1 - t_0)\tilde{w}^{\delta r}(t_2 - t_0)D^{\delta r}_0 + \int_{t_0}^{\min(t_1, t_2)}\tilde{w}^{\delta r}(t_1 - \tau)\tilde{w}^{\delta r}(t_2 - \tau)\nu_3d\tau; \quad (20)$$

$$\bar{s}(\omega) = \begin{bmatrix} s^{pp}(\omega) & s^{pq}(\omega) \\ s^{qp}(\omega) & s^{qq}(\omega) \end{bmatrix} = \Phi(i\omega)\bar{\nu}\Phi(i\omega)^*, \quad (21)$$

$$s^{\delta r}(\omega) = |\Phi^r(i\omega)|^2\nu_3. \quad (22)$$

Here, the asterisk stands for complex conjugation;

$$\bar{m}_t = \begin{bmatrix} m^p_t \\ m^q_t \end{bmatrix}, \quad \bar{m}_0 = \begin{bmatrix} m^p_0 \\ m^q_0 \end{bmatrix};$$
$$\bar{K}_0 = \begin{bmatrix} D^p_0 & K^{pq}_0 \\ K^{pq}_0 & D^q_0 \end{bmatrix}, \quad \bar{\nu} = \begin{bmatrix} \nu_1 & 0 \\ 0 & \nu_2 \end{bmatrix}; \quad (23)$$

$$\alpha_0 = \begin{bmatrix} \mathcal{P}_{10} + \mathcal{P}_{11}\cos\omega_*t + \mathcal{P}_{12}\cos2\omega_*t \\ \mathcal{Q}_{10} + \mathcal{Q}_{11}\cos\omega_*t + \mathcal{Q}_{12}\cos2\omega_*t \end{bmatrix}; \quad (24)$$

$$\alpha'_0 = \mathcal{R}_{10} + \mathcal{R}_{11}\cos\omega_*t + \mathcal{R}_{12}\cos2\omega_*t. \quad (25)$$

In Eqs. (17)–(23), $\Phi(i\omega)$ is the transfer function; $\tilde{w}(t - \tau)$ and $w(t - \tau)$ are weighting functions; and $\Phi^{\delta r}(i\omega)$, $\tilde{w}^{\delta r}(t - \tau)$, and $w^{\delta r}(t - \tau)$ are the respective fundamental solutions of linear equations (1). According

to [9, 10], these quantities are determined by the formulas

$$\Phi(i\omega) = -(\alpha - i\omega I_2)^{-1}$$

$$= -\frac{1}{\Delta(\omega)}\begin{bmatrix} -(D_2 + i\omega) & -N_* \\ N_* & -(D_1 + i\omega) \end{bmatrix}, \quad (26)$$

$$\alpha = \begin{bmatrix} -D_1 & -N_* \\ N_* & D_2 \end{bmatrix}, \quad I_2 = \begin{bmatrix} 1 & 0 \\ 0 & 1 \end{bmatrix};$$

$$\Phi^{\delta r}(i\omega) = (D_3 + i\omega)^{-1}; \quad (27)$$

$$\Delta(\omega) = \omega_c^2 - \omega^2 + 2\varepsilon i\omega,$$
$$\omega_c^2 = N_*^2 + D_1 D_2 \approx N_*^2, \quad 2\varepsilon = D_1 + D_2; \quad (28)$$

$$w(t-\tau) = \begin{bmatrix} w^{pp}(t-\tau) & w^{pq}(t-\tau) \\ w^{pq}(t-\tau) & w^{qq}(t-\tau) \end{bmatrix}, \quad (29)$$
$$\tilde{w}(t-\tau) = w(t-\tau)\mathbf{1}(t-\tau);$$

$$w^{pp}(t-\tau) = e^{-1/2(D_1+D_2)(t-\tau)}$$
$$\times\left[\frac{D_2 - D_1}{2N_*}\sin N_*(t-\tau) + \cos N_*(t-\tau)\right],$$

$$w^{qq}(t-\tau) = e^{-1/2(D_1+D_2)(t-\tau)}$$
$$\times\left[-\frac{D_2 - D_1}{2N_*}\sin N_*(t-\tau) + \cos N_*(t-\tau)\right], \quad (30)$$

$$w^{pq}(t-\tau) = w^{qp}(t-\tau)$$
$$= -e^{-1/2(D_1+D_2)(t-\tau)}\sin N_*(t-\tau).$$

Here, the components of $w(t-\tau)$ are written including squares and products of the quantities $D_{1,2}N_*^{-1}$, $\mathbf{1}(t-\tau)$ is the Heaviside step function, and

$$w^{\delta r}(t-\tau) = e^{-D_3(t-\tau)},$$
$$\tilde{w}^{\delta r}(t-\tau) = e^{-D_3(t-\tau)}\mathbf{1}(t-\tau). \quad (31)$$

If $D_{1,2}N_*^{-1} \ll 1$ and the quantities ν_1, ν_2, and ν_3 are constants, formulas (15), (16), (21), and (22) take the form

$$D^p = \frac{2D_1\nu_2 - (D_2 - D_1)\nu_1}{2D_1(D_1 + D_2)}; \quad (32)$$

$$D^q = \frac{2D_2\nu_1 + (D_2 - D_1)\nu_2}{2D_1(D_1 + D_2)}; \quad (33)$$

$$K^{pq} = \frac{\nu_1 D_2 - \nu_2 D_1}{N_*(D_1 + D_2)}; \quad (34)$$

$$D^{\delta r} = \frac{\nu_3}{2D_3}; \quad (35)$$

$$s^{pp}(\omega) = \Delta_1^{-2}(\omega)[\nu_1(D_2^2 + \omega^2) + \nu_2 N_*^2]; \quad (36)$$

$$s^{qq}(\omega) = \Delta_1^{-2}(\omega)[\nu_1 N_*^2 + \nu_2(D_1^2 + \omega^2)]; \quad (37)$$

$$s^{pq}(\omega) = \Delta_1^{-2}(\omega)N_*[-\nu_1(D_2 + i\omega)$$
$$+ \nu_2(D_1 - i\omega)] = \overline{s^{qp}(\omega)}; \quad (38)$$

$$s^{\delta r}(\omega) = \Delta_2^{-2}(\omega)\nu_3, \quad \Delta_2^2(\omega) = D_3^2 + \omega^2, \quad (39)$$

where

$$\Delta_1^2(\omega) = (N_*^2 + D_1 D_2 - \omega^2)^2 + \omega^2(D_1 + D_2)^2$$
$$\approx (N_*^2 - \omega^2)^2 + \omega^2(D_1 + D_2)^2.$$

The system of Eqs. (7) and (12)–(16) provides the basis for the analytical simulation and the analysis of the spectral correlation characteristics of fluctuations in the Earth's motion.

5. The dynamic spectral correlation and kinetic models of fluctuations in the Earth's motion (Sections 2–4) were used to analyze the measurements for the fundamental problem "Statistical Dynamics of the Earth's Rotation" [11].

The stationary spectral densities $s^{p,\,q,\,\delta r}(\omega)$ found in the approximate (linear) theory [formulas (17)–(39)] are shown in the figure for the white-noise intensities $\nu_1 = \nu_2 = \nu_0$ and $\nu_3 < \nu_0$ and the specific coefficients of the moments of dissipative forces $D_1 = D_2 = D_0$ and $D_3 < D_0$. In this case, the variances, covariances, cova-

riance functions, and spectral densities are given by the approximate expressions

$$D_\infty^{p,q} \approx \frac{\nu_0}{2D_0}, \quad D_\infty^{\delta r} \approx \frac{\nu_3}{2D_3}, \quad K_\infty^{pq} \approx 0; \tag{40}$$

$$\begin{aligned} k^{p,q}(\tau) &= D_\infty^{p,q} e^{-D_0|\tau|} \cos N_* \tau, \\ k^{\delta r}(\tau) &= D_\infty^{\delta r} e^{-D_3|\tau|}; \end{aligned} \tag{41}$$

$$s_1^{p,q} \approx \frac{\nu_0}{N_*^2}, \quad s_2^{p,q} \approx \frac{\nu_0(\omega_*^2 + N_*^2)}{(N_*^2 - \omega_*^2)^2},$$

$$s_3^{p,q} \approx \frac{\nu_0}{2D_0^2}, \quad s_4^{p,q} \approx \frac{\nu_0(4\omega_*^2 + N_*^2)}{(N_*^2 - 4\omega_*^2)^2}, \tag{42}$$

$$s_1^{\delta r} \approx \frac{\nu_3}{D_3^2}, \quad s_2^{\delta r} \approx \frac{\nu_3}{\omega_*^2}, \quad s_3^{\delta r} \approx \frac{\nu_3}{N_*^2}, \quad s_4^{\delta r} \approx \frac{\nu_3}{4\omega_*^2}.$$

According to [4, 5], the estimates of the relaxation time D_0^{-1} range from 10 to 100 years with the standard deviation $\sqrt{D_\infty^{p,q}}$ about 0.02" to 0.04".

The nonlinear components with the coefficients $u_{4,8} \sim 10^{-8}$ at the frequency N_* were included by analytical simulation. The corrections found by statistical simulation for the mathematical expectation, second moments, and spectral density are equal to 2, 6, and 10%, respectively.

In addition to the analysis of the accuracy, formulas (17)–(39) and measurements allow us to identify the parameters **u** (which are important when estimating trends) as well as the basic parameters N_* and $D_{1,2,3}$ of the model.

The statistical analyses show that the spectral correlation models based on the linear theory can ensure a required accuracy in time intervals from 3 to 5 years.

The dynamic Gaussian linear (and nonlinear) spectral correlation models of fluctuations in the Earth's motion can be used to analyze the accuracy and identify the basic dynamic parameters by processing measurements [1–5]. The models describe the features of fluctuations in the Earth's motion and ensure the required accuracy.

The PC software package developed at our institute in 2000–2003 allows us to perform analytical, statistical, and combined simulations of both regular and stochastic motions of the Earth in both nonstationary and stationary regimes.

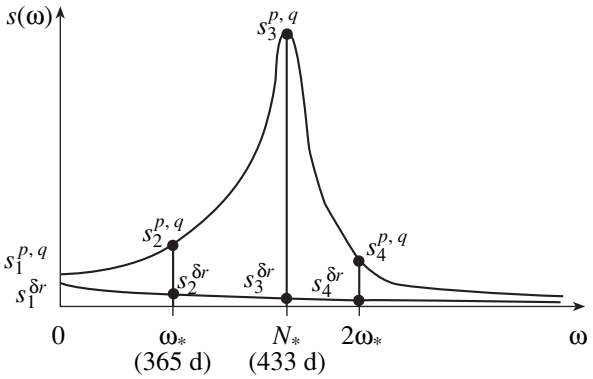

Figure.

ACKNOWLEDGMENTS

We are grateful to V.I. Sinitsyn, Yu.V. Chumin, V.V. Belousov, and E.R. Korepanov for their work developing the software package we used. This work was supported by the Russian Foundation for Basic Research, project nos. 01-02-17250 and 01-01-00758.

REFERENCES

1. L. V. Rykhlova, G. S. Kurbasova, and T. A. Taĭdanova, Astron. Zh. **67**, 151 (1990) [Sov. Astron. **34**, 79 (1990)].
2. L. V. Rykhlova, G. S. Kurbasova, and M. N. Rybalova, Tr. Inst. Astron. Akad. Nauk SSSR **69**, 3 (1991).
3. G. S. Kurbasova and L. V. Rykhlova, Astron. Zh. **75**, 632 (1998) [Astron. Rep. **42**, 558 (1998)].
4. M. Araty, *Linear Stochastic Systems with Constant Coefficients* (Springer-Verlag, Berlin, 1982; Nauka, Moscow, 1989).
5. N. S. Sidorenkov, *Physics of Earth's Rotation Instabilities* (Nauka, Moscow, 2002).
6. Yu. G. Markov and I. N. Sinitsyn, Dokl. Akad. Nauk **385**, 189 (2002) [Dokl. Phys. **47**, 531 (2002)].
7. Yu. G. Markov and I. N. Sinitsyn, Dokl. Akad. Nauk **387**, 482 (2002) [Dokl. Phys. **47**, 867 (2002)].
8. Yu. G. Markov and I. N. Sinitsyn, Dokl. Akad. Nauk **350**, 343 (2003) [Dokl. Phys. **48**, 253 (2003)].
9. V. S. Pugachev and I. N. Sinitsyn, *Stochastic Differential Systems: Analysis and Filtration* (Nauka, Moscow, 1990).
10. V. S. Pugachev and I. N. Sinitsyn, *Theory of Stochastic Systems* (Logos, Moscow, 2002).
11. I. N. Sinitsyn, Yu. G. Markov, V. I. Sinitsyn, *et al.*, in *Proceedings of the International School–Seminar on Automation and Computerization in Science and Engineering, ACS'2002, Moscow, 2002*, http://www.elicsnet.ru.

Translated by V. Chechin

Doklady Physics, Vol. 48, No. 12, 2003, pp. 696–700. Translated from Doklady Akademii Nauk, Vol. 393, No. 5, 2003, pp. 624–628.

MECHANICS

Extrema of the Kinetic Energy and Its Dissipation Rate in Vortex Flows

A. S. Chefranov* and S. G. Chefranov

Presented by Academician G.S. Golitsyn August 22, 2003

Received August 27, 2003

Conditions for minimizing the kinetic energy of a flow of an ideal incompressible fluid with constant vorticity are obtained by the variational method. On this basis, the corresponding Kelvin theorem stating that such an extremum is realized for the linear superposition of the potential velocity field with the homogeneously spiral vortex regime of the Gromeka–Beltrami type is generalized. It is shown that one of the modifications of the Helmholtz–Rayleigh theorem, which also separate Gromeka–Beltrami inertialess flows but with respect to the minimization of the dissipation rate of the flow energy, is an analogue of the well-known theorem on minimization of the energy of a magnetic field with fixed total vorticity.

1. INTRODUCTION

Exact solutions of the time-independent equations of the vortex dynamics of an ideal incompressible fluid in the Gromeka–Beltrami form [1, 2] have been known for more than a century. In these flows, the velocity $\mathbf{v}$ is collinear to its curl $\boldsymbol{\omega} = \mathrm{curl}\mathbf{v}$; i.e., $\boldsymbol{\omega} = k\mathbf{v}$, where $k = \dfrac{\boldsymbol{\omega}\mathrm{curl}(\boldsymbol{\omega})}{\omega^2}$. For k = const, the corresponding flow is a homogeneously spiral vortex flow with nonzero vorticity $H = \dfrac{(\boldsymbol{\omega}\mathbf{v})}{2}$. Such flows are convenient for description of observed tornado-like vortices [3]. The vorticity of these vortices is much larger than that of other atmospheric vortices without such a pronounced three-dimensional structure, such as tornado vortices, dust devils, and water tornado [4]. The homogeneously spiral vortex regime is also observed at a sufficient distance from the underlying surface in experiments on simulation of tornado-like vortices [5].

At the same time, such flows are considered in many works on general and geophysical hydrodynamics as exotic and rare in nature (see, e.g., [6]). Gromeka–Beltrami flows are often not mentioned even when discussing the corresponding phenomena, such as inertial waves in a rotating fluid, which are well known and often discussed in hydrodynamics and particularly in geophysical hydrodynamics [6]. Indeed, Batchelor [6] did not even mention that these waves are a realization of homogeneously curled vortex Gromeka–Beltrami flows (as can be easily shown). Attitude to Gromeka–Beltrami solutions began to change in the 1980s, when numerical simulations showed that a turbulent flow could contain regions of low energy dissipation, where the tendency of the alignment of the velocity and vorticity vectors is observed [7]. According to the generalization of the Helmholtz–Rayleigh theorem [2], inertialess flows, in particular Gromeka–Beltrami flows, are characterized by the minimum rate of energy dissipation. However, only inhomogeneously spiral flows, where k in the relation $\boldsymbol{\omega} = k(\mathbf{x})\mathbf{v}$ is the coordinate function, were considered in [2].

In this work, we obtain modifications of the Helmholtz–Rayleigh theorem that correspond to the minimum dissipation rates of the kinetic energy of a vortex flow at fixed energy or fixed helicity and separate homogeneously spiral vortex flows with k = const. In addition, the Kelvin theorem [2, 6] on the minimization of the kinetic energy of a potential flow is generalized for the superposition of potential flows with homogeneously spiral vortex flows for the case, where the flow vorticity is invariant and can be fixed in the corresponding variational problem. Moreover, we revise the known Arnold theorem [8] on the minimum kinetic energy for vortex stationary solutions of the Euler equations. Previously, this theorem ignored the invariance of vorticity for ideal fluid flows. Comparison with similar theorems in magnetic hydrodynamics [9] is made. As is shown, the statement that the energy dissipation rate in a fluid flow with fixed integral vorticity $\overline{H}$ is minimal for the Gromeka–Beltrami homogeneously spiral vortex flows with k = const is similar to the statement that

Obukhov Institute of Atmospheric Physics, Russian Academy of Sciences, Pyzhevskii per. 3, Moscow, 109017 Russia

** e-mail: schefranov@mail.ru*

the energy of a magnetic field with invariant integral vorticity is minimal for force-free fields.

2. GENERALIZATION OF THE KELVIN THEOREM ON THE ENERGY MINIMUM

2.1. We consider the variational isoperimetric problem (more precisely, the more general Boltz problem [10]) of the minimization of the kinetic energy functional

$$T = \rho_0 \int_V d^3x \frac{\mathbf{v}^2}{2}$$

for an ideal incompressible fluid in the presence of the differential constraint $\mathrm{div}\mathbf{v} = 0$ and the integral constraint associated with the total vorticity invariant

$$\overline{H} = \frac{\rho_0}{2} \int_V d^3x (\boldsymbol{\omega}\mathbf{v}),$$

where $\rho_0 = \mathrm{const}$ is the fluid density and V is the region occupied by the fluid. It is assumed that the hydrodynamic fields of velocity $\mathbf{v}$ and $\boldsymbol{\omega} = \mathrm{curl}\mathbf{v}$ are equal to zero at the boundary of the region V. If these fields are fixed by boundary conditions, we assume that the variations of these fields is equal to zero at the integration-domain boundary S.[1] The functional that must be varied has the form

$$F = \int_V d^3x \left[\rho_0 \frac{v^2}{2} + \frac{\mu_1 \rho_0}{2} (\mathbf{v} \cdot \mathrm{curl}\mathbf{v}) + \mu_2(\mathbf{x}) \mathrm{div}\mathbf{v} \right], \quad (1)$$

where μ_1 and μ_2 are the Lagrange multipliers.

Substituting $\mathbf{v} = \mathbf{v}_0 + \mathbf{v}_1$, where $\mathbf{v}_1$ is the low velocity variation, into Eq. (1), equating the first variation of the functional F to zero, and assuming that

$$F_S = \int_S ds_j \left[\mu_2 v_{1j} - \mu_1 \frac{\rho_0}{2} \varepsilon_{jik} v_{0i} v_{1k} \right] = 0):,$$

we arrive at the system

$$\mathbf{v} + \mu_1 \mathrm{curl}\mathbf{v} = \mathrm{grad}\mu_2, \quad \Delta\mu_2 = 0, \quad \mu_1 = -\frac{\tilde{T}}{\overline{H}_0}, \quad (2)$$

where the subscript 0 is omitted in $\mathbf{v}_0$ and $\tilde{T}$ is the kinetic energy for $\mathrm{grad}\mu_2 = 0$ on the surface S and can parametrically depend on μ_1 (see the example in the next section). This system corresponds to the constraint equations and corresponding Euler–Ostrogradsky equations for $\mu_1 = \mathrm{const}$ and $\overline{H} = \overline{H}_0 = \mathrm{const}$.

System (2) with $\mu_1 = 0$ provides the Kelvin theorem [2, 6] on the minimum of the flow kinetic energy, which is reached for potential irrotational velocity fields. In this case, μ_2 in Eqs. (2) satisfies the Laplace equation for a flow of the incompressible fluid in the region V. At the same time, the inclusion of the invariance of the total vorticity of the flow $\overline{H}$ for $\mu_1 \neq 0$ modifies the Kelvin theorem. In this case, the minimum of the kinetic energy can be reached either for homogeneous Gromeka–Beltrami flows (for $\mu_2 = 0$ or $\mathrm{grad}\mu_2 = 0$) or for any superposition of such flows with a certain potential flow (for $\mathrm{grad}\mu_2 \neq 0$) in the form

$$\mathbf{v} = \nabla\mu_2 + \tilde{\mathbf{v}}, \quad \mathrm{curl}\tilde{\mathbf{v}} = k\tilde{\mathbf{v}}, \quad \mathrm{div}\tilde{\mathbf{v}} = 0, \quad (3)$$

where $k = -\dfrac{1}{\mu_1} = \mathrm{const}$ because $\mu_1 = \mathrm{const}$ in Eqs. (2). Explicit expressions for $\tilde{\mathbf{v}}$ will be represented in the next section. The representation of $\mathbf{v}$ in the form of the superposition of potential and vortex fields is truly used in hydrodynamics [2, 6].

The generalization obtained for the Kelvin theorem agrees with the Arnold theorem [8] on the minimization of the kinetic energy of an ideal incompressible fluid for stationary vortex solutions of the Euler equations. Moreover, the generalization refines this theorem. Homogeneous vortex Gromeka–Beltrami flows are particular solutions of the time-independent hydrodynamic equations. At the same time, energy minimization is realizable for homogeneously spiral vortex flows of the Gromeka–Beltrami type, when the conditions of the Arnold theorem must be supplemented by the inevitable invariance of the total vorticity of a flow of the ideal incompressible fluid. According to the reciprocity principle [10], the generalization of the Kelvin theorem, which is derived on the basis of the above modified isoperimetric problem, makes it possible to determine the possibility of reaching the maximum total vorticity at fixed energy for homogeneous vortex flows (3) satisfying Eqs. (2). This conclusion justifies the corresponding statement presented without proof in [3] and agrees with the observed properties of turbulent coherent structures, when a fluid flow includes individual "spots" with maximum vorticity that are surrounded by regions with relatively high dissipation of turbulence energy [7, 11].

2.2. The field $\tilde{\mathbf{v}}$ corresponding to Eqs. (2) and (3) can be represented in the cylindrical coordinates as [1]

$$\tilde{v}_z = BJ_0(kr), \quad \tilde{v}_\varphi = BJ_1(kr), \quad \tilde{v}_r = 0,$$

where J_0 and J_1 are the zeroth and first-order Bessel functions, respectively. This solution can describe a tor-

[1] It is actually sufficient to assume that the corresponding integrals over the surface bounding the fluid region V—including $V \to \infty$—are equal to zero.

nado-like spiral vortex localized in the cylindrical region of radius R for $\tilde{v}_\varphi = \left.\frac{d\tilde{v}_z}{dr}\right|_{r=R} = 0$ if $kR = \gamma_{1n}$, where γ_{1n}, $n = 1, 2, \ldots$ are the zeros of the Bessel function J_1. For $\mu_2 = 0$, the quantity $\tilde{T}$ in Eqs. (2) can be determined as

$$\tilde{T} = \frac{\pi\rho_0}{2} LB^2R^2J_0^2(\gamma_{ln}),$$

if this cylindrical vortex is limited by the vertical scale L. In this case, the corresponding discrete μ_1 values allowed by the variational principle can be estimated from Eqs. (2), where $\bar{H}_0$ is fixed by the constraint. The discrete allowable values of the vortex radius $R = R_n$ is determined by the expression

$$R_n = \frac{2\bar{H}_0}{\pi\rho_0 LB^2\gamma_{1n}J_0^2(\gamma_{1n})}, \quad n = 1, 2, \ldots. \qquad (4)$$

It is the relation between geometric and dynamic parameters of this cylindrical vortex, which has nontrivial stable topological structure (particularly for $n > 1$) due to the finite vorticity corresponding to the invariant topological charge. Since $L \sim R$ for observed tornado-like vortices [4], expression (4) provides the following estimate for discrete values of the scale-invariant similarity criterion corresponding to these vortices [12]:

$$\Pi = \Pi_n = \frac{H_v R_n}{B^2}, \quad \Pi_n = \frac{1}{2}\gamma_{1n}J_0^2(\gamma_{1n}), \quad n = 1, 2, \ldots, \qquad (5)$$

where $H_v \equiv \frac{\bar{H}_0}{\rho_0 V_n}$ and $V_n = \pi R_n^3$. In [12], the possibility of discretization of the similarity criterion Π was also noted for homogeneously spiral flows. However, this discretization was determined only by the possibility of an integer ratio of the total height of the vortex to the height step of the spiral of this vortex [3]. At the same time, formula (5) yields the sequence $\Pi_1 \approx 3.08$, $\Pi_2 \approx 3.012$, $\Pi_3 \approx 0.266$, $\Pi_4 \approx 0.323$, etc., that is, in contrast to [12], nonmonotonic in n. The nontrivial topological features of the homogeneously spiral cylindrical tornado-like vortex corresponding to the exact solution of the hydrodynamic equations are taken into account in formula (5) more precisely than in [12]. We emphasize that the value $\Pi \approx 3$ obtained for the similarity criterion agrees well with the criterion value corresponding to the experimental tornado model [13]. According to the parameters of tornado and tornado-like vortices observed in nature [4], Π can range from 0.2 to 20.

3. EXTREMA OF THE ENERGY DISSOCIATION RATE

The time-independent equations of magnetic hydrodynamics are mathematically similar to the corresponding equations for an ideal incompressible fluid [11]. It is of interest to compare the variational principles determining the limiting steady structure for both magnetic and hydrodynamic fields. In particular, the above generalization of the Kelvin variational principle is formulated similarly to the known magnetohydrodynamic theorem on the minimum energy

$$E = \frac{1}{8\pi}\int d^3x\mathbf{h}^2$$

of a magnetic field with allowance for the invariance of the corresponding integral vorticity

$$S = \int d^3x(\mathbf{Ah})$$

of this field for force-free fields, whose vector $\mathbf{h} = \mathrm{curl}\mathbf{A}$ is collinear to the current field vector $\mathbf{j}$ [9]. In addition, there is a certain analogue between force-free fields and Gromeka–Beltrami flows, where the velocity field $\mathbf{v}$ and vortex field $\boldsymbol{\omega}$ correspond to the $\mathbf{h}$ and $\mathbf{j}$ fields, respectively [11].

However, there is a fundamental difference between this variational principle and the above generalization of the Kelvin theorem. Indeed, an analogue of the S invariant is absent in hydrodynamics if correspondence is established between the $\mathbf{v}$ and $\mathbf{h}$ fields, as is usually the case [11]. Only the integral vorticity $\bar{H}$ rather than $\xi = \int d^3x\mathbf{va}$, where $\mathbf{v} = \mathrm{curl}\,\mathbf{a}$, is invariant in hydrodynamics. At the same time, if correspondence is established between $\mathbf{v}$ and vector potential $\mathbf{A}$ instead of $\mathbf{h}$, the energy dissipation integral

$$I = \nu\rho_0\int d^3x(\mathrm{curl}\mathbf{v})^2$$

rather than the energy of the flow corresponds to the quantity E. In this case, the integral vorticity

$$\bar{H} = \frac{\rho_0}{2}\int d^3x(\mathbf{v}\mathrm{curl}\mathbf{v})$$

corresponds to the quantity S. However, the integral vorticity is not an invariant of motion of a viscous fluid for $\nu \neq 0$, where ν is the kinematic viscosity. The energy integral T of motion of the fluid also is not an invariant for $\nu \neq 0$. Therefore, the results of the preceding section for the three-dimensional dynamics of the ideal incompressible fluid are not directly similar to the outwardly resembling theorem of magnetic hydrodynamics.

At the same time, the variational problem of the extremum energy dissipation rate for a viscous incom-

pressible fluid under some integral constraints can be considered. Let us consider the problem of the minimum functional I determining the average energy dissipation rate in the fluid among all solenoidal velocity fields with the same vorticity $\bar{H}$ and energy T. The functional corresponding to this problem has the form

$$F_1 = \int d^3x\left[\eta\frac{(\mathrm{curl}\mathbf{v})^2}{2} + \frac{\lambda_1\rho_0(\mathbf{v}\mathrm{curl}\mathbf{v})}{2} + \frac{\lambda_2\rho_0 v^2}{2} + \lambda_3(\mathbf{x})\mathrm{div}\mathbf{v}\right], \quad (6)$$

where $\eta = \nu\rho_0$ is the dynamic viscosity.

In particular, for $\lambda_2 = \lambda_3 = 0$, the variational problem for F_1 exactly corresponds to the problem of the extremum energy of the magnetic field with fixed vorticity [9]. In this case, the field of the vector potential **A** in [9] corresponds to the **v** field in Eq. (6). For $\lambda_2 \neq 0$ and $\lambda_3 \neq 0$, equating the first variation of functional (6) to zero and assuming that

$$F_{1S} = \int_S ds_i\left[\lambda_3 v_{1i} + \varepsilon_{ijk}v_{1j}\left(\eta\omega_{0k} + \frac{\lambda_1\rho_0}{2}v_{0k}\right)\right] = 0):,$$

we arrive at the relation

$$\mathrm{curlcurl}\mathbf{v} + \tilde{\lambda}_1\mathrm{curl}\mathbf{v} + \tilde{\lambda}_2\mathbf{v} = \mathrm{grad}\tilde{\lambda}_3,$$
$$\Delta\tilde{\lambda}_3 = 0, \quad \tilde{\lambda}_2 = \pm\left(\frac{ca - b^2}{Ba - A^2}\right)^{1/2}, \quad \tilde{\lambda}_1 = \frac{A\tilde{\lambda}_2 - b}{a}, \quad (7)$$

where $\tilde{\lambda}_i = \dfrac{\lambda_i}{\eta}$ ($i = 1, 2, 3$), the expressions for $\tilde{\lambda}_1$ and $\tilde{\lambda}_2$ are obtained from the constraints $T = T_1 = \mathrm{const}$ and $\bar{H} = H_1 = \mathrm{const}$, $A = -\dfrac{2H_1}{\rho_0}$, $B = \dfrac{2T_1}{\rho_0}$,

$$a = \int d^3x\boldsymbol{\omega}^2, \quad b = \int d^3x(\boldsymbol{\omega}\cdot\mathrm{curl}\boldsymbol{\omega}),$$
$$\text{and} \quad c = \int d^3x(\mathrm{curl}\boldsymbol{\omega})^2,$$

if $\nabla\lambda_3 = 0$ on the surface S. Since $ca \geq b^2$ and $Ba \geq A^2$ according to the Cauchy–Schwarz inequality, $\mathrm{Im}\tilde{\lambda}_2 = 0$. For $\tilde{\lambda}_2 = \tilde{\lambda}_3 = 0$, the velocity field in Eqs. (7) satisfies Eqs. (2) and (3).

In particular, for $\lambda_3 = 0$, any homogeneously spiral vortex field $\boldsymbol{\omega} = k\mathbf{v}$ for $k = -\dfrac{\lambda_1}{2\nu}$ automatically satisfies the condition of zero surface integral F_{1S} for any variation $\mathbf{v}_1$, which corresponds to the natural boundary conditions [14]. In this case, λ_1 and λ_2 have the form $\left(\text{because } k = \dfrac{H_1}{T_1}\right)$

$$\lambda_1 = -2\nu\frac{H_1}{T_1}, \quad \lambda_2 = \nu\frac{H_1^2}{T_1^2}, \quad (8)$$

determined from the constraints rather than from Eqs. (7), where $ac = b^2$ and $Ba = A^2$ for $\boldsymbol{\omega} = k\mathbf{v}$.

We emphasize that condition (7) at $\tilde{\lambda}_1\mathrm{curl}\mathbf{v} + \tilde{\lambda}_2\mathbf{v} = 0$ formally coincides with the criterion of the minimum energy dissipation rate according to the generalization presented in [2] for the Helmholtz–Rayleigh theorem. However, only inhomogeneously spiral variants of the vortex Gromeka–Beltrami flow can consistently satisfy the condition $-\Delta\mathbf{v} = \mathrm{grad}\tilde{\lambda}_3$ in [2]. Therefore, the indicated coincidence is not formal only for $\dfrac{\lambda_2}{\lambda_1} = -k \neq \mathrm{const}$. At the same time, $\dfrac{\lambda_2}{\lambda_1} = -\dfrac{k}{2} = \mathrm{const}$ according to formulas (8).

Thus, the conclusions for the minimum dissipation rate of the kinetic energy for steady homogeneously spiral vortex flows modify the corresponding Helmholtz–Rayleigh theorem [2]. Moreover, these conclusions agree with the principle of the minimum entropy production under given external (boundary) conditions for nonequilibrium steady states of various natural objects [14, 15].

The results are obtained only by analyzing the first variations of the functionals F and F_1. Strictly speaking, these results determine only the necessary conditions of the existence of the corresponding relative extrema. To determine the type of extrema and stability of solutions, it is necessary to analyze the signs of the second variations of the functionals.

ACKNOWLEDGMENTS

We are grateful to G.S. Golitsyn for his attention to the work. This work was supported by the Russian Foundation for Basic Research (project nos. 01-05-64300, 01-07-90211).

REFERENCES

1. I. S. Gromeka, *Some Cases of the Motion of an Incompressible Liquid: Collection of Scientific Works* (Akad. Nauk SSSR, Moscow, 1952).
2. D. Serrin, *Mathematical Foundations of Classical Mechanics* (NITs "Regul. Khaot. Din.," Izhevsk, 2001).
3. M. V. Kurganskiĭ, Dokl. Akad. Nauk **371**, 240 (2000).
4. R. Chizheleski, Izv. Akad. Nauk, Fiz. Atmos. Okeana **35**, 174 (1999).

5. B. M. Boubnov and P. V. Rhines, *Turbulent Mixing in Geophysical Flows*, Ed. by P. F. Linden and J. M. Redondo (CIMNE, Barcelona, 2001), pp. 35–54.
6. G. Batchelor, *An Introduction to Fluid Dynamics* (Cambridge University Press, Cambridge, 1967; Mir, Moscow, 1973).
7. R. B. Pelz, V. Yakhot, S. A. Orszag, *et al.*, Phys. Rev. Lett. **54**, 2505 (1985).
8. V. I. Arnol'd, Prikl. Mat. Mekh. **29**, 846 (1965).
9. J. B. Taylor, Phys. Rev. Lett. **33**, 1139 (1974).
10. L. Ya. Tslaf, *Calculus of Variations and Integral Equations* (Nauka, Moscow, 1966).
11. H. K. Moffatt, J. Fluid Mech. **159**, 359 (1985).
12. S. G. Chefranov, Izv. Akad. Nauk, Fiz. Atmos. Okeana **39**, 759 (2003).
13. V. F. Tarasov and V. G. Makarenko, Dokl. Akad. Nauk SSSR **305**, 297 (1989) [Sov. Phys. Dokl. **34**, 199 (1989)].
14. R. S. Schechter, *The Variational Methods in Engineering* (McGraw-Hill, New York, 1967; Mir, Moscow, 1971).
15. G. S. Golitsyn and I. I. Mokhov, Izv. Akad. Nauk SSSR, Fiz. Atmos. Okeana **14**, 378 (1978).

Translated by R. Tyapaev

Doklady Physics, Vol. 48, No. 12, 2003, pp. 701–704. Translated from Doklady Akademii Nauk, Vol. 393, No. 6, 2003, pp. 766–769.

MECHANICS

Dynamic Model of Small Formation Comminution in Two Immiscible Liquids

V. A. Vinokurov* and A. A. Karpukhin

Presented by Academician V. A. Sadovnichiĭ June 8, 2003

Received June 16, 2003

Since the 1930s, especially after the assimilation of industrial synthesis of a large number of thermoplastics and rubbers, the scope of the use of polymer mixtures is steadily expanding. The volume of production of polymer mixtures increases annually by 7–10%. Polymer mixtures are produced by various methods: by mixing latices or water dispersions with the subsequent coagulation and agitation, by mixing solutions of polymers with the subsequent desiccation or precipitation, by mixing polymers and oligomers with the subsequent solidification of the oligomers, and by mixing polymers at a temperature higher than a vitrification temperature or a melting point. The last method is widely used in industry.

The properties of polymer compositions are determined both by the properties of initial components and by the phase structure of the mixture formed when mixing according to the ratio of components and the dispersivity of phase formations.

Mathematical models of mixing two fluids were proposed in [1–4]. This process was experimentally studied in [5, 6]. Unfortunately, these models are poorly detailed and, therefore, cannot be used in practice.

In this study, a mathematical model of the mutual dispersion of polymers was developed so that it provides the calculation of the size of formations in the dispersion phase as a function of the known parameters of the system.

FORMULATION OF THE PROBLEM

We consider a system of two immiscible liquids. The total volume of the system and the volumes of the components are assumed constant in the dispersive mixing process. We study comminution of first component formations in the dispersion phase. The second component that is a viscoelastic fluid and serves as the matrix for the dispersion component is called the dispersion medium. An obligatory condition for breakdown of formations is the presence of the velocity gradient in the matrix.

In this study, we use the following designations: r is the formation radius, N is the number of formations in the dispersion phase, t is time, V is the volume of the dispersion phase, V_0 is the total volume of the composition, $\varphi = V/V_0$ is the relative volume of the dispersion phase, α is the coefficient characterizing the collision of formations leading to coalescence, β is the dispersion efficiency, σ is the interphase tension at the interface between the dispersion formation and the matrix, E is Young's modulus of the dispersion phase, h is the radius of the capture region, $\dot{\gamma}$ is the shear rate for the mixing machinery, τ is the shear stress, η is the viscosity, ν is the relative velocity of formations, and κ is the velocity gradient.

The model is based on the following assumptions:

(i) At every time t, the dispersion phase of the system involves $N(t)$ of perfectly spherical formations with the same radius $r(t)$.

(ii) The volume of the dispersion phase is constant in the process:

$$V = N\frac{4}{3}\pi r^3 = \text{const}. \quad (1)$$

(iii) Dispersion proceeds by dividing a spherical formation of radius r into two spherical formations of radius $r/\sqrt[3]{2}$.

(iv) Formations are dispersed due to the mechanical work executed by the motor of the mixing machinery. Only a fraction of this work is immediately expended to dispersion. The energy consumption for dispersion is determined from the formula $Q_d = \beta Q_f$, where $\beta \in [0; 1]$ is the model parameter and Q_f is the power released in the melt volume due to internal friction. The power Q_f is determined from the formula [7] $Q_f = \tau\dot{\gamma}V_0$. Therefore,

$$Q_d = \beta\tau\dot{\gamma}V_0. \quad (2)$$

Moscow State University of Design and Technology, ul. Sadovnicheskaya 33, Moscow, 113806 Russia

** e-mail: vinokur@narod.ru*

1028-3358/03/4812-0701$24.00

(v) Simultaneously with dispersion, the coalescence of formations proceeds. This process is simulated by a pair coalescence of two colliding formations of the same radius into a single formation. Coalescence takes place if the impact parameter $h' < h$, where $h = \alpha \cdot 2r$ and $\alpha \in [0; 1]$ is the coefficient determining the possibility of formations coalescing in the collision (a system parameter).

We consider the proposed model of comminution of formations in the dispersion phase.

DYNAMICS OF COMMINUTION OF FORMATIONS

The dispersion rate is estimated in the thermodynamic approach; i.e., the rate dN/dt of increase in the number of formations in the dispersion phase is assumed to be determined by the formula

$$\frac{dN}{dt} = \frac{Q_d}{e_1}, \quad (3)$$

where e_1 is the energy required for dividing the ball of radius r into two balls of radius $r/\sqrt[3]{2}$. It is assumed that

$$e_1 = e_{1,E} + e_{1,\sigma}, \quad (4)$$

where $e_{1,E}$ is the energy of deformation of a formation and $e_{1,\sigma}$ is the energy of creation of a new surface.

Using Hooke's law, we estimate the energy of deformation of one formation by the expression

$$e_{1,E} = \Theta_1 E \cdot \frac{4}{3}\pi r^3, \quad (5)$$

where Θ_1 is the tuning coefficient, which is equal to 3/2 in the simplest case. The second term in formula (4) is associated with the difference in the surface area of a formation before and after the breakdown:

$$e_{1,\sigma} = 2\sigma \cdot 4\pi\left(\frac{r}{\sqrt[3]{2}}\right)^2 - \sigma \cdot 4\pi r^2 = \Theta_2 \sigma \cdot 4\pi r^2, \quad (6)$$

where $\Theta_2 = 3(\sqrt[3]{2} - 1)$.

In view of Eqs. (2) and (4)–(6), expression (3) for the rate of increase in the number of formations takes the form

$$\frac{dN}{dt} = \frac{\beta\tau\dot{\gamma}N}{\varphi\left(\frac{\Theta_1}{2}E + \Theta_2\frac{\sigma}{r}\right)}. \quad (7)$$

DYNAMICS OF FORMATION COALESCENCE

When the dispersion formations move in the matrix, they can collide and, when the impact parameter $h' < h$, coalesce. The dynamics of coalescence of dispersion formations is determined by the regimes of motion of the medium. In this study, we consider two types of motion: plane-parallel and disordered flows of the matrix.

PLANE-PARALLEL FLOW OF THE MATRIX

In the Cartesian coordinate system, each plane layer z = const of the plane-parallel flow moves with a velocity $\nu = \kappa z$ along the y axis. It is assumed that spherical formations of the dispersion phase do not change their shape when moving in the medium. In this case, the calculation shows that the rate of coalescence-induced decrease in the number of formations is

$$\frac{dN}{dt} = -\Theta_3\kappa\varphi N, \quad (8)$$

where $\Theta_3 = 4\alpha^3/\pi$.

DISORDERED FLOW OF THE MATRIX

The number of collisions between formations in the disordered flow of the dispersion medium is calculated similarly to the statistical calculation of the number of collisions between molecules in an ideal gas. Under these assumptions, the rate of coalescence-induced decrease in the number of formations is equal to

$$\frac{dN}{dt} = -\Theta_4\frac{\varphi\nu N}{r}, \quad (9)$$

where $\Theta_4 = 3\alpha^2/2$.

DYNAMICS EQUATIONS FOR THE RADIUS OF DISPERSION FORMATIONS

The dynamics of formation size variation in the dispersion phase are described under the assumption that two opposite processes—dispersion and coalescence—proceed simultaneously. The overall rate of the process is determined by the sum of their rates. From this viewpoint, we consider two models of the dynamics of formation size variation in the dispersion phase, namely, plane-parallel and disordered flows of polymer melt.

According to aforementioned formulas (7) and (8), the rate of change in the number of formations in the plane-parallel flow is determined by the expression

$$\frac{dN}{dt} = \left(\frac{\beta\tau\dot{\gamma}}{\varphi\left(\Theta_5 E + \Theta_2\frac{\sigma}{r}\right)} - \Theta_3\kappa\varphi\right)N, \quad (10)$$

where $\Theta_5 = \frac{3}{2}\Theta_1$.

Combining formulas (7) and (9) for the dynamics of change in the number of formations in the disordered flow, we obtain the expression

$$\frac{dN}{dt} = \left(\frac{\beta\tau\dot{\gamma}}{\varphi\left(\Theta_5 E + \Theta_2 \frac{\sigma}{r}\right)} - \Theta_4 \frac{\varphi\nu}{r} \right) N. \quad (11)$$

According to assumption (1) that the volume of the dispersion phase is constant, the number of formations N is a function of the radius:

$$N = \frac{3V}{4\pi} \cdot \frac{1}{r^3}. \quad (12)$$

Relation (12) makes it possible to pass from differential equations (10) and (11) to the corresponding differential equations for the radius r as a time function. After substitution (12), differential equation (10) reduces to the differential equation

$$\frac{dr}{dt} = -r\frac{rb_1 - c_1}{rb + c}, \quad (13)$$

where

$$b = \Theta_5 E, \quad c = \Theta_2 \sigma, \quad b_1 = \frac{1}{3}\left(\frac{\beta\tau\dot{\gamma}}{\varphi} - \Theta_3\Theta_5 E\kappa\varphi\right),$$

$$\text{and} \quad c_1 = \frac{1}{3}\Theta_2\Theta_3\sigma\kappa\varphi.$$

Thus, we obtain the basic differential equation (13) describing the dynamics of the radius of formations in the dispersion phase in the plane-parallel flow.

Using the same substitution, we transform Eq. (11) for the disordered flow to the form

$$\frac{dr}{dt} = -\frac{r^2 a - rbq - qc}{rb + c}, \quad (14)$$

where $a = \dfrac{\beta\tau\dot{\gamma}}{3\varphi}$ and $q = \dfrac{1}{3}\Theta_4\varphi\nu$.

Both differential equations (13) and (14) have a single stable rest point $r = r_\infty$ at the positive semiaxis $r > 0$. An arbitrary trajectory is attracted to this point for $t \to +\infty$.

For the plane-parallel flow of the matrix,

$$r_\infty = \frac{4\alpha^3\varphi^2\kappa\sigma}{\pi\beta\tau\dot{\gamma} - 6\alpha^3\varphi^2\kappa E}. \quad (15)$$

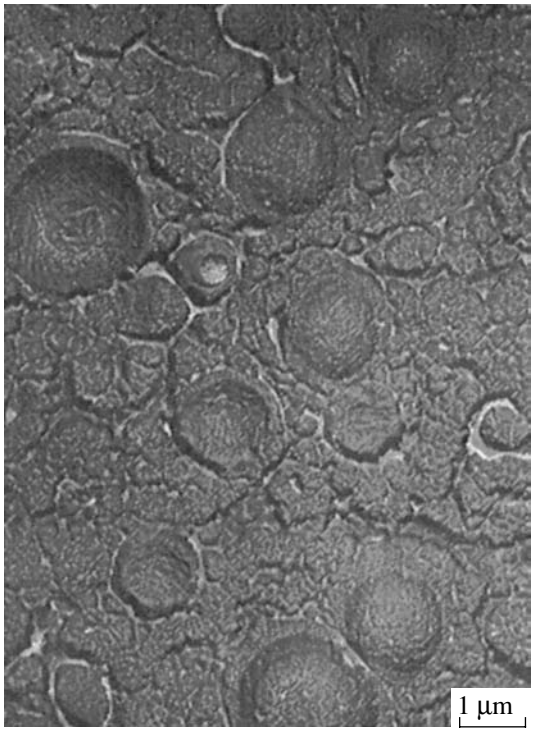

Electron microphotograph of the plasticized composition of polyvinylchloride and butadiene acrylonitrile rubber.

For the disordered flow,

$$r_\infty = \frac{9\alpha^2\varphi^2\nu E + \sqrt{(9\alpha^2\varphi^2\nu E)^2 + 96\alpha^2\beta\varphi^2\nu\dot{\gamma}\sigma}}{8\beta\tau\dot{\gamma}}. \quad (16)$$

DISCUSSION

The suitability of the models of calculating the ultimate size of formations in the dispersion phase was tested by comparing the calculated values with the measured sizes of formations in the dispersion phase in the microphotographs of polymer mixtures. The figure exemplifies the electron microphotograph of a polymer mixture of plasticized polyvinylchloride and butadiene acrylonitrile rubber obtained under the following technological conditions: $T = 185°C$, $\varphi = 0.2$, and $\dot{\gamma} = 120\ s^{-1}$. The size of formations in the dispersion phase ranges from 1×10^{-6} to 2×10^{-6} m.

For these parameters, formulas (15) and (16) yields the ultimate formation radius $r_\infty = 2 \times 10^{-13}$ and 7.1×10^{-7} m, respectively. Thus, formula (15) is unsuitable for estimating the sizes of formations in the dispersion phase, while formula (16) is in good agreement with the experimental results.

An advantage of the proposed model over the preceding ones [1–4] is the concrete analysis of the factors determining dispersive mixing. This analysis allows both control over this process and prediction of the for-

mation sizes in the dispersion phase, the structure of this phase, and, thus, the consumption characteristics of polymer systems.

REFERENCES

1. G. J. Taylor, Proc. R. Soc. London, Ser. A **146**, 501 (1934).
2. S. Tomotika, Proc. R. Soc. London, Ser. A **150**, 332 (1935).
3. S. Tomotika, Proc. R. Soc. London, Ser. A **153**, 302 (1936).
4. N. Tokita, in *Proceedings of ACS Rubber Division Meeting, San Francisco, 1976*, Repr. no. 26.
5. Yu. P. Miroshnikov, in *Equipment and Technology of Processing Rubbers, Polymers, and Rubber Mixtures: Collection of Articles* (Yaroslavsk. Politekhn. Inst., Yaroslavl, 1978), pp. 35–37.
6. Yu. P. Miroshnikov, Doctoral Dissertation (Mosk. Inst. Tonk. Khim. Tekhnol., Moscow, 1996).
7. A. Ya. Malkin and V. P. Begishev, *Chemical Formation of Polymers* (Khimiya, Moscow, 1991).
8. V. N. Kuleznev, *Polymer Blends* (Khimiya, Moscow, 1980).

Translated by V. Bukhanov

Doklady Physics, Vol. 48, No. 12, 2003, pp. 705–709. Translated from Doklady Akademii Nauk, Vol. 393, No. 6, 2003, pp. 770–775.

MECHANICS

Nonlinear Laws of Motion and Explanation of the Motion of Inertoids

É. R. Smol'yakov

Presented by Academician S.V. Emel'yanov September 16, 2003

Received September 18, 2003

Newton's laws are nonlinearly generalized so that the "strange" motion of Tolchin's inertoids, which is not explained by classical mechanics, can be explained and predicted.

In the mid-1930s, Tolchin [1] designed a simple mechanism, which he called an inertoid, which moved due to a periodic change in its internal momentum. Since that time, numerous experiments were carried out with such mechanisms at various laboratories in different countries over nearly 70 years. All criticism of these experiments has been unfounded because all possible effects of friction, aerodynamics, etc., are weaker than the observed effect of the motion of an inertoid, by a factor from the range 0.001–0.1. The motion of these mechanisms has not yet been explained in the framework of classical (or Einsteinian) mechanics. Tolchin attempted to intuitively explain this motion by the action of "tangential inertial forces" [1, p. 87]. However, this explanation is empty. It is more realistic to assume that all known theories of motion (Newtonian, Einsteinian, Shipov's [2], etc.) are too "linearized" to take into account the features of the motion of inertoids. Their motion can be satisfactorily described only in a substantially nonlinear simple "extended" Newtonian model [3].

In this work, we extend this model and show that it can explain center-of-mass motion that is pronounced in numerous experiments with a Tolchin inertoid ("four-dimensional" gyroscope) [1] and is due to proper control over the momentum. Moreover, the parameters of the inertoid can be optimized in agreement with experimental results. Thus, mechanisms moving in vacuum and in any medium without both loss of their mass and any active contact with the environment can be designed and optimized.

Proposing the most general available mathematical model of the world, Shipov [2] attempted to prove that the center-of-mass motion of an isolated mechanical system under the action of controllable internal rotations could be described by "torsion interaction" theory. Shipov wrote [2, p. 191], "The torsion conservation law is the practical conclusion that exchange between the momentum and angular momentum can change the momentum of the center of mass of an isolated mechanical system." However, this statement has not been proven by Shipov and cannot be corroborated in the framework of his "overly linearized" model.

Shipov's theory, which undoubtedly provides more extended representation of both *vacuum* as an "accumulator" of all existing things and inertial forces, explains many ununderstandable phenomena. However, the aim of this theory was the explanation of center-of-mass motion due to internal forces. This aim has not been achieved despite the substantial extension (compared to classical mechanics) of the role of inertial forces. Shipov wrote about inertial forces [2, pp. 195–196],

"(i) They are generated by the inertial fields T^i_{jk} and enter into both translational

$$\frac{Du^i}{ds} + T^i_{jk}u^k u^i = 0 \qquad (3.161)$$

and rotational

$$\frac{De^i_a}{ds} + T^i_{jk}\frac{dx^k}{ds}e^i_a = 0 \qquad (3.162)$$

equations of motion;

(ii) inertial fields T^i_{jk} are determined by the torsion of absolute parallelism geometry

$$\Omega^i_{jk} = -\Delta^i_{[jk]} = -\frac{1}{2}e^i_a(e^a_{j,k} - e^a_{k,j}),$$

which characterizes the elastic properties of space and is local;

(iii) being of vacuum nature, inertial forces can be treated neither as internal nor as external for any isolated system."

Shipov wrote [2, p. 197], "new concept of inertial fields and forces make it possible to go beyond the scope of some theorems of classical mechanics. In particular, it is the conservation theorem for the center-of-

Moscow State University,
Vorob'evy gory, Moscow, 119992 Russia

1028-3358/03/4812-0705$24.00

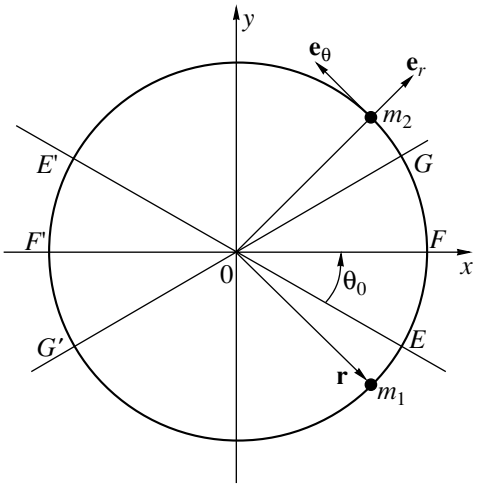

Figure.

mass momentum of an isolated mechanical system. According to this theorem, internal forces cannot change the center-of-mass momentum of an isolated mechanical system. The theorem was proved under the following conditions [4]: internal forces satisfy Newton's third law and internal forces are forces that act in the internal volume bounded by the isolated-system walls."

In his attempts to explain the Tolchin effect, Shipov emphasizes that the inertial field (tensor T^i_{jk}) appears in his equations of torsion mechanics for both translational and rotational motions. However, the motion of an inertoid can hardly be explained by taking into account only the second derivatives. Explanation should be sought in a certain nonlinear theory of motion, such as the extended Newton's law [3] or, in a more complete form, generalized Newton's law (1) proposed below. The applicability of this law is corroborated at least implicitly, because it explains the center-of-mass motion of Tolchin's inertoids, which had remained unexplained for nearly 70 years, and provides the possibility of optimizing the parameters of this mechanism.

We consider dynamic systems where only gravitational and inertial forces, as well as forces which we call forces of the coupling of a body with vacuum, are manifested. In addition, we assume that the total force F acting on the body with mass m is expandable in a Taylor series whose terms are not all equal to zero simultaneously. Thus, the equation of motion takes the form

$$F_0 + \sum_{i=0}^{\infty} K_i \mathbf{r}^{(i)} = 0, \qquad (1)$$

where $\mathbf{r}^{(i)}$ is the ith time derivative of the radius vector in a certain coordinate system and F_0 and K_i are dimensional coefficients, which can depend on the configuration properties of the body and space.

Series (1) extends a similar series from [3] by including the three following terms: the term F_0 determining the coupling of the body with vacuum, the term $K_0\mathbf{r}$ responsible for the gravitational force, and the term $K_1\frac{d\mathbf{r}}{dt}$, which is related to the momentum for $K_1 = m$. Different terms in Eq. (1) are nonzero in dependence on the shape of the body, the character of the motion of masses in it, and external (gravitational) fields.

We consider the motion of an inertoid in the polar coordinate system whose unit vectors are shown in the figure. In this coordinate system, the position of a material point is specified by the radius vector $\mathbf{r} = rE_r$ and angle θ measured in the (x, y) plane from the x axis $(0 \le \theta \le 2\pi)$. Successive derivatives of the radius vector are given by the expressions

$$\dot{\mathbf{r}} = \dot{r}\mathbf{e}_r + r\dot{\theta}\mathbf{e}_\theta, \qquad (2)$$

$$\ddot{\mathbf{r}} = (\ddot{r} - r\dot{\theta}^2)\mathbf{e}_r + (r\ddot{\theta} + 2\dot{r}\dot{\theta})\mathbf{e}_\theta, \qquad (3)$$

$$\mathbf{r}^{(3)} = (r^{(3)} - 3\dot{r}\dot{\theta}^2 - 3r\dot{\theta}\ddot{\theta})\mathbf{e}_r + (3\ddot{r}\dot{\theta} + r\theta^{(3)} - r\dot{\theta}^3 + 3\dot{r}\ddot{\theta})\mathbf{e}_\theta, \qquad (4)$$

$$\mathbf{r}^{(4)} = (r\dot{\theta}^4 + r^{(4)} - 6\ddot{r}\dot{\theta}^2 - 12\dot{r}\dot{\theta}\ddot{\theta} - 3r\ddot{\theta}^2 - 4r\dot{\theta}\theta^{(3)})\mathbf{e}_r + (r\theta^{(4)} + 4r^{(3)}\dot{\theta} + 6\ddot{r}\ddot{\theta} - 4\dot{r}\dot{\theta}^3 + 4\dot{r}\theta^{(3)} - 6r\dot{\theta}^2\ddot{\theta})\mathbf{e}_\theta. \qquad (5)$$

The simplest Tolchin's inertoid [1] is a mechanical system consisting of two identical masses $m_1 = m_2 = m$ that rotate about the O axis in the opposite directions and are located at the ends of inelastic rods whose momentum changes periodically for a short time (by means of an electromotor and a brake) during each rotation period.

The figure illustrates the simplified mathematical model of an inertoid. According to experiments with inertoids [1, 2], the pulsed displacement of its center of mass O along the x axis in the second half-period of mass rotation is opposite to that in the half-period. The displacement of the center of mass in one direction is much larger than that in the opposite direction so that center-of-mass motion over many periods is translational. This motion occurs due to the specific control of its momentum. For convenience of calculations, we consider masses m_1 and m_2 as unit masses.

When the first and second masses rotating in opposite directions reach the points E and G (figure) where they have the same circular velocity $|v_0|$, these masses begin to be accelerated with a constant acceleration $|r\ddot{\theta}| = a > 0$ until they meet at point F with the identical velocity $|v_1| > |v_0|$. Further, moving by inertia along the

arcs GE' and EG', they reach points E' and G', respectively, at a certain time. At this time, the brake is turned on and provides a constant negative acceleration with the same absolute value as that under acceleration. Both masses have the same circular velocity $|v_0|$ when they meet at the point F'. Then, they move by inertia along the arcs $G'E$ and $E'G$ with the circular velocity $|v_0|$ to points E and G, respectively. Afterwards, the described process repeats anew.

Below, we will show that the center of mass of the model under consideration cannot move in the framework of classical mechanics, but such motion is allowed by generalized Newton's law (1). Moreover, the parameters of the inertoid can be optimized for any physical constants of this law, and the conclusions agree with experimental results.

First, we calculate change in the x projection of the angular momentum of the rotating masses and check if it is equal to zero. To calculate the x projection of the inertia force $\ddot{\mathbf{r}} = -r\dot{\theta}^2\mathbf{e}_r + r\ddot{\theta}\,\mathbf{e}_\theta$, we express the unit vectors $\mathbf{e}_r$ and $\mathbf{e}_\theta$ of the polar coordinate system shown in the figure in terms of the unit vectors $\mathbf{e}_x$ and $\mathbf{e}_y$ of the Cartesian coordinate system:

$$\ddot{\mathbf{r}} = -r\dot{\theta}^2(\mathbf{e}_x\cos\theta + \mathbf{e}_y\sin\theta) + r\ddot{\theta}(-\mathbf{e}_x\sin\theta + \mathbf{e}_y\cos\theta) = (-r\dot{\theta}^2\cos\theta - r\ddot{\theta}\sin\theta)\mathbf{e}_x + (-r\dot{\theta}^2\sin\theta + r\ddot{\theta}\cos\theta)\mathbf{e}_y.$$

Therefore, the x projection of the vector $\ddot{\mathbf{r}}$ has the form $F_2 = -r\dot{\theta}^2\cos\theta - r\ddot{\theta}\sin\theta$, and the x projection of the momentum changes during time interval $(0, t)$ by the value

$$J_2 = \int_0^t F_2 dt. \tag{6}$$

First, this integral is calculated for the first mass in its acceleration section EF with the preliminary calculation of auxiliary quantities. Integrating the constant acceleration $r\ddot{\theta} > 0$ of the first mass in its acceleration section EF in the time interval $(0, t_1)$, i.e., from the angle $\theta = -\theta_0$ to the angle $\theta = 0$ reached at $t = t_1$, we obtain

$$\dot{\theta} = \frac{at}{r} + \dot{\theta}_0, \quad \theta = \frac{a}{2r}t^2 + \dot{\theta}_0 t + \theta_0, \tag{7}$$

where $\dot{\theta}_0 > 0$ and $\theta_0 < 0$ (angle θ_0 corresponds to the point E in the figure). Therefore,

$$t = \frac{1}{a}\left[-v_0 + \sqrt{v_0^2 + 2ar(\theta - \theta_0)}\right];$$

where the first mass rotating counterclockwise has a velocity $v_0 = \dot{\theta}_0 r$ at the point E. The circular velocity of the first mass in the section EF is equal to

$$r\dot{\theta} = v = v_0 + at = \sqrt{v_0^2 + 2ar(\theta - \theta_0)} \triangleq \sqrt{A},$$

where A is introduced for further reduction of notation. The velocity at point F is equal to

$$v(t_1) \triangleq v_1 = \sqrt{v_0^2 - 2ar\theta_0}.$$

In view of the above relations, integral (6) over the section EF of the motion of the first mass is obviously calculated as

$$J_2^{EF} = -\int_0^{t_1}\frac{1}{r}(r\dot{\theta})^2\cos\theta dt - a\int_0^{t_1}\sin\theta dt$$

$$= -\int_{\theta_0}^{0}\sqrt{A}\cos\theta d\theta - ar\int_{\theta_0}^{0}\frac{1}{\sqrt{A}}\sin\theta d\theta \tag{8}$$

$$= -\int_{\theta_0}^{0}\sqrt{A}d(\sin\theta) - ar\int_{\theta_0}^{0}\frac{1}{\sqrt{A}}\sin\theta d\theta = v_0\sin\theta_0,$$

where one of the integrals is calculated by parts. Thus, change in the x projection of the momentum of the first mass in the section EF is equal to $J_2^{EF} = v_0\sin\theta_0$, where $\theta_0 < 0$. Since the opposing motion of the second mass over the section GF is the mirror image of the motion of the first mass about the x axis, we immediately obtain $J_2^{GF} = v_0\sin\theta_0$ for the second mass.

We now calculate the deceleration motion of the second mass over the arc $G'F'$ with the preliminary integration of the constant acceleration (deceleration) $r\ddot{\theta} = a$, where $a > 0$ because opposing motion is considered. We obtain $r\dot{\theta} = at - v_1$, where $v_1 > 0$ because the velocity $-v_1$ corresponds to opposing motion (to the θ angle direction accepted in the figure). Recall that v_1 is the velocity of the second mass in the section EG' of its free motion from point F (where its acceleration to velocity v_1 finishes) to point G'. In addition, we obtain

$$\theta = \frac{a}{2r}t^2 - \frac{v_1}{r}t + (\pi - \theta_0),$$

$$t = \frac{1}{a}(v_1 - \sqrt{v_1^2 - 2ar(\pi - \theta - \theta_0)}),$$

$$r\dot{\theta} = at - v_1 = -\sqrt{v_1^2 - 2ar(\pi - \theta - \theta_0)}$$

$$= \sqrt{v_0^2 - 2ar(\theta - \pi)} \triangleq \sqrt{B}; \quad dt = -\frac{rd\theta}{\sqrt{B}},$$

where the symbol B is introduced to simplify further calculations. For convenience of calculations, motion

over the arc $G'F'$ is considered to occur in the time interval $(0, t_1)$, where $t_1 = \frac{1}{a}(v_1 - \sqrt{v_1^2 - 2ar\theta_0})$. In view of the above notation and calculations, the integral $J_2^{G'F'}$ is calculated similarly to the integral J_2^{EF} and is equal to $J_2^{G'F'} = -v_1\sin\theta_0$.

Taking into account that the opposing motion of the first mass over the (deceleration) arc $E'F'$ is the mirror image of the motion of the first mass about the x axis, we obtain $J_2^{E'F'} = -v_1\sin\theta_0$ for the first mass. As is easily calculated and immediately follows from similar calculations in [3], the free motion of both masses in the section $E'G$ and EG' does not change the x projection of the momentum.

For the free motion of the first mass in the section FG,

$$r\dot{\theta} = v_1, \quad \theta = \frac{v_1}{r}t, \quad dt = \frac{r}{v_1}d\theta,$$

and, therefore,

$$J_2^{FG} = -\int_0^{t_1}\frac{(r\dot{\theta})^2}{r}\cos\theta dt = -v_1\int_0^{-\theta_0}\cos\theta d\theta = v_1\sin\theta_0.$$

Thus, $J_2^{FE} = v_1\sin\theta_0$. Similar calculations in the section $F'G'$ of the free motion of the first mass give $J_2^{G'F'} = -v_0\sin\theta_0$ and, therefore, $J_2^{F'E'} = -v_0\sin\theta_0$. Thus, the total change in the x projection of the momentum of the inertoid is equal to zero in classical mechanics. Therefore, according to classical mechanics, the Tolchin's inertoid cannot move (without the reactive force).

Now, we carry out calculations by using generalized Newton's law (1) and expression (4) for the third derivative $\mathbf{r}^{(3)}$ of the radius vector $\mathbf{r}$:

$$\mathbf{r}^{(3)} = (r^{(3)} - 3\dot{r}\dot{\theta}^2 - 3r\dot{\theta}\ddot{\theta})\mathbf{e}_r + (3\dot{r}\ddot{\theta} + r\theta^{(3)} - r\dot{\theta}^3 + 3\dot{r}\ddot{\theta})\mathbf{e}_\theta.$$

For r = const and $\ddot{\theta}$ = const, Eq. (4) yields

$$\mathbf{r}^{(3)} = -3r\dot{\theta}\ddot{\theta}\mathbf{e}_r - r\dot{\theta}^3\mathbf{e}_\theta.$$

The third derivative determines the rate of varying the force (acceleration) and can be a "driving force," the more so that the dimension of the "momentum" of this driving force coincides with the force dimension.

The x projection of the vector $\mathbf{r}^{(3)}$ is equal to

$$F_3 = -3r\dot{\theta}\ddot{\theta}\cos\theta + r\dot{\theta}^3\sin\theta,$$

and integral (6) of this projection is equal to

$$J_3^{EF} = -\frac{3a}{r}\int_0^{t_1}(r\dot{\theta})\cos\theta dt + \frac{1}{r^2}\int_0^{t_1}(r\dot{\theta})^3\sin\theta dt$$
$$-3a\int_{\theta_0}^{0}\cos\theta d\theta + \frac{1}{r}\int_{\theta_0}^{0}A\sin\theta d\theta = 3a\sin\theta_0$$
$$+\frac{1}{r}\int_{\theta_0}^{0}[v_0^2 - 2ar\theta_0 + 2ar\theta]\sin\theta d\theta$$
$$= \sin\theta_0 + 2a\theta_0 - \frac{v_0^2}{r}(1 - \cos\theta_0),$$

where $A = v_0^2 + 2ar(\theta - \theta_0)$.

Taking into account that the opposing motion of the second mass over the (deceleration) arc $E'F'$ is the mirror image of the motion of the first mass about the x axis, we obtain $J_3^{GF} = J_3^{EF}$.

The integral $J_3^{G'F'}$ determining the motion of the second mass in its deceleration section $G'F'$ is equal to

$$J_3^{G'F'} = -\frac{3a}{r}\int_0^{t_1}(r\dot{\theta})\cos\theta dt + \frac{1}{r^2}\int_0^{t_1}(r\dot{\theta})^3\sin\theta dt$$
$$= -3a\int_{\pi-\theta_0}^{\pi}\cos\theta d\theta + \frac{1}{r}\int_{\pi-\theta_0}^{\pi}B\sin\theta d\theta$$
$$= a\sin\theta_0 + 2a\theta_0\cos\theta_0 + v_0^2(1 - \cos\theta_0),$$

where $B = v_0^2 + 2ar(\theta - \pi)$.

In view of the same symmetry with respect to the x axis, $J_3^{E'F'} = J_3^{G'F'}$.

For the free motion of both the first mass in the section FG and the second mass in the section FE,

$$J_3^{FG} = J_3^{FE} = \frac{1}{r}v_1^2(1 - \cos\theta_0).$$

For the free motion of both the first mass in the section $F'G'$ and the second mass in the section $F'E'$,

$$J_3^{F'G'} = J_3^{F'E'} = \frac{1}{r}v_0^2(1 - \cos\theta_0).$$

Since the total value of the integral J for both masses in the sections GE' and $G'E$ is equal to zero, the total integral J_3 determining the center-of-mass motion of the inertoid per one period of the rotation of masses is equal to

$$J_3 = 4[a\sin\theta_0 + 2a\theta_0\cos\theta_0]. \quad (9)$$

Therefore, the acceleration $|a|$ has the determining importance for the velocity of the center of mass of inertoids (this velocity increases with the acceleration). In addition, equating the partial derivative to zero, we arrive at the relation $\tan\theta_0 = \frac{3}{2\theta_0}$ from which the optimum value $|\theta_0^{opt}| = 56.5°$ is obtained. This value can be corrected by including higher derivatives of the radius vector **r**.

A similar calculation of the "action" of the x projection of the fourth derivative provides

$$J_4 = \frac{3a}{r}(v_1 - v_0)(1 - \cos\theta). \quad (10)$$

Thus, with the inclusion of unknown coefficients K_3 and K_4 in law (1), we obtain

$$J_{3,4} = 4K_3 a(\sin\theta_0 + 2\theta_0\cos\theta_0) + 3K_4\frac{a}{r}(v_1 - v_0)(1 - \cos\theta_0). \quad (11)$$

Since coefficients in law (1) are unknown (they can depend on dynamics), the parametric optimization of expressions (11) is difficult and is not carried out.

Any theory of the motion of inertoids is absent (only filming of motion has been carried out [2]). Therefore, the effect of parameters on their motion has not yet been studied. Comparison of the motion of several variants of inertoids only showed that their velocity is maximal for relatively small angles $|\theta_0| \approx 30°$. Now, inertoids and possibly other constructions (e.g., proposed in [3, 5]) can be purposefully designed to ensure the maximum velocity of their centers of mass due to internal forces without any reaction forces. Thus, even without knowledge of its physical parameters, the generalized Newton's law makes it possible not only to explain the motion of inertoids, which was not explained for nearly 70 years, but also to optimize the parameters of their motion.

In conclusion, we note that the centers of mass of constructions with asymmetric rotations (such as those considered in [3, 5]) must move continuously according to the generalized Newton's law (rather than by forward–backward jumps, which are characteristic for Tolchin's inertoids). This is their advantage over Tolchin's inertoids. Moreover, the center of mass of conic constructions can be accelerated due not only to higher derivatives, but also to interaction with vacuum (through the term F_0 in the law of motion given by Eq. (1)) if these constructions rotate fast enough to eliminate their coupling with vacuum [5].

ACKNOWLEDGMENTS

This work was supported by the Russian Foundation for Basic Research (project nos. 01-01-00543 and 03-01-00329) and by the Division of Information Technologies and Computing Systems, Russian Academy of Sciences (project no. 1.3).

REFERENCES

1. V. N. Tolchin, *Inertoid. Inertial Forces as a Source of Translational Motion* (Permsk. Knizhn. Izd., Perm, 1977).
2. G. I. Shipov, *Theory of Physical Vacuum* (Nauka, Moscow, 1997).
3. V. A. Gelovani and E. R. Smol'yakov, Dokl. Akad. Nauk **375**, 159 (2000).
4. I. I. Ol'khovskiĭ, *Course of Theoretical Mechanics for Physicists* (Nauka, Moscow, 1970).
5. E. R. Smol'yakov and V. E. Smol'yakov, Preprint GUMDN (Moscow, 2003).

Translated by R. Tyapaev

Doklady Physics, Vol. 48, No. 12, 2003, pp. 710–714. Translated from Doklady Akademii Nauk, Vol. 393, No. 6, 2003, pp. 776–780.

MECHANICS

Calculation of the Structure of Periodic Flows in a Continuously Stratified Fluid with Allowance for Diffusion

Yu. D. Chashechkin* and A. V. Kistovich**

Presented by Academician D.M. Klimov June 11, 2003

Received June 18, 2003

Interest in dissipation in inhomogeneous fluids is stimulated by the search for mechanisms of formation of the fine structure of both the ocean and the atmosphere and by the necessity of development of methods for calculating linear and nonlinear waves as well as concomitant boundary layer flows. Singular components of the complete solutions are of increasing interest due to the use of microscopic electromechanical systems as well as micro- and nanotechnologies in control systems of power-intensive devices. The internal structure of boundary layers depends on the dimensionality of the space of the problem. Two different boundary layers can exist in a three-dimensional periodic flow in a stratified viscous medium [1]. One of them is an analogue of the periodic Stokes flow [2]. Its thickness is determined by the wave frequency and kinematic viscosity of the medium. The thickness of the other inner-boundary layer, which is specific for a stratified medium, depends on the Stokes scale and the geometry of the problem (slope of waves and radiating surfaces) [3]. Since the equations of motion are nonlinear, large-scale (regular) and small-scale (singular) elements interact with each other and with other flow components. Owing to this circumstance, the number of the mechanisms of excitation of internal waves increases, and a range of conditions under which this effect occurs extends [4].

Inclusion of diffusion increases both the order of the governing system of equations and the number of forms of periodic motions, which complicates analysis of the problem. In this work, the complete solution to the linearized problem of generation of three-dimensional internal waves with allowance for viscosity and diffusion has been constructed for the first time. A procedure of constructing solutions to multiscale singularly perturbed equations depends on the ratio between the kinematic viscosity ν and the salt diffusion coefficient D. For this reason, we analyze only the case of large values of the Schmidt number $\mathrm{Sc} = \frac{\nu}{D}$, which are typical for both aqueous solutions of metal salts and seawater.

We consider an exponentially stratified fluid whose density decreases with the height z as

$$\rho_0(z) = \rho_{00}\exp\left(-\frac{z}{\Lambda}\right);$$

where Λ is the buoyancy scale, the direction of the z axis is opposite to the gravitational acceleration $\mathbf{g}$, and $N = \sqrt{\frac{g}{\Lambda}} = \frac{2\pi}{T_\mathrm{b}}$ is the buoyancy frequency (T_b is the buoyancy period).

In the Boussinesq approximation that allows for the diffusion of the stratifying component, the linearized system of the equations of motion of a viscous incompressible fluid has the form

$$\begin{aligned}\rho_0\frac{\partial\mathbf{u}}{\partial t} &= -\nabla P + \nu\rho_0\Delta\mathbf{u} - \sigma g\mathbf{e}_z,\\ \frac{\partial\sigma}{\partial t} - \frac{u_z}{\Lambda} &= D\Delta\sigma, \quad \nabla\cdot\mathbf{u} = 0.\end{aligned} \tag{1}$$

Here, P, σ, and $\mathbf{u}$ are perturbations of pressure, of salinity, and of fluid velocity, respectively, which are assumed to be constant, and $\mathbf{e}_z$ is the unit vector of the z axis. In the linearized equation of the state which relates the density and the stratifying impurity (salinity), the coefficient of saline contraction is included in the figure of salinity perturbation.

Taking into account the symmetry of three-dimensional internal waves, we chose a part of a vertical cylinder with the height a and radius R as a source of periodic perturbations. It performs either vertical vibrations or torsional vibrations about the z axis. The time factor

Institute for Problems in Mechanics,
Russian Academy of Sciences,
pr. Vernadskogo 101/1, Moscow, 117526 Russia
** e-mail: chakin@ipmnet.ru*
*** e-mail: akist@vniiftri.ru*

1028-3358/03/4812-0710$24.00

$e^{-i\omega t}$ will be omitted below. The nonslip and impermeability boundary conditions for the velocity and substance, respectively, on the radiating surface and the condition of damping of all perturbations at infinity have the form

$$u_r|_{r=R} = 0, \quad u_\varphi|_{r=R} = U_\varphi(\varphi, z),$$
$$u_z|_{r=R} = U_z(\varphi, z), \quad D\frac{\partial\sigma}{\partial r}\bigg|_{r=R} = 0, \qquad (2)$$
$$P, u_r, u_\varphi, u_z, \sigma|_{r\to\infty, z\to\pm\infty} \to 0.$$

The equations

$$[(\omega - iD\Delta)(\omega - i\nu\Delta)\Delta - N^2\Delta_\perp]\Phi = 0,$$
$$(\omega - i\nu\Delta)\Psi = 0, \qquad (3)$$

for the components Ψ and Φ of the toroidal–poloidal representation of the velocity $\mathbf{u} = \nabla\times(\mathbf{e}_z\Psi) + \nabla\times\nabla\times(\mathbf{e}_z\Phi)$ [5] follow from Eqs. (1). Here, Δ is the total Laplacian and

$$\Delta_\perp = \frac{1}{r}\frac{\partial}{\partial r}\left(r\frac{\partial}{\partial r}\right) + \frac{1}{r^2}\frac{\partial^2}{\partial\varphi^2}$$

is the horizontal Laplacian. The equation for the salinity perturbation σ coincides with the equation for the potential Φ, while the condition of zero divergence $\nabla\cdot\mathbf{u} = 0$ is automatically satisfied.

Since source motion is axially symmetric, a solution to Eqs. (3) is sought in the form of the following expansion in plane waves:

$$\Psi = \int_{-\infty}^{+\infty} E(k)H_0^{(1)}(\kappa_\nu r)e^{ikz}dk,$$
$$\Phi = \int_{-\infty}^{+\infty} (A(k)H_0^{(1)}(k_w r) + B(k)H_0^{(1)}(k_\nu r)$$
$$+ C(k)H_0^{(1)}(k_D r))e^{ikz}dk, \qquad (4)$$
$$\sigma = \frac{1}{D\Lambda}\int_{-\infty}^{+\infty}\left(\frac{A(k)k_w^2}{k_w^2 - \kappa_D^2}H_0^{(1)}(k_w r)\right.$$
$$\left. + \frac{B(k)k_\nu^2}{k_\nu^2 - \kappa_D^2}H_0^{(1)}(k_\nu r) + \frac{C(k)k_D^2}{k_D^2 - \kappa_D^2}H_0^{(1)}(k_D r)\right)e^{ikz}dk,$$

where $H_0^{(1)}$ is the Hankel function of the first kind. The wavenumbers k_w, k_ν, k_D, κ_ν, and κ_D found from the solution to the dispersion equation obtained after the substitution of solution (4) into system (3) have the form

$$k_w = |k|\tan\theta + i\frac{\nu + D}{2N\cos^2\theta}|k|^3,$$
$$k_\nu = (\mp 1 + i)\sqrt{\frac{N}{\Omega}}\cos\theta,$$
$$k_D = \frac{1+i}{2}\sqrt{\frac{N\Omega}{D\nu}}, \quad \kappa_\nu^2 = \frac{i\omega}{\nu} - k^2, \quad \kappa_D^2 = \frac{i\omega}{D} - k^2, \qquad (5)$$
$$\Omega = (\nu + D)\sin\theta + \sqrt{(\nu - D)^2\sin^2\theta + 4\nu D},$$
$$\theta = \arcsin\frac{\omega}{N}.$$

The roots κ_ν and κ_D are chosen so that perturbations are damped at infinity ($\mathrm{Im}\,\kappa_\nu$, $\mathrm{Im}\,\kappa_D > 0$) and waves exist (i.e., the upper and lower signs are taken in the k_ν expression for $\omega \le N$ and $\omega \ge N$, respectively). If the generator frequency ω exceeds the buoyancy frequency N, then

$$k_w = \frac{|k|}{\sqrt{\omega^2 - N^2}}\left(i\omega + \frac{\nu + D}{2N(\omega^2 - N^2)}k^2\right) \qquad (6)$$

and waves are not emitted in the linear approximation. Instead, a region where the wave component of the periodic motion is exponentially damped is formed near the source. For a spectral component with the wavenumber $\mathbf{k}$, the width of this region is equal to $\delta_w = |\mathbf{k}|^{-1}\sqrt{1 - \frac{N^2}{\omega^2}}$.

The spectral amplitudes A, B, C, and D are found from the system of algebraic equations obtained after the substitution of solution (4) into boundary conditions (2). For large Schmidt numbers, the awkward solution of this system reduces to the simple form

$$A(k) \approx -\frac{H_1^{(1)}(k_\nu R)\bar{U}_z(k)}{k_\nu k_w H_0^{(1)}(k_\nu R)H_1^{(1)}(k_w R)}, \quad B(k) \approx \frac{\bar{U}_z(k)}{k_\nu^2 H_0^{(1)}(k_\nu R)},$$
$$C(k) \approx \frac{k^2 k_\nu H_1^{(1)}(k_\nu R)\bar{U}_z(k)}{R\kappa_\nu\kappa_D^2 k_D^3 H_0^{(1)}(k_\nu R)H_1^{(1)}(k_D R)}, \quad D(k) \approx \frac{\bar{U}_\varphi(k)}{\kappa_\nu H_1^{(1)}(\kappa_\nu R)}, \qquad (7)$$

where

$$\bar{U}_z(k) = \frac{1}{2\pi}\int_{-\infty}^{+\infty} U_z(z)e^{-ikz}dk,$$
$$\bar{U}_\varphi(k) = \frac{1}{2\pi}\int_{-\infty}^{+\infty} U_\varphi(z)e^{-ikz}dk \qquad (8)$$

are the spectral amplitudes of the vibration velocity of the radiating surface.

The term containing the spectral density $A(k)$ in the solution given by Eqs. (4) and (7) describes outgoing internal waves, while the terms with $B(k)$, $C(k)$, and $D(k)$ describe a family of boundary layers on the radiator surface. The term $D(k)$ determines a *viscous wave boundary layer* of thickness $\delta_\omega = \sqrt{\frac{2\nu}{\omega}}$, which also exists in a homogeneous fluid [6], while the expressions with $B(k)$ and $C(k)$ give *inner wave boundary layers* of a mixed type, which have the transverse scales

$$\lambda_\nu = \frac{\lambda}{\cos\theta}, \quad \lambda_D = \frac{2\delta_\nu\delta_D}{\lambda}, \quad \delta_\nu = \sqrt{\frac{\nu}{N}}, \quad \delta_D = \sqrt{\frac{D}{N}}, \tag{9}$$
$$\lambda = \sqrt{(\delta_\nu^2 + \delta_D^2)\sin\theta + \sqrt{(\delta_\nu^2 - \delta_D^2)\sin^2\theta + 4\delta_\nu^2\delta_D^2}}.$$

Here, the inequality $\lambda_\nu \geq \lambda_D$ is satisfied for any ratio between the kinematic coefficients ν and D, where equality is achieved at $\nu = D$. In the case under consideration ($\nu \gg D$), the leading terms of expansions of λ_ν and λ_D in the small parameter $\frac{D}{\nu}$ coincide with the scales corresponding to the wavenumbers κ_ν and κ_D; i.e.,

$$\lambda_\nu \approx \sqrt{\frac{2\nu}{\omega}}, \quad \lambda_D \approx \sqrt{\frac{2D}{\omega}} \tag{10}$$

and fields of velocity and density split partially.

The vertical cylinder does not violate the condition of stability of the initial density distribution. Therefore, relations (4) do not contain the $E(k)H_0^{(1)}(\kappa_D r)$ terms characterizing the diffusion-induced unsteady flow, where the scales of variations in the density and velocity are quite different [7]. If the radiating surface is inclined, a *density wave boundary layer* of thickness $\lambda_s = \frac{1}{\mathrm{Im}\kappa_D} = \sqrt{\frac{2D}{\omega}}$ is also formed and additional terms appear in integral relations (4).

Salinity, as well as vertical and radial velocity components, are unperturbed by the torsional vibrations of the radiating surface. In this case, the viscous periodic boundary layer is formed:

$$u_\varphi \approx -\frac{U_\varphi}{\pi}\int_{-\infty}^{+\infty}\frac{\sin\frac{ak}{2}}{k}\frac{H_1^{(1)}(\kappa_\nu r)}{H_1^{(1)}(\kappa_\nu R)}e^{ikz}dk, \tag{11}$$

but waves are not radiated in the linear approximation.

If the source radius is much larger than the characteristic scale of the formed boundary layer ($|\kappa_\nu R|$, $|\kappa_\nu r| \gg 1$), then, in the low-viscosity approximation $\left(\frac{k^2\nu}{\omega} \ll 1\right)$, relation (11) reduces to the form

$$u_\varphi \approx -\frac{U_\varphi}{\pi}\sqrt{\frac{R}{r}}I_1, \tag{12}$$

where

$$I_1 \approx \int_{-\infty}^{+\infty}\frac{\sin\frac{ak}{2}}{k}e^{ikz}\exp\left(\frac{i}{\sqrt{2\nu}}(\kappa_- + i\kappa_+)\rho\right)dk$$
$$\approx \exp\left((i-1)\sqrt{\frac{\omega}{2\nu}}\rho\right)\int_{-\infty}^{+\infty}\frac{\sin\frac{ak}{2}}{k}e^{ikz} \tag{13}$$
$$\times \exp\left(-(1+i)\sqrt{\frac{\omega}{2\nu}}\frac{k^2\rho}{2}\right)dk,$$
$$\kappa_\pm = \sqrt{\sqrt{k^4\nu^2 + \omega^2} \pm k^2\nu}, \quad \rho = r - R.$$

According to Eq. (13), the flow intensity in the viscous wave boundary layer decreases exponentially with the scale $\delta_\omega = \sqrt{\frac{2\nu}{\omega}}$. The factor $\sqrt{\frac{R}{r}}$ characterizes the geometric attenuation caused by the cylindrical symmetry of the problem.

The velocity distribution around a thin source of torsional vibrations, which has a radius much smaller than either the viscous wave scale or the thickness of the viscous boundary layer ($|\kappa_\nu R|, |\kappa_\nu r| \ll 1$), has the form

$$u_\varphi \approx -\frac{U_\varphi}{\pi}\frac{R}{r}\int_{-\infty}^{+\infty}\frac{\sin\frac{ak}{2}}{k}e^{ikz}dk = U_\varphi\frac{R}{r}\begin{cases}1, & |z| < \frac{a}{2}\\ \frac{1}{2}, & |z| = \frac{a}{2}\\ 0, & |z| > \frac{a}{2}.\end{cases} \tag{14}$$

Therefore, the flow decays linearly rather than exponentially with distance from the source surface. Consequently, the periodic motions primarily differ near micro- and macroinhomogeneities.

If vibrations are vertical, two families of inner boundary layers of viscous and mixed types are formed on the cylindrical belt of the height a. In the inner

boundary layer of the first type, perturbations of velocity and salinity are given by the relations

$$u_r \approx U_z \frac{H_1^{(1)}(k_\nu r)}{H_0^{(1)}(k_\nu R)}\left(\delta\left(z-\frac{a}{2}\right)-\delta\left(z+\frac{a}{2}\right)\right),$$

$$u_z \approx U_z \frac{H_0^{(1)}(k_\nu r)}{H_0^{(1)}(k_\nu R)}\begin{cases}1, & |z|<\dfrac{a}{2}\\ \dfrac{1}{2}, & |z| = \dfrac{a}{2}\\ 0, & |z|>\dfrac{a}{2},\end{cases}$$

$$\sigma \approx \frac{i\nu U_z}{2\Lambda\omega(\nu+D)}\frac{H_0^{(1)}(k_\nu r)}{H_0^{(1)}(k_\nu R)}\left(f\left(z-\frac{a}{2}\right)-f\left(z+\frac{a}{2}\right)\right), \quad (15)$$

$$f(x) = \operatorname{sgn}(x)\left(1-\exp\left(-(1-i)\frac{\alpha}{\sqrt{2}}|x|\right)\right),$$

$$\alpha = \sqrt{\frac{(\nu+D)\omega}{\nu D}}.$$

Singularities appear in Eq. (15) at the edges of the cylindrical segment, because calculations performed under the condition $D \ll \nu$ are approximate. In the exact expressions for the radial velocity, infinite discontinuities are smoothed and transformed to narrow zones of the bounded radial motion near source edges. A decrease in the vertical velocity component u_z is exclusively geometric, and the velocity boundary layer is not formed. However, the density boundary layer having the characteristic scale $\lambda_\rho = \sqrt{2\nu D/(\nu+D)\omega}$ is formed due to the combined action of periodic perturbations and diffusion.

In the inner wave boundary layer of the second type, perturbations are described by the expressions

$$u_r \approx -\frac{iU_z k_\nu}{\pi R k_D^2}\frac{H_1^{(1)}(k_\nu R)H_1^{(1)}(k_D r)}{H_0^{(1)}(k_\nu R)H_1^{(1)}(k_D R)}\int_{-\infty}^{+\infty}\frac{k^2\sin\dfrac{ak}{2}}{\kappa_\nu\kappa_D^2}e^{ikz}dk,$$

$$u_z \approx -\frac{U_z k_\nu}{\pi R k_D}\frac{H_1^{(1)}(k_\nu R)H_0^{(1)}(k_D r)}{H_0^{(1)}(k_\nu R)H_1^{(1)}(k_D R)}\int_{-\infty}^{+\infty}\frac{k\sin\dfrac{ak}{2}}{\kappa_\nu\kappa_D^2}e^{ikz}dk, \quad (16)$$

$$\sigma \approx \frac{U_z k_\nu}{D\Lambda\pi R k_D}\frac{H_1^{(1)}(k_\nu R)H_0^{(1)}(k_D r)}{H_0^{(1)}(k_\nu R)H_1^{(1)}(k_D R)}\int_{-\infty}^{+\infty}\frac{k\sin\dfrac{ak}{2}}{\kappa_\nu\kappa_D^2(k_D^2-\kappa_D^2)}e^{ikz}dk.$$

In the zero approximation with respect to the Schmidt number, these expressions do not contain salinity perturbations. In the first approximation, solution (16) describes the boundary layer characterized by different scales of variation for velocity ($\delta_\omega = \sqrt{\dfrac{2\nu}{\omega}}$) and salinity ($\delta_S = \sqrt{\dfrac{2D}{\omega}}$). The pattern of the physical fields is determined by the expressions consisting of the Hankel functions and by the integrals on the right-hand sides of the corresponding expressions.

Inner gravitational waves are generated only by a vertically vibrating source of the considered type. The radiated wave field is antisymmetric with respect to the central horizontal plane. In the upper wave cone, the velocity components and salinity perturbations are described by the expressions

$$u_r \approx \frac{iU_z}{\pi k_\nu}\frac{H_1^{(1)}(k_\nu R)}{H_0^{(1)}(k_\nu R)}\int_0^\infty \sin\frac{ak}{2}\frac{H_1^{(1)}(k_w r)}{H_0^{(1)}(k_w R)}e^{ikz}dk,$$

$$u_z \approx \frac{U_z}{\pi k_\nu}\frac{H_1^{(1)}(k_\nu R)}{H_0^{(1)}(k_\nu R)}\int_0^\infty \frac{\sin\dfrac{ak}{2}}{k}k_w\frac{H_0^{(1)}(k_w r)}{H_1^{(1)}(k_w R)}e^{ikz}dk, \quad (17)$$

$$\sigma \approx -\frac{U_z}{D\Lambda\pi k_\nu}\frac{H_1^{(1)}(k_\nu R)}{H_0^{(1)}(k_\nu R)}\int_0^\infty \sin\frac{ak}{2}$$

$$\times\frac{k_w}{(k_w^2-\kappa_D^2)}\frac{H_0^{(1)}(k_w r)}{H_1^{(1)}(k_w R)}e^{ikz}dk.$$

The structure of the wave field is conic in the coordinate system concomitant with the wave beam (p, q), where the q and p axes are directed along the beam and phase velocity, respectively ($r = R + p\sin\theta + q\cos\theta$, $z = -p\cos\theta + q\sin\theta$, $\sin\theta = \dfrac{\omega}{N}$). The function ([8])

$$F_d(k) = \exp\left(ikp - \frac{(\nu+D)k^3 q}{2N\cos\theta}\right) = F(q, p, k) \quad (18)$$

appears in the integrands in Eqs. (17). It contains the *dissipative wave scale*

$$L_d = \frac{\sqrt[3]{(\nu+D)g}}{N}, \quad (19)$$

which is similar to the viscous wave scale L_ν in the diffusionless medium [9]. The ratio of the size of the source to the scale L_d (19) determines the modal structure of the radiated beam.

The table presents the vertical displacements h of particles in the wave cone that are calculated by formula (17) for three values of the cylinder radius. Here, $\Phi(q) = \dfrac{2N\cos\theta}{(\nu+D)q}$ and $a' = a\cos\theta$ is the projection of the height of the moving cylinder part onto the p axis.

Table

Source	Displacement in the conic beam $\lvert h(p, q)\rvert$	Displacement in the beam axis $\lvert h(0, q)\rvert$
$\lvert k_w R\rvert \gg 1$, $\lvert k_\nu R\rvert \gg 1$, $R \gg L_d$	$\frac{U_z \tan\theta}{\pi N}\sqrt{\frac{\nu + D}{\omega}}\int_0^\infty \sin\frac{ka'}{2} F_d dk$	$\frac{U_z a \sin\theta}{6\pi N}\Phi^{2/3}(q)\sqrt{\frac{(\nu + D)R}{\omega(R + q\cos\theta)}}\Gamma\left(\frac{2}{3}\right)$
$\lvert k_w R\rvert \ll 1$, $\lvert k_\nu R \gg 1\rvert$	$\frac{U_z R}{N\sqrt{2\pi r}}\int_0^\infty \sqrt{k}\sin\frac{ka'}{2} F_d dk$	$\frac{U_z aR}{6N}\Phi^{5/6}(q)\sqrt{\frac{(\nu + D)\cos\theta}{2\pi N q}}\Gamma\left(\frac{5}{6}\right)$
$\lvert k_w R\rvert \ll 1$, $\lvert k_\nu R \ll 1\rvert$	$\frac{U_z(\nu + D)\sin^{5/2}\theta\cos^{1/2}\theta}{\omega^2 \ln(k_\nu R/2)\sqrt{2\pi r}}\int_0^\infty \sqrt{k}\sin\frac{ka'}{2} F_d dk$	$\frac{U_z a(\nu + D)}{6N^2 \ln(k_\nu R/2)}\Phi^{5/6}(q)\sqrt{\frac{\tan\theta}{2\pi q}}\Gamma\left(\frac{5}{6}\right)$

The first row of the table presents the results for a radiator radius exceeding the scales of all introduced perturbations: beam width, wavelength of the internal waves, thickness of the inner wave boundary layer λ_ν, and the dissipative wave scale L_d. The second row shows the results for the intermediate radius that exceeds the scales of the boundary flows but is smaller than the characteristic wavelengths of the internal waves. The third row presents the results for a radius much smaller than all scales of the problem. Disregarding the effects of diffusion, our results agree with the results of [10].

REFERENCES

1. Yu. V. Kistovich and Yu. D. Chashechkin, Preprint No. 674, IPM RAN (Institute of Applied Mechanics, Russian Academy of Sciences, Moscow, 2001).
2. G. G. Stokes, Trans. Cambridge Philos. Soc. **9**, 8 (1851).
3. Yu. V. Kistovich and Yu. D. Chashechkin, Prikl. Mekh. Tekh. Fiz. **42**, 52 (2001).
4. Yu. V. Kistovich and Yu. D. Chashechkin, Dokl. Akad. Nauk **382**, 772 (2002) [Dokl. Phys. **47**, 163 (2002)].
5. D. D. Holm and Y. Kimura, Phys. Fluids A **3**, 1033 (1991).
6. H. Schlichting, *Boundary Layer Theory*, 6th ed. (McGraw-Hill, New York, 1968; Nauka, Moscow, 1974).
7. A. V. Kistovich and Yu. D. Chashechkin, Dokl. Akad. Nauk **325**, 833 (1992).
8. M. J. Lighthill, *Waves in Fluid* (Cambridge Univ. Press, Cambridge, 1978; Mir, Moscow, 1981).
9. S. A. Makarov, V. I. Neklyudov, and Yu. D. Chashechkin, Izv. Akad. Nauk USSR, Fiz. Atmos. Okeana **26**, 744 (1990).
10. Yu. V. Kistovich and Yu. D. Chashechkin, Prikl. Mat. Mekh. **63**, 611 (1999).

Translated by Yu. Verevochkin